Regulation of Human Hsp70 by its Nucleotide Exchange Factors (NEFs)

by

Jennifer N. Rauch

A dissertation submitted in partial fulfillment
of the requirements for the degree of
Doctor of Philosophy
(Biological Chemistry)
in the University of Michigan
2015

Doctoral Committee:

Adjunct Associate Professor Jason E. Gestwicki, co-chair, University of California at San Francisco
Associate Professor Zhaohui Xu, co-chair
Professor Robert T. Kennedy
Professor Richard R. Neubig, Michigan State University
Assistant Professor Daniel Southworth

Dedication

This work is dedicated to my parents, Dr. Jack Rauch and Dr. Terry Hayrynen-Rauch. Their constant love and support has encouraged me to always strive for success. Without them, this work would not be possible.

Acknowledgements

Many people have supported the work of this thesis. First and foremost, I need to thank my mentor, Jason Gestwicki. Jason is a brilliant scientist and excellent teacher who has taught me many lessons throughout my tenure in his lab. His patience and positive reinforcement have always been essential to my successes. Even when I was convinced an experiment wouldn't work or everything was doomed for failure, his relentless confidence and enthusiasm has always persevered. His attitude towards science is something I admire, and hope to emulate in the future. I have treasured my time in the lab and I feel lucky to have had him as my mentor.

I would like to thank my committee members: Dr. Zhaohui Xu, Dr. Robert Kennedy, Dr. Richard Neubig, and Dr. Dan Southworth. They have always taken time to provide feedback on my research throughout my graduate career and have provided support and engaging insight that has made this work possible.

Next, I would like to thank the members of the Gestwicki Lab. My first teachers in the lab – Yoshi Miyata, Andrea Thompson, Matt Smith, and Leah Makley. From BCA assays to Electron Microscopy, your insight, advice, and technical skills have been instrumental. I will always be grateful for the lessons you taught me. I would also like to thank Tomoko Komiyama. Tomoko was an inspiring woman, whose zeal, dedication, and perseverance will forever encourage me; she is sincerely missed. To the rest of the members of the Gestwicki Lab, both past and present, I want to thank you for the constant camaraderie. It is an amazing thing to work with a group of people that you consider friends. I have enjoyed every moment of scientific debate, as well as every impromptu lab dance party.

I am grateful for all of my family and friends who have supported me. I especially thank my brother Andy, nephew Leo, and aunts and uncles. Your confidence in me has always been my rock – I hope I have made you proud.

I would also thank my boyfriend, Dr. Cody Vild. It is hard to explain how incredible it is to have such an amazing best friend. Cody is a remarkable scientist who has always supported and, more importantly, challenged me. His beliefs in my abilities are unparalleled and his encouragement has propelled me more times than I can count. I am grateful for all of our years together and I look forward to many more.

Lastly, I would like to thank my parents for their role in this work. Without them, I would have never imagined a career in science. I thank my father for gracing me with his intellectual prowess and effervescent humor. His contagious personality and undying enthusiasm have always made me smile. I thank my mother for being an amazing role model and the strongest woman I know. I continue to strive to be more like her every day.

Preface

This thesis is a compilation of published and unpublished work dissecting the role of human Hsp70 nucleotide exchange factors (NEFs). NEFs help guide Hsp70 biology and are an important component of the proteostasis network. In Chapter 1, we introduce Hsp70, the various classes of NEFs, and reasons for targeting the Hsp70-NEF interaction. A portion of this chapter was published as: Assimon VA*, Gilles AT*, **Rauch JN***, Gestwicki JE. Hsp70 protein complexes as drug targets. Current Pharmaceutical Design. 2013; 19(3):404-17. Chapter 2 describes the systematic biochemical characterization of two NEF families, Hsp105 and the BAG proteins. This chapter represents work published as **Rauch JN** and Gestwicki JE. *Binding of human nucleotide exchange factors to heat shock protein 70 (Hsp70) generates functionally distinct complexes in vitro*. Journal of Biological Chemistry. 2014; 289(3):1402-14. In Chapter 3, we move on to develop a novel high throughput screening platform to aid in the discovery of Hsp70-NEF inhibitors. Work from this chapter was published as **Rauch JN***, Nie J*, Buchholz TJ, Gestwicki JE, Kennedy RT. *Development of a capillary electrophoresis platform for identifying inhibitors of protein-protein interactions*. Analytical Chemistry. 2013; 85(20):9824-31. Then in Chapter 4 we focus on the specific NEF BAG3 and its role in bridging two major chaperone families. This work is currently in preparation to be submitted as a manuscript. Finally, in Chapter 5 we summarize the work provided in this thesis and discuss future work needed to expand on the ideas presented here. The appendix contains work that was published as Miyata Y*, **Rauch JN***, Jinwal UK, Thompson AD, Srinivasan S, Dickey CA, Gestwicki JE. *Cysteine reactivity distinguishes redox sensing by the heat-inducible and constitutive forms of heat shock protein 70***.** Chemistry & Biology. 2012; 19:1391-9.

Table of Contents

List of Figures

Abstract

Regulation of Human Hsp70 by its Nucleotide Exchange Factors (NEFs)

by

Jennifer N. Rauch

Heat shock protein 70 (Hsp70) is an abundant and ubiquitous molecular chaperone that is responsible for maintenance of the human proteome. Hsp70 is known to play key roles in virtually every cellular process that involves proteins, including their folding, stabilization, trafficking, and turnover. Accordingly, Hsp70 has become an attractive drug target for neurodegenerative and hyperproliferative disorders; however it is difficult to imagine strategies for inhibiting its pathobiology without impacting its essential roles. Fortunately, Hsp70 does not work alone, and instead employs a large network of co-chaperone proteins, which can tune Hsp70 activity and influence disease state. These co-chaperone proteins provide potential handles for targeting Hsp70 without disrupting overall proteostasis.

One such class of co-chaperones proteins known as the Nucleotide Exchange Factors (NEFs), are a particular appealing target. NEFs bind Hsp70 and help to facilitate the exchange of ADP for ATP. The biochemistry of the NEF family of co-chaperones has classically been investigated using the prokaryotic NEF, GrpE, as a model. However, the eukaryotic cytosol does not contain a GrpE homolog. Rather, there are three main sub-classes of human NEFs: Hsp110, HspBP1, and the BAG proteins, all of which are structurally distinct with little sequence homology. Consistent with their diverse structures, they also differ in their mode of binding to Hsp70 and their roles in guiding Hsp70 biology. For example, BAG2

is associated with proteasomal degradation of the Hsp70 substrate, tau, while BAG1-Hsp70 is linked to increased tau stability. These observations suggest that the formation of specific NEF-Hsp70 complexes may help decide the fate of Hsp70-bound substrates. Additionally, these findings illustrate that differential disruption of specific Hsp70-NEF contacts might be beneficial in disease.

In this thesis work I have systematically characterized the human Hsp70 NEFs, including how they interact with Hsp70, how the influence Hsp70 biochemistry and how they can bridge Hsp70 with other classes of chaperone proteins. I have used high throughput screening methods to search for chemical matter that can modulate Hsp70-NEF interactions, and we have shown that inhibitors of Hsp70-NEF interactions can be beneficial for treating disease. This thesis work has significantly advanced our knowledge of human Hsp70 regulation, and has provided groundwork for future studies on other Hsp70 co-chaperones and proteostasis components.

Chapter 1

The Nucleotide Exchange Factors (NEFs) of Heat Shock Protein 70 (Hsp70): Background and Potential as Drug Targets.

1.1 Abstract

Heat shock protein 70 (Hsp70) plays critical roles in proteostasis and is an emerging target for multiple diseases. However, competitive inhibition of the enzymatic activity of Hsp70 has proven challenging and, in some cases, may not be the most productive way to redirect Hsp70 function. Another approach is to inhibit Hsp70's interactions with important co-chaperones, such as J-proteins, nucleotide exchange factors (NEFs), or tetratricopeptide repeat (TPR) domain proteins. These co-chaperones normally bind Hsp70 and guide its many, diverse cellular activities. Complexes between Hsp70 and co-chaperones have been shown to have specific functions, such as pro-folding, pro-degradation or pro-trafficking. In addition, Hsp70 complexes have been shown to be important in helping Hsp70 select substrates from the proteome. Thus, one promising strategy is to block protein-protein interactions with co-chaperones or to target allosteric sites that disrupt these contacts. Such an approach might re-shape the proteome and restore healthy proteostasis. In this chapter we focus on a specific group of Hsp70 co-chaperones, the NEFs. We discuss what is known about their function, disease relevance, and how they could be targeted to influence Hsp70 biology.

1.2 The diversity of Hsp70 function

Heat shock protein 70 (Hsp70) is an abundant and ubiquitous molecular chaperone that plays a central role in protein quality control [2, 3]. Hsp70 binds to protein substrates to assist with their folding [4-6], degradation , transport [9],

regulation [6] and aggregation prevention [8]. The capacity of Hsp70 to carry out these widely divergent functions arises, in part, from three features. First, evolution has given rise to multiple homologous Hsp70 genes in eukaryotes [3]. These Hsp70s populate all of the major subcellular compartments. For example, the cytosol of human cells has two major isoforms of Hsp70, a stress-inducible form (Hsp72/HSP1A1) and a constitutive form (Hsc70/HSPA8). Similarly, BiP (HSPA5) is the form in the endoplasmic reticulum and mortalin (HSPA9) in the mitochondria. Another source of functional diversity in Hsp70s is cooperation with other chaperones, such as Hsp90 or Hsp60 [10, 11]. Cooperation between Hsp70 and Hsp90, for example, is critical to the function of nuclear hormone receptors [12]. Finally, the full diversity of Hsp70 activities is achieved through cooperation with a large network of co-chaperones [11], including J proteins, nucleotide exchange factors (NEFs), and tetratricopeptide repeat (TPR)-domain containing proteins [11]. These factors bind to Hsp70 and guide its many chaperone activities. In addition, each class of co-chaperones includes many distinct examples in mammalian cells, such that multiple J proteins, for example, compete for binding to the same site on Hsp70.

1.2.1 Structure and Function of Hsp70 and Its Complexes

Hsp70 consists of two domains, a 45 kDa N-terminal nucleotide binding domain (NBD) and a 25 kDa C-terminal substrate-binding domain (SBD) connected by a short flexible linker [12]. The NBD of Hsp70 is further divided into two subdomains, lobes I and II, that are each divided into an “A” and “B” region (Figure 1.1). These lobes form a cleft that binds ATP with a nucleotide-binding cassette that is related to hexokinase and actin [2, 13]. Hsp70’s SBD is composed of a 15 kDa β-sandwich subdomain with a hydrophobic groove for polypeptide binding and a 10 kDa α-helical region which forms a “lid” over the polypeptide-binding site [14]. Hsp70 preferentially binds hydrophobic regions of proteins and can therefore bind newly synthesized linear peptides or exposed regions on partially unfolded proteins [14, 15]. The lack of strong sequence specificity allows Hsp70 to bind a variety of client proteins including signal

transduction proteins, clathrin, nuclear hormone receptors, and cytoskeletal proteins [16].

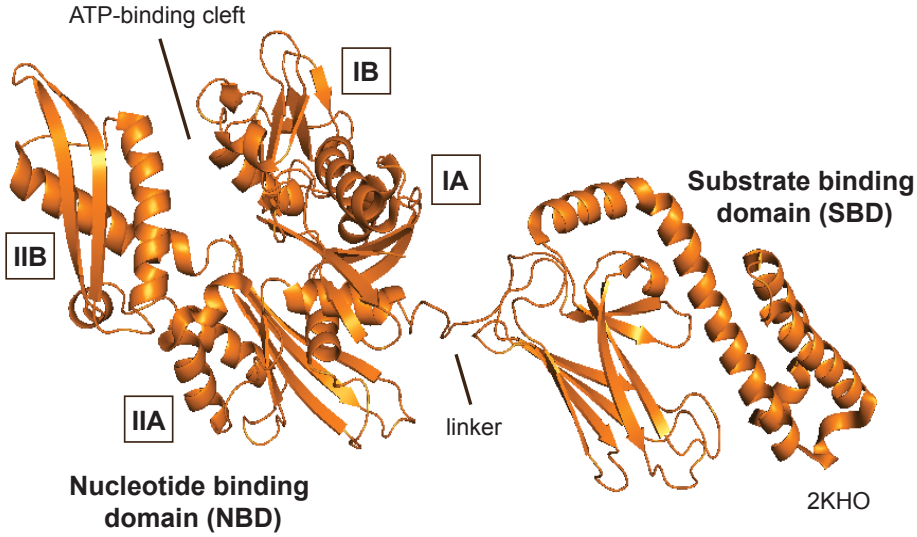

Figure 1.1: Hsp70 is composed of two domains. A nucleotide binding domain (NBD) that is responsible for binding and hydrolyzing ATP, and a substrate binding domain (SBD) that is responsible for binding client proteins. The NBD is divided into four lobes: IA, IB, IIA, and IIB. The SBD has a β-sandwich subdomain and an α-helical lid region.

The ATPase cycle of Hsp70s has been largely studied in the context of the highly conserved, prokaryotic DnaK. In this chaperone, ATP hydrolysis involves critical allostery between the NBD and SBD. In the ATP-bound state, Hsp70 has a low affinity for substrate and retains an “open” substrate-binding cleft, but conversion to the ADP-bound state causes the α-helical lid region to close (Figure 1.2) [18]. In DnaK, this crosstalk between the NBD and SBD appears to be bidirectional, because substrate binding also promotes nucleotide hydrolysis [18]. Thus, ATP hydrolysis in Hsp70s is thought to be a major determinant of their chaperone functions. For example, mutations in the ATP-binding cassette have dramatic effects on chaperone functions *in vitro* and *in vivo* [18]. However, recent mutagenesis studies have further shown that the relationship between ATP hydrolysis and chaperone functions is indirect [19]. For example, some mutations in DnaK that dramatically reduce ATP turnover have only modest effects on luciferase refolding. These observations suggest that inhibiting the ATPase activity of Hsp70 might not always directly lead to proportional changes in functional outcomes, such as reduced client stability. Rather, modifying the

interactions with co-chaperones might have a more predictable effect on chaperone functions [20].

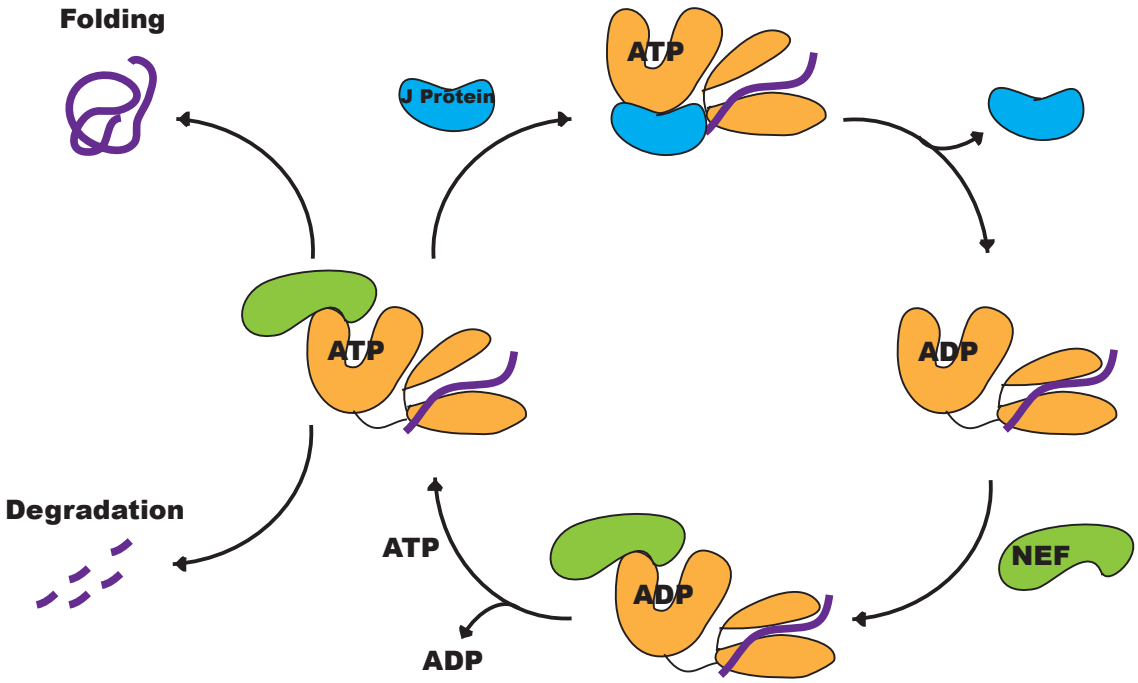

Figure 1.2. Hsp70 in an ATP state binds substrate with low affinity. J proteins accelerate ATP hydrolysis driving Hsp70 to the ADP state and promote a high affinity for substrates. NEFs facilitate the exchange of ADP for ATP and reset the cycle for folding or degradation.

1.2.2 Co-Chaperones Regulate Hsp70 Structure and Activity

The major families of co-chaperones bind to distinct interaction surfaces on Hsp70. The J protein co-chaperones bind Hsp70 at lobe IIA of the NBD and accelerate the rate of ATP hydrolysis [21]. The NEF co-chaperones bind lobes IB and IIB of Hsp70's NBD and facilitate the release of ADP, which has also been shown to accelerate Hsp70's ATPase rate [22]. By accelerating nucleotide exchange on Hsp70, NEFs also cause substrate release from Hsp70. Likewise, TPR domain containing co-chaperones bind Hsp70's C-terminus and have been shown to modulate the fates of Hsp70 client proteins [22-24]. Thus, the major families of co-chaperones bind Hsp70 to regulate its enzymatic activity, its localization and its choice of substrates.

1.2.3 Approaches to Targeting Hsp70

What is the best way to chemically target Hsp70? One possible approach is to inhibit ATPase activity with competitive nucleotide analogs, as has been done with Hsp90 inhibitors [24]. The nucleotide-binding cleft of Hsp70 is well defined and relatively deep, suggesting that it might be suitable for development of inhibitors. However, Hsp70 has a relatively high affinity (mid-nanomolar) for nucleotide, 300-fold better affinity than Hsp90 [24-26]. Because the cellular concentration of ATP is typically about 1-5 mM, protein targets with a high affinity for ADP and ATP are much more difficult to inhibit than those with a lower affinity. Further, the ATP-binding cassette in Hsp70 is highly homologous in actin and other abundant proteins. Thus, selectivity for the chaperone might be challenging. Despite these challenges, innovative work performed by Vernalis has produced competitive, orthosteric inhibitors of Hsp70, using structure-based design [25]. Consistent with their design, these compounds inhibit cancer cell viability [26] and this group has even been successful at selectively targeting BiP [25]. However, Massey has reported that the path towards orthostatic, competitive inhibitors of Hsp70 is quantitatively more challenging than the parallel path to other related targets, such as Hsp90 [26]. Consistent with this, allosteric modulators of Hsp70's NBD have recently gained favorable attention. A rational design approach lead Chiosis and colleagues to the small molecule YK5. YK5 forms a covalent adduct with a reactive cysteine (C267) in a pocket above the ATP-binding cassette, inhibits Hsp70 biochemical function, and promotes apoptosis in cancer cells [27]. Likewise, work from our lab has focused on the MKT-077 series. These compounds bind below the ATP binding pocket and stabilize Hsp70 in an "ADP-like" state [28]. The effects of these small molecules on Hsp70 biology will be discussed further in Chapter 5.

Targeting the substrate-binding cleft of Hsp70 is the next logical avenue, given the depth of the site and its known affinity for relatively low molecular mass peptides. This approach has been taken by Chaperone Technologies in their development of antibiotics. For example, a series of 18-20 amino acid peptides,

including drosocin, pyrrhocoricin, and apidaecin, are known to interact with DnaK [27]. Of these peptides, pyrrhocoricin exhibited broad-spectrum antibacterial activity. Competition experiments indicated that this peptide has two binding sites on DnaK, one of which is thought to be adjacent to the substrate-binding pocket. Interestingly, pyrrhocoricin has activity against bacteria but not mammalian cells [29-31], suggesting that the SBD could be leveraged to gain selectivity between different isoforms of Hsp70. Indeed, another natural product, Novolactone, has recently been shown to target the SBD of human Hsp70. This compound acts as a covalent modifier and shows selectivity for cytosolic and ER localized Hsp70s due to the presence of glutamate at position 444 (E444) [29]. While these works highlight the efficiency of SBD-targeted compounds, it is unclear whether this strategy could be implemented in the development of therapeutics for different Hsp70 related diseases.

Given the significant challenges associated with the targeting of either the nucleotide- or substrate-binding regions of Hsp70, additional strategies are worth pursuing. A number of additional Hsp70 inhibitors have been identified, but their mechanisms are not known yet [31-33]. To supplement this collection of compounds, targeting the protein-protein interactions (PPIs) between Hsp70 and its many co-chaperones may be an effective approach.

1.3 NEFs are an emerging target

Nucleotide exchange factors (NEF) provide a potential “handle” for targeting the Hsp70 chaperone complex. NEFs bind Hsp70 and help to facilitate the exchange of ADP for ATP. The biochemistry of the NEF family of co-chaperones has classically been investigated using the prokaryotic NEF, GrpE, as a model [31]. However, the eukaryotic cytosol does not contain a GrpE homolog. Rather, there are three main sub-classes of human NEFs: Hsp110, HspBP1, and the BAG proteins, all of which are structurally distinct with little to no sequence homology (Figure 1.3). Consistent with their diverse structures, they also differ in their mode of binding to Hsp70s and their roles in guiding Hsp70 biology. For

example, BAG2 is associated with proteasomal degradation of the Hsp70 substrate, tau, while BAG1-Hsp70 is linked to increased tau stability [34-37]. These observations suggest that the formation of specific NEF-Hsp70 complexes may help decide the fate of Hsp70-bound substrates. Also, these observations suggest that differential disruption of specific Hsp70-NEF contacts might be beneficial for treating disease. For example, members of the NEF family are differentially expressed in multiple diseases, including cancer, Alzheimer's, cardiomyopathies, and ischemia [36-39], highlighting the rationale for developing chemical modulators of NEF-Hsp70 interactions.

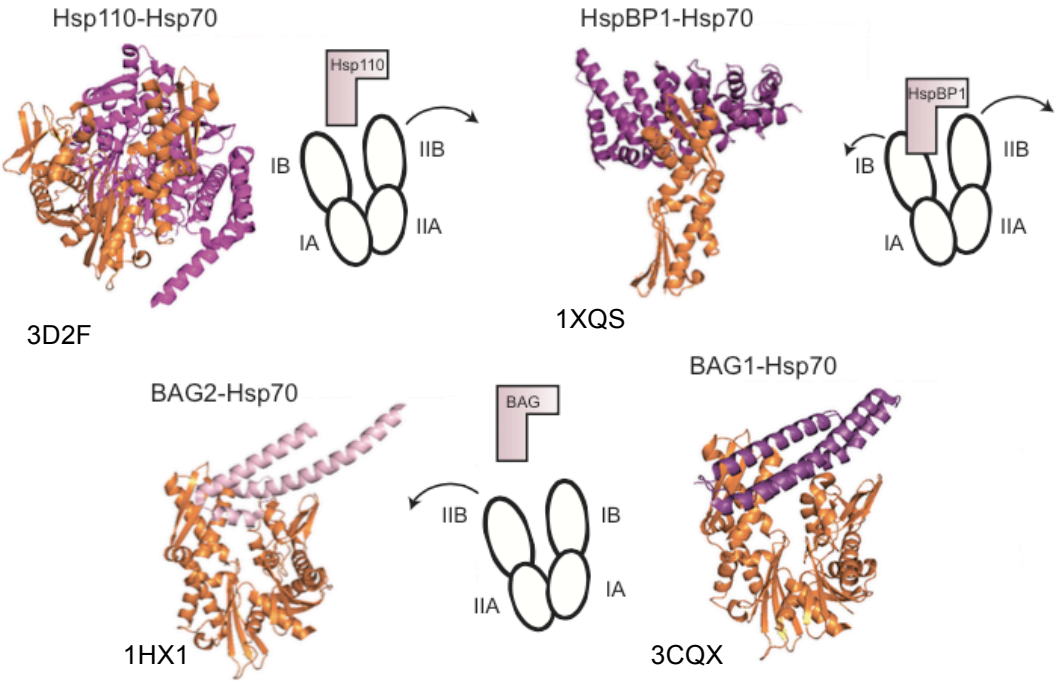

Figure 1.3. Structures of Hsp70-NEF complexes. Crystal structure of yeast Hsp110, Sse1, and human Hsp70 NBD. Complex formation between Hsp70 and Hsp110 leads to a rotation in lobe IIB allowing nucleotide release. Crystal structure of HspBP1 and lobe II of Hsp70's NBD. HspBP1 wraps around lobe IIB displacing lobe I and opening the nucleotide cleft. Crystal structures of Hsp70 NBD in complex with the BAG domain of BAG1 and BAG2. Association between Hsp70 and the BAG proteins cause an outward rotation of lobe II, promoting nucleotide exchange. In all figures Hsp70 is colored in orange and NEFs are colored in purple with PDB codes indicated.

1.3.1 Hsp110 Family

Heat shock protein 110 (Hsp110) was originally observed and classified as a heat shock protein based on the appearance of a 110 kDa band in the lysates of

Chinese Hamster Ovary (CHO) cells upon heat shock [39, 40]. In humans the major cytosolic Hsp110 protein is called Hsp105 (HSPH1) and it has two major isoforms α and β [41]. Hsp105α is constitutively expressed and upregulated by a variety of stressors, whereas the alternatively spliced isoform Hsp105β is only induced upon heat shock [41]. The Hsp110 family is evolutionarily conserved from yeast to humans [41]. While research has primarily focused on *Homo sapiens* and *S. cerevisiae* (yeast) Hsp110 proteins, genes for Hsp110 family members have been annotated in over 80 species. The high level of conservation across species (25% identity from humans to yeast) is indicative of the essential function of this group of proteins [43].

Hsp110 proteins are evolutionary relatives of the Hsp70 family, and in fact were originally classified as an Hsp70 sub-family. While sequence conservation between Hsp70 and Hsp110 proteins is only ~30%, structural analyses have shown they share the same features and are likely derived from ancestral DnaK [44]. For example, Hsp110 proteins (like Hsp70s) are composed of two domains, a nucleotide binding domain (NBD) and a substrate-binding domain (SBD), which are connected by a flexible linker. In addition, Hsp110s also contain a variable C-terminal extension with little predicted structure. While the overall domain architecture is reminiscent of the Hsp70 family, the major structural differences are found in the SBD. Unlike Hsp70, Hsp110 members contain an acidic insertion in the SBD and their C-terminal extensions tend to be longer (>100 AA). Functionally, although Hsp110 has been reported to bind ATP [45], only human Hsp110 (HSPH1) has been reported to have intrinsic ATPase activity [43, 45-48]. Thus, Hsp110s share some structural similarity with Hsp70s but they differ in important ways.

Early studies demonstrated that Hsp110 overexpression was sufficient to confer thermal tolerance to cells and prevent aggregation of proteins *in vitro* [47]. Despite the structural similarity to Hsp70, Hsp110 only functions as a holdase and has no ability to refold substrates without the help of the Hsp70 machinery

[45, 47-50]. Regardless, Hsp110 has been shown to be a very efficient chaperone that can bind peptide substrates with low nM affinity and perhaps is even more effective than Hsp70 at stabilizing unfolded proteins [47, 51, 52]. Studies looking at the substrate binding properties of Hsp110 vs. Hsp70 proteins have found that, while both proteins use their respective SBDs to interact with clients, they vary in several binding properties including sequence preference, binding kinetics, and nucleotide requirements [51]. Interestingly, swapping of loop regions within the SBD of either partner was sufficient to confer specificity, as well as convert Hsp70 from its normal foldase function to an Hsp110-like holdase [53]. This functional difference is important because Hsp110's holdase activity appears to be hijacked by cancer cells. Specifically, Hsp110 stabilizes anti-apoptotic factors and prevents apoptosis [54, 55]. In line with this thinking, Hsp110 is overexpressed in a variety of human tumors [56, 57] and siRNA knockdown of Hsp110 or expression of a naturally occurring dominant negative mutant, Hsp110ΔE9, have been shown to sensitize cancer cells and induce apoptosis in human cancer cells, but not in control fibroblasts [58].

As a NEF for Hsp70, Hsp110 has been implicated in various cellular processes, including co-translational and post-translational folding [60], stabilization and secretion of proteins [61], maturation and signaling of glucocorticoid receptor [63], as well as degradation of Hsp70 clients [63, 64]. Overexpression of Hsp110 has been shown to be protective for various neurodegenerative diseases [65]. Likewise, Hsp110 knockout mice exhibit an age-dependent accumulation of phosphorylated tau that is associated with the appearance of neurofibrillary tangles and neurodegeneration [67, 68].

X-ray crystal structures of the *S. cerevisiae* Hsp110 (Sse1) have been solved alone [68], as well as in complex with Hsp70 [69]. The Hsp110-Hsp70 complex structure shows that the protein-protein interaction between the two covers a large surface area involving both partners' NBDs (Figure 1.3). An extensive network of intermolecular contacts along each partner's NBD is consistent with

the measured stability of the complex. The binding of Hsp110 to Hsp70 causes several rotations in Hsp70's NBD, especially in lobe IIB, allowing ADP release, thus providing a structural mechanism for Hsp110's NEF activity (Figure 1.3)

The large buried surface area between Hsp70 and Hsp110 may make targeting this interaction difficult. The problem in PPI systems like this is that binding energy is often distributed across a large and complex topology, precluding easy inhibition by small (<500 Da) molecules. However, inhibiting PPIs with large surface areas is not unprecedented and compounds with potency values in the low nM range have been reported [71]. A common feature of previous successful strategies is that the small molecules tend to target so-called "hotspots" of the PPI, meaning that the inhibitor binds in a region on one partner containing a small number of residues that are responsible for the majority of the binding strength [72]. Thus, it will be important to identify residues that are critical to the Hsp70-NEF interaction. Another common feature of successful PPI inhibitors is that they bind in allosteric sites to impact the topology of protein-protein contact surfaces from a distance. This approach lets the small molecule bind in a relatively concise pocket and impact larger surfaces to block PPIs. It seems likely that similar mechanisms will need to be employed to target the Hsp110-Hsp70 interaction. This will be important based on the genetic findings that the Hsp70-Hsp110 interface might be a critical anti-cancer target.

1.3.2 HspBP1

Similar issues are important in considering the potential for inhibition of the other major classes of NEFs. The Hsp binding protein 1 (HspBP1) was originally identified in a yeast two-hybrid screen for Hsp70 interacting proteins using a human heart cDNA library [74]. Since then, sequence homologs to HspBP1 have been identified throughout the eukaryotic domain, as well as paralogous ER proteins in mammals and yeast [75].

HspBP1 is a 40 kDa protein that is composed of two structural domains, one N-terminal domain that is largely unstructured and a C-terminal domain that is mostly α-helical and is responsible for HspBP1 binding to Hsp70 [77]. This C-terminal region has been shown to be sufficient for eliciting Hsp70 nucleotide release and inhibiting Hsp70 dependent refolding of luciferase [76]. Insight into HspBP1 NEF function came from the crystal structure of HspBP1's C-terminal domain solved in complex with lobe II of Hsp70's NBD [76, 77]. The armadillo repeats of the HspBP1 structure wrap around lobe II of the Hsp70 NBD (Figure 1.3) and due to steric hindrance cause a large displacement of lobe I relative to lobe II [78]. This shift facilitates nucleotide exchange, increases NBD hydrogen deuterium exchange, and increases protease susceptibility [78].

While little research has fully examined substrate client fate upon HspBP1 binding to Hsp70, HspBP1 has been shown to be a potent inhibitor of Hsp70 refolding activity even at substoichiometric concentrations [80]. Inhibiting Hsp70 function can obviously have detrimental effects to the cell; however, in tumor cells where Hsp70 functions to prevent apoptotic death and promote tumorigenesis, inhibiting Hsp70 can be beneficial. In line with this thinking, patients who have higher ratios of HspBP1/Hsp70 have been shown to have less aggressive tumors and are more susceptible to anti-cancer drugs and chemotherapies [79]. Furthermore, anti-cancer drugs themselves have been shown to upregulate HspBP1 expression in tumor cell lines [81]. This line of evidence suggests that increasing HspBP1 levels and/or activating HspBP1-Hsp70 complexes could be a potential therapeutic for specific tumor types.

1.3.3 BAG Family

Additional lessons about how to potentially target the Hsp70-NEF interaction are illustrated by the BAG family of co-chaperones, which includes BAG1-6. BAG proteins are defined by a characteristic C-terminal BAG domain that binds lobe IB and IIB of Hsp70's NBD and facilitates nucleotide release [20, 82]. This BAG domain typically consists of ~100 amino acids and forms a three-helix bundle

with the second and third helices providing the binding interfaces for Hsp70 [20]. The association between the BAG domain and Hsp70 causes a 14° rotation in lobe II, which results in an opening of the nucleotide binding cleft and promotes ADP release (Figure 1.3) [22]. Interestingly, while all BAG proteins interact with Hsp70 through their conserved BAG domains, their N-terminal region is highly variable (Figure 1.4). This diversity is likely to be key for pathway specificity and BAG proteins may use these domains to determine the timing and location of nucleotide-dependent delivery of Hsp70-bound cargo.

1.3.3.1 BAG1

BAG1 is the founding member of the BAG protein family. It was initially discovered by two independent research groups using immunochemical screening methods to identify interacting partners of the anti-apoptotic protein Bcl-2 and the glucocorticoid receptor, respectively [83]. The former researchers entitled their protein Bcl-2-associated AnthanoGene-1 (BAG1) [86]. Four human BAG1 isoforms are expressed through alternative initiation sites and are designated BAG1L (p50, Hap50), BAG1M (p46, Rap46, Hap46), BAG1S (p36, Hap33), and p29 (Hap29) [87]. BAG1S is the most abundant isoform expressed in cells, followed by BAG1L and BAG1M, while p29 is not consistently detected [88-90]. BAG1 isoforms share a common C-terminus, containing the BAG domain and an Ubiquitin-like (UBL) domain, while their N-termini differ based on the translation initiation site (Figure 1.4). Besides their BAG and UBL domains, longer isoforms of BAG1 (M & L) also contain TXSEEX repeats, a DNA-binding domain (DBD), and BAG1L contains a nuclear localization signal (NLS). These various domains help to dictate interacting partners as well as cellular function and localization of each BAG1 isoform (for review see [89]).

BAG1 regulates the fate of Hsp70-bound client proteins. For example, the UBL domain of BAG1 allows for BAG1-Hsp70 complexes to associate with the proteasome and promotes the degradation of specific client proteins such as the glucocorticoid receptor, BCR-ABL and huntingtin protein (Htt) [90-92]. However,

BAG1 has also been shown to inhibit proteasomal degradation of other Hsp70 clients, such as tau and CFTR [92]. These observations suggest that chemically targeting BAG1-Hsp70 complexes could be used to reshape the proteome. Work towards that goal has been reported by Sharp *et. al*, in which they performed a

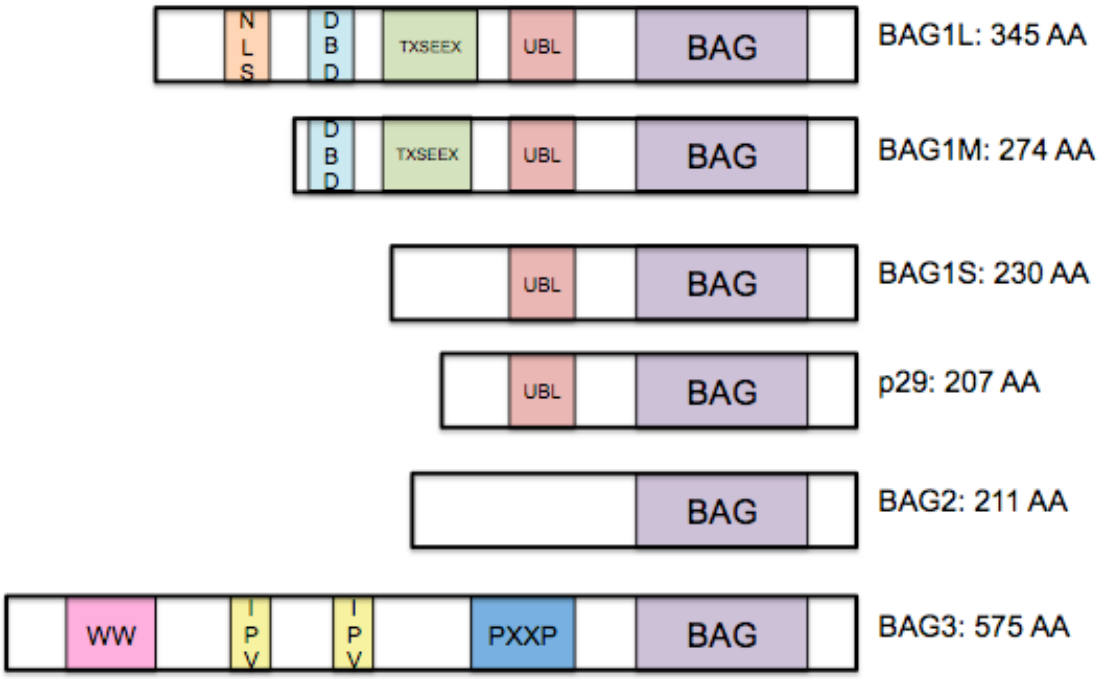

Figure 1.4. Domain architecture of BAG proteins. While all proteins share a common C-terminal BAG domain (used to interact with Hsp70), their N-termini are highly variable in composition and structure.

screen for inhibitors of the BAG1-Hsp70 interaction using GST pulldowns. After hit validation, NSC71948 (Thioflavin S), was selected for further study [80]. This compound inhibits ERK phosphorylation and growth of ZR-75-1 human breast cancer cells. This group has further gone on to isolate the active component of the complex Thioflavin S mixture (Thio-2), and show that this molecule might have therapeutic potential for BRAF inhibitor-resistant cell lines [94]. While these studies suggest that targeting a BAG-Hsp70 complex is both feasible and beneficial, further studies are still needed. For example, the binding sites and mechanisms of these molecules are not yet clear.

1.3.3.2 BAG2

The BAG family members BAG2 and BAG3 were identified in a yeast two hybrid screen with the NBD of Hsc70 as bait and were named based on their structural and functional similarity to BAG1 [95-97]. However, the crystal structure of BAG2's BAG domain revealed that BAG2 does not adopt the canonical three-helix bundle and instead forms a dimeric structure with each monomer consisting of only two long antiparallel helices [96]. Due to these structural differences, the BAG2 residues responsible for binding Hsp70 are different than the BAG1-Hsp70 interface. These differences and how they might be exploited to develop BAG2 specific modulators will be discussed in Chapter 5.

In regards to BAG2's NEF duties, like BAG1, BAG2 regulation of Hsp70 function has substrate specific consequences. While BAG2 has been shown to stabilize various Hsp70 clients (CFTR, PINK1, SCA3) [97-99] and prevent their proteasomal degradation, it has also been shown to increase the proteasomal degradation of tau in an ubiquitin-independent manner [99]. These mostly protective roles of BAG2 suggest compounds that promote Hsp70-BAG2 association could be clinically relevant.

1.3.3.3 BAG3

BAG3 is one of the largest BAG proteins and contains multiple protein-protein interaction (PPI) motifs. On top of its BAG domain, BAG3 also has a WW domain for PPxY protein binding [100], multiple PXXP motifs allowing association with SH3 proteins [101], and two IPV motifs used for small heat shock protein (sHsp) binding [102-107] (Figure 1.4). Despite having these various PPI regions, BAG3 has little predicted structure outside of its BAG domain. This is consistent with experimental evidence that BAG3 has a large hydrodynamic radius, a low sedimentation coefficient, high susceptibility to proteolysis, and elutes early on size exclusion columns [103]. The intrinsic disorder of BAG3 may be important for its role as a scaffolding protein and this will be discussed further in Chapter 4.

BAG3 has gained a lot of attention in the last few years, both for its integral role in basic cell biology functions like autophagy, as well as for its ever growing list of disease relevant functions and mutations. In a series of remarkable papers, it has been shown that BAG3 is essential for selective autophagy of misfolded proteins [104-109]. The association of BAG3 with dynein allows Hsp70 substrates, both ubiquitinated and non-ubiquitinated, to be targeted to aggresomes. This has been investigated for multiple substrates including mutant SOD1 [107], α-synuclein [102], and polyQ-huntingtin [108]. Aggresome targeting is dependent on BAG3 function and BAG3 knockout cells are unable to clear these protein aggregates [109]. Indeed, in astrocytes affected by protein aggregation diseases BAG3 has been shown to be upregulated [110]. However, it is still unclear if upregulation of BAG3 during late stages of neurodegeneration will be effective for decreasing disease severity, or if BAG3 is only effective for clearing acute forms of stress damage.

In striated skeletal muscle and cardiac tissue BAG3 function is critical. BAG3 is highly expressed in these muscle cells and is integral to the maintenance of Z-discs [111]. Consistent with this BAG3 null mice display no phenotype during development, but postnatally show degenerated muscle growth and die before week 4 of age [112]. In humans, a whole suite of BAG3 mutations have been reported to cause various forms of myopathy, a majority of which fall into known PPI regions of BAG3 [113].

In comparison to other BAG proteins, BAG3 is unique in that it is the only member induced under stress conditions, mainly through activation of heat shock factor 1 (HSF1) [114-118]. HSF1 is required for tumor initiation and maintenance in a variety of cancer models, which suggests a role for BAG3 in tumor formation [115]. In support of this notion, it has been shown that the BAG3-Hsp70 complex stabilizes a number of key oncogenes, suppressing apoptosis [116-120]. Accordingly, silencing of BAG3 in multiple tumor lines sensitizes the cells to chemotherapy, suggesting that the BAG3-Hsp70 complex is an especially

attractive cancer drug target [119]. Work towards inhibiting the BAG3-Hsp70 interaction will be discussed in Chapter 3.

1.4 Analysis and Prospectus

There are compelling reasons to target the PPIs between Hsp70 and its co-chaperones. These contacts help shape Hsp70 activities and, as such, they might be targeted to re-direct the protein quality control system. Molecules that disrupt the assembly and disassembly of the Hsp70 complex might supplement other types of Hsp70 inhibitors, such as competitive inhibitors of ATP and substrate binding, providing a more complete suite of chemical probes and potential therapeutics. However, the number of PPIs in the Hsp70 complex means that there are a large number of contacts yet to be explored.

PPIs are notoriously difficult to inhibit and the specific interactions involved in binding to Hsp70 are particularly challenging, given their large buried surface areas. What strategies might be used to disrupt these contacts? Based on growing evidence from other PPI inhibitors discovery programs [121, 122], it seems likely that compounds that are able to bind to allosteric sites might be in the best position to target the types of PPIs in the Hsp70 system. Another key tool will likely be the development of HTS platforms that are specifically suited to finding inhibitors of PPIs. Recent developments in this area, including AlphaLisa, flow cytometry protein interaction assay (FCPIA) and gray box screening [121], might lower the barrier to uncovering suitable compounds. These possibilities will be explored in more detail in Chapter 3. Also, the creation of chemical libraries enriched for more complex small molecules (*e.g.* natural product-like, *etc*) may further accelerate discovery in this area [123]. A clever combination of these methods might overcome the challenges associated with targeting the Hsp70 complex.

One major question that looms large over this field is how the global proteome will respond to inhibitors of Hsp70 (both orthostatic and allosteric). This concept

has not been rigorously tested and it remains uncertain how cells will respond to different types of Hsp70 inhibitors. What will happen to protein stability and turnover when Hsp70 function is blocked or even “tuned”? The answers to this question may depend on how the molecule works (*e.g.* competitive inhibitor of ATP binding, allosteric inhibitor of NEF proteins, *etc.*) and whether it is selective for specific Hsp70 paralogs. In the case of NEFs, it is still unknown whether the structural differences between the major NEF classes can be exploited to produce selective inhibitors of the various families. Similarly, can different members of the BAG family be individually targeted? Further, it isn’t yet clear how many NEF functions are dependent on Hsp70 and how many are independent. It seems likely that the only way to address these significant concerns is to develop potent inhibitors and then use them to develop empirical models.

My thesis is focused on understanding how NEFs interact with Hsp70, how these interactions could be targeted, and how inhibitors of the Hsp70-NEF contact might influence Hsp70 biology. In Chapter 2, I biochemically characterize the interactions between Hsp70 and human NEFs. In Chapter 3, I discuss the use of emerging technologies to discover inhibitors of Hsp70-NEF interactions. This work was done in close collaboration with the Kennedy laboratory. In Chapter 4, I dissect the role of BAG3 in stabilizing Hsp70-sHsp complexes. This work was done in collaboration with the Southworth, Conklin, and Kampinga laboratories. In Chapter 5, I discuss future work that will enable drug discovery in the Hsp70-NEF space and potential applications of that work. The appendix describes my work dissecting the mechanism of an Hsp70 modulator, methylene blue.

1.5 Notes

A portion of this chapter has been published as Assimon VA*, Gilles AT*, Rauch JN*, Gestwicki JE. Hsp70 protein complexes as drug targets. *Current Pharmaceutical Design*. 2013; 19(3):404-17. (*co-first authors).

1.6 References

1. Bukau, B., J. Weissman, and A. Horwich, *Molecular chaperones and protein quality control.* Cell, 2006. **125**(3): p. 443-51.
2. Frydman, J., *Folding of newly translated proteins in vivo: the role of molecular chaperones.* Annu Rev Biochem, 2001. **70**: p. 603-47.
3. Hartl, F.U., A. Bracher, and M. Hayer-Hartl, *Molecular chaperones in protein folding and proteostasis.* Nature, 2011. **475**(7356): p. 324-32.
4. Arndt, V., C. Rogon, and J. Hohfeld, *To be, or not to be--molecular chaperones in protein degradation.* Cell Mol Life Sci, 2007. **64**(19-20): p. 2525-41.
5. Kettern, N., et al., *Chaperone-assisted degradation: multiple paths to destruction.* Biol Chem, 2010. **391**(5): p. 481-9.
6. Pratt, W.B. and D.O. Toft, *Regulation of signaling protein function and trafficking by the hsp90/hsp70-based chaperone machinery.* Exp Biol Med (Maywood), 2003. **228**(2): p. 111-33.
7. Tyedmers, J., A. Mogk, and B. Bukau, *Cellular strategies for controlling protein aggregation.* Nat Rev Mol Cell Biol, 2010. **11**(11): p. 777-88.
8. Brocchieri, L., E. Conway de Macario, and A.J. Macario, *hsp70 genes in the human genome: Conservation and differentiation patterns predict a wide array of overlapping and specialized functions.* BMC Evol Biol, 2008. **8**: p. 19.
9. Mayer, M.P. and B. Bukau, *Hsp70 chaperones: cellular functions and molecular mechanism.* Cell Mol Life Sci, 2005. **62**(6): p. 670-84.
10. Bertelsen, E.B., et al., *Solution conformation of wild-type E. coli Hsp70 (DnaK) chaperone complexed with ADP and substrate.* Proc Natl Acad Sci U S A, 2009. **106**(21): p. 8471-6.
11. Bork, P., C. Sander, and A. Valencia, *An ATPase domain common to prokaryotic cell cycle proteins, sugar kinases, actin, and hsp70 heat shock proteins.* Proc Natl Acad Sci U S A, 1992. **89**(16): p. 7290-4.
12. Wang, H., et al., *NMR solution structure of the 21 kDa chaperone protein DnaK substrate binding domain: a preview of chaperone-protein interaction.* Biochemistry, 1998. **37**(22): p. 7929-40.
13. Zhu, X., et al., *Structural analysis of substrate binding by the molecular chaperone DnaK.* Science, 1996. **272**(5268): p. 1606-14.
14. Young, J.C., J.M. Barral, and F. Ulrich Hartl, *More than folding: localized functions of cytosolic chaperones.* Trends Biochem Sci, 2003. **28**(10): p. 541-7.
15. Gaestel, M., *Molecular chaperones in signal transduction.* Handb Exp Pharmacol, 2006(172): p. 93-109.
16. Mayer, M.P., et al., *Multistep mechanism of substrate binding determines chaperone activity of Hsp70.* Nat Struct Biol, 2000. **7**(7): p. 586-93.
17. Vogel, M., M.P. Mayer, and B. Bukau, *Allosteric regulation of Hsp70 chaperones involves a conserved interdomain linker.* J Biol Chem, 2006. **281**(50): p. 38705-11.

18. Chang, L., et al., *Mutagenesis reveals the complex relationships between ATPase rate and the chaperone activities of Escherichia coli heat shock protein 70 (Hsp70/DnaK).* J Biol Chem, 2010. **285**(28): p. 21282-91.
19. Ahmad, A., et al., *Heat shock protein 70 kDa chaperone/DnaJ cochaperone complex employs an unusual dynamic interface.* Proc Natl Acad Sci U S A, 2011. **108**(47): p. 18966-71.
20. Sondermann, H., et al., *Structure of a Bag/Hsc70 complex: convergent functional evolution of Hsp70 nucleotide exchange factors.* Science, 2001. **291**(5508): p. 1553-7.
21. Williamson, D.S., et al., *Novel Adenosine-Derived Inhibitors of 70 kDa Heat Shock Protein, Discovered Through Structure-Based Design.* Journal of Medicinal Chemistry, 2009. **52**(6): p. 1510-1513.
22. Massey, A.J., *ATPases as drug targets: insights from heat shock proteins 70 and 90.* J Med Chem, 2010. **53**(20): p. 7280-6.
23. Massey, A.J., et al., *A novel, small molecule inhibitor of Hsc70/Hsp70 potentiates Hsp90 inhibitor induced apoptosis in HCT116 colon carcinoma cells.* Cancer Chemother Pharmacol, 2011. **66**(3): p. 535-45.
24. Macias, A.T., et al., *Adenosine-derived inhibitors of 78 kDa glucose regulated protein (Grp78) ATPase: insights into isoform selectivity.* J Med Chem, 2010. **54**(12): p. 4034-41.
25. Rodina, A., et al., *Identification of an allosteric pocket on human hsp70 reveals a mode of inhibition of this therapeutically important protein.* Chem Biol, 2013. **20**(12): p. 1469-80.
26. Rousaki, A., et al., *Allosteric drugs: the interaction of antitumor compound MKT-077 with human Hsp70 chaperones.* J Mol Biol, 2011. **411**(3): p. 614-32.
27. Hassan, A.Q., et al., *The Novolactone Natural Product Disrupts the Allosteric Regulation of Hsp70.* Chem Biol, 2014.
28. Cellitti, J., et al., *Small molecule DnaK modulators targeting the beta-domain.* Chem Biol Drug Des, 2009. **74**(4): p. 349-57.
29. Harrison, C., *GrpE, a nucleotide exchange factor for DnaK.* Cell Stress Chaperones, 2003. **8**(3): p. 218-24.
30. Jinwal, U.K., et al., *Chemical manipulation of hsp70 ATPase activity regulates tau stability.* J Neurosci, 2009. **29**(39): p. 12079-88.
31. Howe, M.K., et al., *Identification of an allosteric small-molecule inhibitor selective for the inducible form of heat shock protein 70.* Chem Biol, 2014. **21**(12): p. 1648-59.
32. Carrettiero, D.C., et al., *The cochaperone BAG2 sweeps paired helical filament- insoluble tau from the microtubule.* J Neurosci, 2009. **29**(7): p. 2151-61.
33. Elliott, E., P. Tsvetkov, and I. Ginzburg, *BAG-1 associates with Hsc70.Tau complex and regulates the proteasomal degradation of Tau protein.* J Biol Chem, 2007. **282**(51): p. 37276-84.
34. Souza, A.P., et al., *HspBP1 levels are elevated in breast tumor tissue and inversely related to tumor aggressiveness.* Cell Stress Chaperones, 2009. **14**(3): p. 301-10.

35. Elliott, E., O. Laufer, and I. Ginzburg, *BAG-1M is up-regulated in hippocampus of Alzheimer's disease patients and associates with tau and APP proteins.* J Neurochem, 2009. **109**(4): p. 1168-78.
36. Knoll, R., et al., *The cardiac mechanical stretch sensor machinery involves a Z disc complex that is defective in a subset of human dilated cardiomyopathy.* Cell, 2002. **111**(7): p. 943-55.
37. Nakamura, J., et al., *Targeted disruption of Hsp110/105 gene protects against ischemic stress.* Stroke, 2008. **39**(10): p. 2853-9.
38. Subjeck, J.R., et al., *Heat shock proteins and biological response to hyperthermia.* Br J Cancer Suppl, 1982. **5**: p. 127-31.
39. Ishihara, K., K. Yasuda, and T. Hatayama, *Molecular cloning, expression and localization of human 105 kDa heat shock protein, hsp105.* Biochim Biophys Acta, 1999. **1444**(1): p. 138-42.
40. Wakatsuki, T. and T. Hatayama, *Characteristic expression of 105-kDa heat shock protein (HSP105) in various tissues of nonstressed and heat-stressed rats.* Biol Pharm Bull, 1998. **21**(9): p. 905-10.
41. Easton, D.P., Y. Kaneko, and J.R. Subjeck, *The hsp110 and Grp1 70 stress proteins: newly recognized relatives of the Hsp70s.* Cell Stress Chaperones, 2000. **5**(4): p. 276-90.
42. Shaner, L., R. Sousa, and K.A. Morano, *Characterization of Hsp70 binding and nucleotide exchange by the yeast Hsp110 chaperone Sse1.* Biochemistry, 2006. **45**(50): p. 15075-84.
43. Oh, H.J., et al., *The chaperoning activity of hsp110. Identification of functional domains by use of targeted deletions.* J Biol Chem, 1999. **274**(22): p. 15712-8.
44. Mattoo, R.U., et al., *Hsp110 is a bona fide chaperone using ATP to unfold stable misfolded polypeptides and reciprocally collaborate with Hsp70 to solubilize protein aggregates.* J Biol Chem, 2013. **288**(29): p. 21399-411.
45. Oh, H.J., X. Chen, and J.R. Subjeck, *Hsp110 protects heat-denatured proteins and confers cellular thermoresistance.* J Biol Chem, 1997. **272**(50): p. 31636-40.
46. Dragovic, Z., et al., *Molecular chaperones of the Hsp110 family act as nucleotide exchange factors of Hsp70s.* EMBO J, 2006. **25**(11): p. 2519-28.
47. Goeckeler, J.L., et al., *Overexpression of yeast Hsp110 homolog Sse1p suppresses ydj1-151 thermosensitivity and restores Hsp90-dependent activity.* Mol Biol Cell, 2002. **13**(8): p. 2760-70.
48. Yamagishi, N., et al., *Characterization of stress sensitivity and chaperone activity of Hsp105 in mammalian cells.* Biochem Biophys Res Commun, 2011. **409**(1): p. 90-5.
49. Yamagishi, N., et al., *Hsp105 but not Hsp70 family proteins suppress the aggregation of heat-denatured protein in the presence of ADP.* FEBS Lett, 2003. **555**(2): p. 390-6.
50. Goeckeler, J.L., et al., *The yeast Hsp110, Sse1p, exhibits high-affinity peptide binding.* FEBS Lett, 2008. **582**(16): p. 2393-6.

51. Xu, X., et al., *Unique peptide substrate binding properties of 110-kDa heat-shock protein (Hsp110) determine its distinct chaperone activity.* J Biol Chem, 2012. **287**(8): p. 5661-72.
52. Yamagishi, N., et al., *Hsp105 family proteins suppress staurosporine-induced apoptosis by inhibiting the translocation of Bax to mitochondria in HeLa cells.* Exp Cell Res, 2006. **312**(17): p. 3215-23.
53. Yamagishi, N., Y. Saito, and T. Hatayama, *Mammalian 105 kDa heat shock family proteins suppress hydrogen peroxide-induced apoptosis through a p38 MAPK-dependent mitochondrial pathway in HeLa cells.* FEBS J, 2008. **275**(18): p. 4558-70.
54. Kai, M., et al., *Heat shock protein 105 is overexpressed in a variety of human tumors.* Oncol Rep, 2003. **10**(6): p. 1777-82.
55. Oda, T., et al., *Prognostic significance of heat shock protein 105 in lung adenocarcinoma.* Mol Med Rep, 2009. **2**(4): p. 603-7.
56. Hosaka, S., et al., *Synthetic small interfering RNA targeting heat shock protein 105 induces apoptosis of various cancer cells both in vitro and in vivo.* Cancer Sci, 2006. **97**(7): p. 623-32.
57. Dorard, C., et al., *Expression of a mutant HSP110 sensitizes colorectal cancer cells to chemotherapy and improves disease prognosis.* Nat Med, 2011. **17**(10): p. 1283-9.
58. Yam, A.Y., et al., *Hsp110 cooperates with different cytosolic HSP70 systems in a pathway for de novo folding.* J Biol Chem, 2005. **280**(50): p. 41252-61.
59. Hrizo, S.L., et al., *The Hsp110 molecular chaperone stabilizes apolipoprotein B from endoplasmic reticulum-associated degradation (ERAD).* J Biol Chem, 2007. **282**(45): p. 32665-75.
60. Saxena, A., et al., *Human heat shock protein 105/110 kDa (Hsp105/110) regulates biogenesis and quality control of misfolded cystic fibrosis transmembrane conductance regulator at multiple levels.* J Biol Chem, 2012. **287**(23): p. 19158-70.
61. Mandal, A.K., et al., *Hsp110 chaperones control client fate determination in the hsp70-Hsp90 chaperone system.* Mol Biol Cell, 2010. **21**(9): p. 1439-48.
62. Yamagishi, N., et al., *Hsp105 reduces the protein aggregation and cytotoxicity by expanded-polyglutamine proteins through the induction of Hsp70.* Exp Cell Res, 2010. **316**(15): p. 2424-33.
63. Yamashita, H., et al., *Heat-shock protein 105 interacts with and suppresses aggregation of mutant Cu/Zn superoxide dismutase: clues to a possible strategy for treating ALS.* J Neurochem, 2007. **102**(5): p. 1497-505.
64. Ishihara, K., et al., *Hsp105alpha suppresses the aggregation of truncated androgen receptor with expanded CAG repeats and cell toxicity.* J Biol Chem, 2003. **278**(27): p. 25143-50.
65. Eroglu, B., D. Moskophidis, and N.F. Mivechi, *Loss of Hsp110 leads to age-dependent tau hyperphosphorylation and early accumulation of insoluble amyloid beta.* Mol Cell Biol, 2010. **30**(19): p. 4626-43.

66. Liu, Q. and W.A. Hendrickson, *Insights into Hsp70 chaperone activity from a crystal structure of the yeast Hsp110 Sse1.* Cell, 2007. **131**(1): p. 106-20.
67. Polier, S., et al., *Structural basis for the cooperation of Hsp70 and Hsp110 chaperones in protein folding.* Cell, 2008. **133**(6): p. 1068-79.
68. Schuermann, J.P., et al., *Structure of the Hsp110:Hsc70 nucleotide exchange machine.* Mol Cell, 2008. **31**(2): p. 232-43.
69. Wilson, C.G. and M.R. Arkin, *Small-molecule inhibitors of IL-2/IL-2R: lessons learned and applied.* Curr Top Microbiol Immunol, 2011. **348**: p. 25-59.
70. DeLano, W.L., et al., *Convergent solutions to binding at a protein-protein interface.* Science, 2000. **287**(5456): p. 1279-83.
71. Wells, J.A. and C.L. McClendon, *Reaching for high-hanging fruit in drug discovery at protein-protein interfaces.* Nature, 2007. **450**(7172): p. 1001-9.
72. Raynes, D.A. and V. Guerriero, Jr., *Inhibition of Hsp70 ATPase activity and protein renaturation by a novel Hsp70-binding protein.* J Biol Chem, 1998. **273**(49): p. 32883-8.
73. Kabani, M., et al., *HspBP1, a homologue of the yeast Fes1 and Sls1 proteins, is an Hsc70 nucleotide exchange factor.* FEBS Lett, 2002. **531**(2): p. 339-42.
74. Chung, K.T., Y. Shen, and L.M. Hendershot, *BAP, a mammalian BiP-associated protein, is a nucleotide exchange factor that regulates the ATPase activity of BiP.* J Biol Chem, 2002. **277**(49): p. 47557-63.
75. McLellan, C.A., D.A. Raynes, and V. Guerriero, *HspBP1, an Hsp70 cochaperone, has two structural domains and is capable of altering the conformation of the Hsp70 ATPase domain.* J Biol Chem, 2003. **278**(21): p. 19017-22.
76. Shomura, Y., et al., *Regulation of Hsp70 function by HspBP1: structural analysis reveals an alternate mechanism for Hsp70 nucleotide exchange.* Mol Cell, 2005. **17**(3): p. 367-79.
77. Andreasson, C., et al., *Insights into the structural dynamics of the Hsp110-Hsp70 interaction reveal the mechanism for nucleotide exchange activity.* Proc Natl Acad Sci U S A, 2008. **105**(43): p. 16519-24.
78. Tzankov, S., et al., *Functional divergence between co-chaperones of Hsc70.* J Biol Chem, 2008. **283**(40): p. 27100-9.
79. Tanimura, S., et al., *Anticancer drugs up-regulate HspBP1 and thereby antagonize the prosurvival function of Hsp70 in tumor cells.* J Biol Chem, 2007. **282**(49): p. 35430-9.
80. Takayama, S., Z. Xie, and J.C. Reed, *An evolutionarily conserved family of Hsp70/Hsc70 molecular chaperone regulators.* J Biol Chem, 1999. **274**(2): p. 781-6.
81. Takayama, S., et al., *BAG-1 modulates the chaperone activity of Hsp70/Hsc70.* EMBO J, 1997. **16**(16): p. 4887-96.

82. Briknarova, K., et al., *Structural analysis of BAG1 cochaperone and its interactions with Hsc70 heat shock protein.* Nat Struct Biol, 2001. **8**(4): p. 349-52.
83. Takayama, S., et al., *Cloning and functional analysis of BAG-1: a novel Bcl-2-binding protein with anti-cell death activity.* Cell, 1995. **80**(2): p. 279-84.
84. Zeiner, M. and U. Gehring, *A protein that interacts with members of the nuclear hormone receptor family: identification and cDNA cloning.* Proc Natl Acad Sci U S A, 1995. **92**(25): p. 11465-9.
85. Yang, X., et al., *Human BAG-1/RAP46 protein is generated as four isoforms by alternative translation initiation and overexpressed in cancer cells.* Oncogene, 1998. **17**(8): p. 981-9.
86. Townsend, P.A., et al., *BAG-1: a multifunctional regulator of cell growth and survival.* Biochim Biophys Acta, 2003. **1603**(2): p. 83-98.
87. Gehring, U., *Multiple, but concerted cellular activities of the human protein Hap46/BAG-1M and isoforms.* Int J Mol Sci, 2009. **10**(3): p. 906-28.
88. Luders, J., J. Demand, and J. Hohfeld, *The ubiquitin-related BAG-1 provides a link between the molecular chaperones Hsc70/Hsp70 and the proteasome.* J Biol Chem, 2000. **275**(7): p. 4613-7.
89. Tsukahara, F. and Y. Maru, *Bag1 directly routes immature BCR-ABL for proteasomal degradation.* Blood, 2010. **116**(18): p. 3582-92.
90. Sroka, K., et al., *BAG1 modulates huntingtin toxicity, aggregation, degradation, and subcellular distribution.* J Neurochem, 2009. **111**(3): p. 801-7.
91. Mendes, F., et al., *BAG-1 stabilizes mutant F508del-CFTR in a ubiquitin-like-domain-dependent manner.* Cell Physiol Biochem, 2012. **30**(5): p. 1120-33.
92. Sharp, A., et al., *Thioflavin S (NSC71948) interferes with Bcl-2-associated athanogene (BAG-1)-mediated protein-protein interactions.* J Pharmacol Exp Ther, 2009. **331**(2): p. 680-9.
93. Enthammer, M., et al., *Isolation of a novel thioflavin S-derived compound that inhibits BAG-1-mediated protein interactions and targets BRAF inhibitor-resistant cell lines.* Mol Cancer Ther, 2013. **12**(11): p. 2400-14.
94. Xu, Z., et al., *Structural basis of nucleotide exchange and client binding by the Hsp70 cochaperone Bag2.* Nat Struct Mol Biol, 2008. **15**(12): p. 1309-17.
95. Arndt, V., et al., *BAG-2 acts as an inhibitor of the chaperone-associated ubiquitin ligase CHIP.* Mol Biol Cell, 2005. **16**(12): p. 5891-900.
96. Che, X., et al., *The BAG2 Protein Stabilises PINK1 By Decreasing its Ubiquitination.* Biochem Biophys Res Commun, 2013.
97. Che, X.Q., et al., *The BAG2 and BAG5 proteins inhibit the ubiquitination of pathogenic ataxin3-80Q.* Int J Neurosci, 2014.
98. Ulbricht, A., et al., *Cellular mechanotransduction relies on tension-induced and chaperone-assisted autophagy.* Curr Biol, 2013. **23**(5): p. 430-5.

99. Doong, H., et al., *CAIR-1/BAG-3 forms an EGF-regulated ternary complex with phospholipase C-gamma and Hsp70/Hsc70.* Oncogene, 2000. **19**(38): p. 4385-95.
100. Fuchs, M., et al., *Identification of the key structural motifs involved in HspB8/HspB6-Bag3 interaction.* Biochem J, 2010. **425**(1): p. 245-55.
101. Shemetov, A.A. and N.B. Gusev, *Biochemical characterization of small heat shock protein HspB8 (Hsp22)-Bag3 interaction.* Arch Biochem Biophys, 2011. **513**(1): p. 1-9.
102. Zhang, X. and S.B. Qian, *Chaperone-mediated hierarchical control in targeting misfolded proteins to aggresomes.* Mol Biol Cell, 2011. **22**(18): p. 3277-88.
103. Minoia, M., et al., *BAG3 induces the sequestration of proteasomal clients into cytoplasmic puncta: implications for a proteasome-to-autophagy switch.* Autophagy, 2014. **10**(9): p. 1603-21.
104. Gamerdinger, M., et al., *Protein quality control during aging involves recruitment of the macroautophagy pathway by BAG3.* EMBO J, 2009. **28**(7): p. 889-901.
105. Gamerdinger, M., et al., *BAG3 mediates chaperone-based aggresome-targeting and selective autophagy of misfolded proteins.* EMBO Rep, 2011. **12**(2): p. 149-56.
106. Xu, Z., et al., *14-3-3 protein targets misfolded chaperone-associated proteins to aggresomes.* J Cell Sci, 2013. **126**(Pt 18): p. 4173-86.
107. Carra, S., S.J. Seguin, and J. Landry, *HspB8 and Bag3: a new chaperone complex targeting misfolded proteins to macroautophagy.* Autophagy, 2008. **4**(2): p. 237-9.
108. Seidel, K., et al., *The HSPB8-BAG3 chaperone complex is upregulated in astrocytes in the human brain affected by protein aggregation diseases.* Neuropathol Appl Neurobiol, 2012. **38**(1): p. 39-53.
109. Arndt, V., et al., *Chaperone-assisted selective autophagy is essential for muscle maintenance.* Curr Biol, 2010. **20**(2): p. 143-8.
110. Homma, S., et al., *BAG3 deficiency results in fulminant myopathy and early lethality.* Am J Pathol, 2006. **169**(3): p. 761-73.
111. Norton, N., et al., *Genome-wide studies of copy number variation and exome sequencing identify rare variants in BAG3 as a cause of dilated cardiomyopathy.* Am J Hum Genet, 2011. **88**(3): p. 273-82.
112. Franceschelli, S., et al., *Bag3 gene expression is regulated by heat shock factor 1.* J Cell Physiol, 2008. **215**(3): p. 575-7.
113. Dai, C., et al., *Heat shock factor 1 is a powerful multifaceted modifier of carcinogenesis.* Cell, 2007. **130**(6): p. 1005-18.
114. Chiappetta, G., et al., *The antiapoptotic protein BAG3 is expressed in thyroid carcinomas and modulates apoptosis mediated by tumor necrosis factor-related apoptosis-inducing ligand.* J Clin Endocrinol Metab, 2007. **92**(3): p. 1159-63.
115. Jacobs, A.T. and L.J. Marnett, *HSF1-mediated BAG3 expression attenuates apoptosis in 4-hydroxynonenal-treated colon cancer cells via*

stabilization of anti-apoptotic Bcl-2 proteins. J Biol Chem, 2009. **284**(14): p. 9176-83.
116. Wang, H.Q., et al., *Inhibition of the JNK signalling pathway enhances proteasome inhibitor-induced apoptosis of kidney cancer cells by suppression of BAG3 expression.* Br J Pharmacol, 2009. **158**(5): p. 1405-12.
117. Festa, M., et al., *BAG3 protein is overexpressed in human glioblastoma and is a potential target for therapy.* Am J Pathol, 2011. **178**(6): p. 2504-12.
118. Liu, P., et al., *BAG3 gene silencing sensitizes leukemic cells to Bortezomib-induced apoptosis.* FEBS Lett, 2009. **583**(2): p. 401-6.
119. Miyata, Y., et al., *High-throughput screen for Escherichia coli heat shock protein 70 (Hsp70/DnaK): ATPase assay in low volume by exploiting energy transfer.* J Biomol Screen, 2010. **15**(10): p. 1211-9.
120. Chang, L., et al., *Chemical screens against a reconstituted multiprotein complex: myricetin blocks DnaJ regulation of DnaK through an allosteric mechanism.* Chem Biol, 2011. **18**(2): p. 210-21.
121. Brodsky, J.L. and G. Chiosis, *Hsp70 molecular chaperones: emerging roles in human disease and identification of small molecule modulators.* Curr Top Med Chem, 2006. **6**(11): p. 1215-25.

Chapter 2

Binding of Human Nucleotide Exchange Factors to Heat Shock Protein 70 (Hsp70) Generates Functionally Distinct Complexes *in Vitro*

2.1 Abstract

As introduced in Chapter 1, proteins with Bcl2-associated anthanogene (BAG) domains act as nucleotide exchange factors (NEFs) for the molecular chaperone, heat shock protein 70 (Hsp70). There are six BAG-family NEFs in humans and each is thought to link Hsp70 to a distinct cellular pathway. However, little is known about how the NEFs compete for binding to Hsp70 or how they might differentially shape its biochemical activities. Towards these questions, we measured binding of human Hsp72 (HSPA1A) to BAG1, BAG2, BAG3 and the structurally unrelated NEF, Hsp105. These studies revealed a clear hierarchy of affinities: BAG3 > BAG1 > Hsp105 >> BAG2. All of the NEFs competed for binding to Hsp70 and their relative affinity values predicted their potency in nucleotide and peptide release assays. Finally, we combined the Hsp70-NEF pairs with co-chaperones of the J protein family, DnaJA1, DnaJA2, DnaJB1 and DnaJB4, to generate sixteen permutations. The activity of the combinations in ATPase and luciferase refolding assays were dependent on the identity and stoichiometry of both the J protein and NEF, such that some combinations were potent chaperones, whereas others were inactive. Given the number and diversity of co-chaperones in mammals, these results suggest that combinatorial assembly is likely to generate a large number of distinct permutations.

2.2 Introduction

Heat shock protein 70 (Hsp70) belongs to a ubiquitous and abundant family of molecular chaperones that regulates protein quality control and homeostasis [2,

3]. Members of this family are thought to play key roles in virtually every cellular process that involves proteins, including folding, stabilization, trafficking and turnover. Accordingly, Hsp70 has become an attractive drug target for neurodegenerative and hyperproliferative disorders [2, 4]; however, it is difficult to envision strategies for selectively inhibiting its pathobiology without impacting its essential roles [4]. To help guide this process, there is an interest in better understanding how Hsp70 is recruited into its various functions.

As discussed in Chapter 1, Hsp70 is a 70 kDa protein that consists of two domains: an N-terminal nucleotide binding domain (NBD) responsible for binding and hydrolyzing ATP and a C-terminal substrate-binding domain (SBD) that binds to “client” proteins. The two domains are allosterically coupled, such that when ATP is bound to the NBD, the SBD binds weakly to clients [126]. When ADP is bound in the NBD, a conformational change enhances the affinity of the SBD for clients [2, 6]. The clients of Hsp70 include a wide range of unfolded, misfolded and partially folded proteins [7]. Indeed, Hsp70 has little ability to discriminate between polypeptide sequences [129] and it is possible that there may be few proteins (or cellular processes) that evade an interaction with Hsp70 at some stage [2].

A key insight into how Hsp70 might be able to “juggle” its multiple functions comes from studies on co-chaperones [9]. Co-chaperones, including the J proteins and the nucleotide exchange factors (NEFs), interact with Hsp70 and guide its various activities. Specifically, the J proteins are a family of co-chaperones that bind to Hsp70 in a region between the NBD and SBD [8]. This interaction stimulates ATP hydrolysis and promotes client binding [10]. In addition, some J proteins interact with clients directly; thus they are believed to recruit proteins to the Hsp70 system [11]. Conversely, the NEFs are co-chaperones that bind the NBD of Hsp70 to accelerate ADP and client release [8]. Some of the NEFs act as scaffolding proteins, linking Hsp70 and its clients to a variety of cellular pathways [11]. Thus, the co-chaperones of Hsp70 are thought

to “tune” the enzymatic activity of the chaperone and help guide its interactions with protein clients and other cellular factors.

Much of our mechanistic knowledge of Hsp70 function comes from studies using the *Escherichia coli* orthologs, which include a single Hsp70 (DnaK), a J protein (DnaJ) and a NEF (GrpE). Although the major components of the eukaryotic system are conserved, the diversity of the system has been greatly expanded through evolution. For example, the human genome contains more than 10 Hsp70s, 13 NEFs and at least 41 J proteins [11-13]. When compared to the prokaryotic system, this increase in potential partners has generated an enormous number of possible combinations. Some of the reasons for this expansion are clear; for example, there are chaperone and co-chaperone components designated for localization in the endoplasmic reticulum (ER) and mitochondria [133]. However, another pressure propelling this evolutionary expansion appears to be functional diversification. Deletion of individual, cytoplasmically expressed J protein genes in yeast often produces a phenotype [133-135], suggesting that they are not redundant [15]. In mammals, auxilin is a J protein that is exclusively dedicated to helping Hsp70 dissociate clathrin triskelions [15, 17]. Other J proteins are unable to compensate for loss of auxilin, suggesting that some co-chaperones may have “evolved” to recruit Hsp70s into specific niche functions.

This concept of functional specialization is further exemplified by the human NEFs, especially the BAG domain proteins [137]. Since the identification of BAG1 [18-20], six members of the BAG family (*i.e.* BAG1-6) have been identified based on the presence of a ~100 amino acid BAG domain. The BAG domain is thought to promote nucleotide release by binding to Hsp70’s NBD ($Hsp70_{NBD}$). This hypothesis is based on structures of human $Hsc70_{NBD}$ in complex with the BAG domains of BAG1 or BAG2, which suggest that the co-chaperones may help “open” the nucleotide-binding cleft to assist ADP dissociation [22, 84, 96]. In addition to their shared BAG domain, the members of the BAG family have

additional domains with specialized functions [138]. BAG1, for example, has an ubiquitin-like (UBL) domain that targets Hsp70 clients to the proteasome [34, 90, 91]. BAG1 also binds to the anti-apoptotic kinase, Raf1, and it works with Hsp70 to stabilize that protein in cancer [25-28]. Conversely, BAG2 has been associated with promoting the degradation of large aggregates, such as phosphorylated tau [34]. BAG3 has multiple protein-protein interaction motifs that link the Hsp70-BAG3 complex to the small heat shock proteins, the signaling molecule PLC-γ, 14-3-3 proteins and the autophagy pathway [101, 106, 108, 139]. Thus, the "choice" of which BAG protein is bound to Hsp70 appears to help determine what will happen to the Hsp70-bound client. In this context, it becomes important to understand the factors that guide the interactions between Hsp70 and these co-chaperones.

Here, we have explored how the major cytoplasmic Hsp70 family members, Hsp72 (HSPA1A) and Hsc70 (HSPA8), interact with the three BAG family members that have been most closely linked to chaperone functions: BAG1, BAG2, and BAG3. We also measured binding of Hsp72 to Hsp105α, which belongs to an evolutionary distinct group of NEFs [140]. We found that these co-chaperones have an apparent binding hierarchy of BAG3 > BAG1 > Hsp105 >> BAG2. The NEF-Hsp70 interactions were sensitive to nucleotide status, with the tightest interactions observed when Hsp72 was nucleotide-free (*e.g.* apo). All of the BAG proteins competed for binding to Hsp72 and they all accelerated nucleotide and substrate release in the relative order expected from their affinities. To understand how this hierarchical binding might influence chaperone functions, we reconstituted Hsp72 with the four NEFs and the four major cytosolic J proteins: DnaJA1, DnaJA2, DnaJB1 and DnaJB4. Using ATP hydrolysis and luciferase refolding assays, we found that some of the permutations were strongly active, whereas other combinations were inactive. These results show how the biochemical properties of mammalian Hsp70s might be diversified by combinatorial assembly with co-chaperones.

2.3 Results

2.3.1 BAG proteins prefer nucleotide-free Hsp70

To understand how BAG proteins regulate Hsp70 function, we first set out to determine how tightly they bind using two different platforms: a flow cytometry protein interaction assay (FCPIA) and isothermal titration calorimetry (ITC). In these studies, we were interested in whether BAG proteins might have similar or different affinities for Hsp70 and whether this affinity was dependent on the nucleotide status of Hsp70. Previous studies had shown that BAG1 had a better affinity for ATP-bound Hsp70 than ADP-bound Hsp70 [19, 20], but this property had not been systematically explored across all of the BAG proteins. For our FCPIA experiments, purified Hsp72 (HSPA1A) was biotinylated and immobilized on streptavidin coated polystyrene beads. Solutions of fluorescently labeled BAG proteins were then incubated with the beads and binding was detected using a flow cytometer. We found that BAG3 (11 ± 2 nM) had the tightest affinity for Hsp72 in the ATP bound form, followed by BAG1 (17 ± 6 nM) and then BAG2 (>1000 nM) (Figure 2.1). The BAG proteins had notably weaker affinity for ADP-

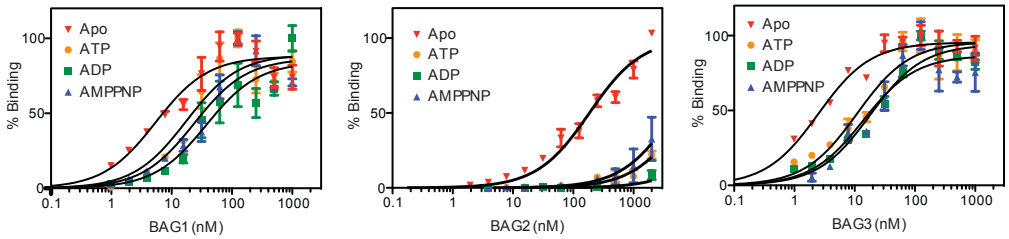

NEF	Apo	ATP	ADP	AMPPNP
BAG1	5.4 ± 1.5 nM	17 ± 6.0 nM	37 ± 12 nM	24 ± 9.0 nM
BAG2	190 ± 40 nM	>1000 nM	>1000 nM	>1000 nM
BAG3	2.5 ± 0.4 nM	11 ± 2.0 nM	18 ± 4.0 nM	14 ± 5.0 nM

Figure 2.1 Binding of Hsp72 (HSPA1A) to BAG1–3 by FCPIA. Hsp72 was immobilized on beads, and binding to fluorescent BAG1–3 was measured. Experiments were performed in triplicate on three independent days with at least two different protein preparations. A representative result is shown. Error bars represent SEM. AMPPNP, adenosine 5'-(β,γ-imino)triphosphate.

Hsp70, with BAG3 binding with a K_D of 18 ± 4 nM and BAG1 at 37 ± 12 nM. Similar results were observed when ADP was replaced with the non-hydrolyzable nucleotide analog, AMP-PNP (Figure 2.1). Surprisingly, we found that all three BAG proteins had their best affinity for apo-Hsp70, with the K_D values enhanced

~ 4 fold compared to the ATP-bound form. Together, these results demonstrated that all of the BAG proteins prefer the apo form of Hsp70 and that BAG3 binds tighter than BAG1 or BAG2.

2.3.2 BAG proteins compete for binding to Hsp70

Structural studies suggest that only one BAG protein can bind to Hsp70 at a time because they share a similar interaction surface on the NBD [20, 31]. To test this model, we labeled each of the BAG proteins with either Alexa Fluor 647 or Alexa Fluor 488 and then used the Alexa 488-labeled samples to compete with the Alexa 647-labeled samples. In the FCPIA platform, we were able to measure both the loss of the Alexa-647 signal and the increase in bound Alexa 488-labeled protein (see schematic in Figure 2.2). The advantage of this approach is that we could simultaneously measure release of the bound BAG protein and the binding of the competitor. Using this method, each BAG protein competed with itself and with the other BAG proteins (Figure 2.2). Consistent with the previous results, BAG3 was the best competitor, followed by BAG1 and then BAG2 (Figure 2.2). As a control, we attempted to displace BAG1 with the

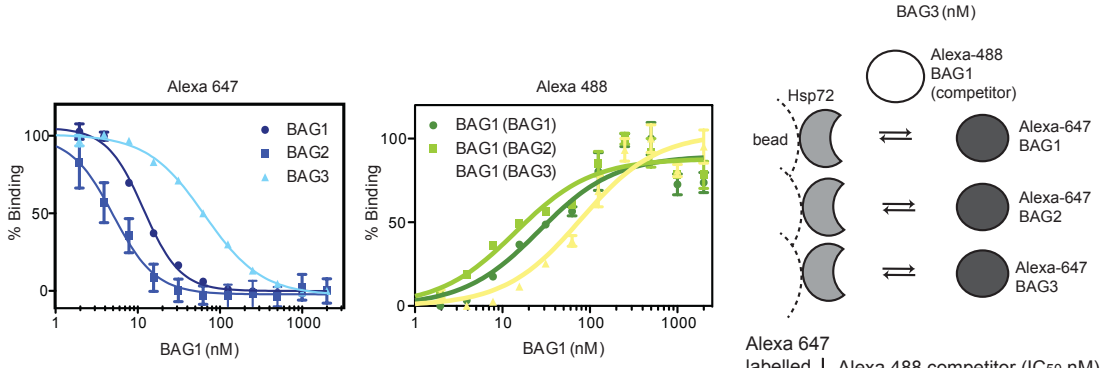

Alexa 647 labelled protein | Alexa 488 competitor (IC_{50} nM)

	BAG1	BAG2	BAG3
BAG1	24 ± 1.0	140 ± 23	15 ± 5.0
BAG2	5.1 ± 1.1	40 ± 16	1.7 ± 0.8
BAG3	65 ± 3.0	1300 ± 600	31 ± 5.0

Figure 2.2 BAG proteins compete for binding to Hsp70. Using the FCPIA platform, the relative ability of Alexa Fluor 488-labeled BAG1–3 to compete for binding with Alexa Fluor 647-labeled BAG1–3 was determined. A schematic of the method is shown. Experiments were performed in triplicate. Error bars represent SEM.

tetratricopeptide repeat (TPR) protein, CHIP. CHIP is known to bind Hsp70 in a distinct location at the C-terminus [20, 31], so it would not be expected to

interfere with binding of Hsp70 to BAG proteins. Consistent with this idea, CHIP could not compete with labeled BAG1 (Figure 2.3). To further confirm the role of nucleotide influence on BAG-Hsp70 interactions, we performed nucleotide competition experiments (Figure 2.4A) with ATP and ADP. We found that nucleotide was able to displace all the BAG proteins tested with relatively high (~10-fold excess) IC_{50} values.

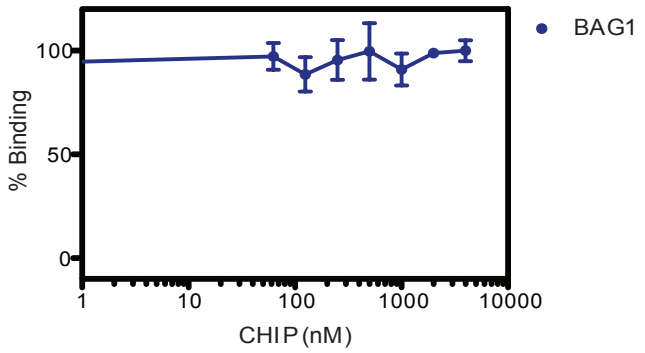

Figure 2.3 A representative TPR protein, CHIP, does not compete with BAG1 for binding to Hsp70. Results are the average of experiments in triplicate and the error bars represent SEM.

2.3.3 BAG proteins exhibit a hierarchy of binding affinities

Using ITC, we then confirmed the affinities of the BAG proteins for Hsp72 (Figure 2.4B). These binding studies were performed using the NBD of Hsp72 (residues 1-394), because this region is thought to be sufficient for binding BAG proteins [20] and it is more soluble in the ITC platform. We found that BAG3 bound apo-$Hsp72_{NBD}$ with the tightest affinity (K_D = 3.3 ± 1.0 nM), followed by BAG1 (7.7 ± 2.4 nM) and BAG2 (170 ± 40 nM). The rank order of the affinity values mirrored those obtained using full length Hsp70 in the FCPIA platform, suggesting that the NBD is indeed the only region of Hsp70 required for the interaction. To explore the minimal region of BAG1 required, we measured binding of $Hsp72_{NBD}$ to the truncated BAG domain (BAG1C; residues 107-219). The affinities of BAG1C for $Hsp72_{NBD}$ in the apo-, ATP- and ADP-bound states were uniformly weaker than the affinities of Hsp72 for full length BAG1. For example, BAG1C bound ATP-$Hsp72_{NBD}$ with an affinity of 95 ± 16 nM, while full length BAG1 bound 8-fold

(A) Nucleotides weaken BAG1-3 binding to Hsp72

NEF	ATP	ADP
BAG1	1.5 ± 0.3μM	1.5 ± 0.2μM
BAG2	1.1 ± 0.5μM	2.1 ± 0.5μM
BAG3	1.9 ± 0.8μM	0.8 ± 0.5μM
BAG1C	0.6 ± 0.3μM	0.9 ± 0.3μM

(B) Isothermal calorimetry on Hsp72 binding to BAG1-3 supports a hierarchy of affinity values

NEF	Apo	1mM ATP	1mM ADP	N
BAG1	7.7 ± 2.4 nM	12 ± 3.0 nM	36 ± 7.0 nM	0.960-1.02
BAG2	170 ± 40 nM	380 ± 110 nM	930 ± 480 nM	0.503-0.595
BAG3	3.3 ± 1.0 nM	10. ± 1.0 nM	41 ± 8.0 nM	0.927-1.02
BAG1C	29 ± 7.0 nM	95 ± 16 nM	110 ± 20 nM	0.967-0.982

Figure 2.4 Affinity of BAG1-3 for Hsp72 is dependent on nucleotide status which weaken the interaction. (A) The binding of BAG1–3 and BAG1C (100 nM) to Hsp72 was measured by FCPIA, and the inhibitory values (Ki) for ATP and ADP are shown. (B) Binding of BAG1–3 and the truncated BAG domain of BAG1 (BAG1C) to purified $Hsp72_{NBD}$ (residues 1–394) was measured by ITC. The results confirmed the relative hierarchy of affinity values. Note that BAG2 is a dimer. Thus, the N value of 0.5 suggests a complex of one BAG2 dimer per $Hsp72_{NBD}$.

tighter (12 ± 3 nM) (Figure 2.4B). These results suggest that regions outside the BAG domain contribute to binding Hsp72. Finally, the ITC studies also provided an estimate of the stoichiometry of the complexes. BAG1, BAG1C and BAG3 all yielded N values of ~1, suggesting formation of a 1:1 complex with $Hsp72_{NBD}$, while BAG2 behaved as a dimer (N ~ 0.5), consistent with previous reports [96]. Collectively, these studies revealed that BAG proteins have a hierarchy of binding to Hsp72 and that nucleotide status is important in controlling their affinity. To test whether other Hsp70 family proteins share this characteristic, we repeated the FCPIA-based binding studies with the constitutive Hsp70, termed Hsc70 (HSPA8). The results were similar to those obtained with Hsp72, with BAG3 being the tightest-binding NEF and the apo-state being the most amenable for binding BAG proteins (Figure 2.5). Thus, these features appear to be

(A) BAG1-3 binding to Hsc70 by FCPIA

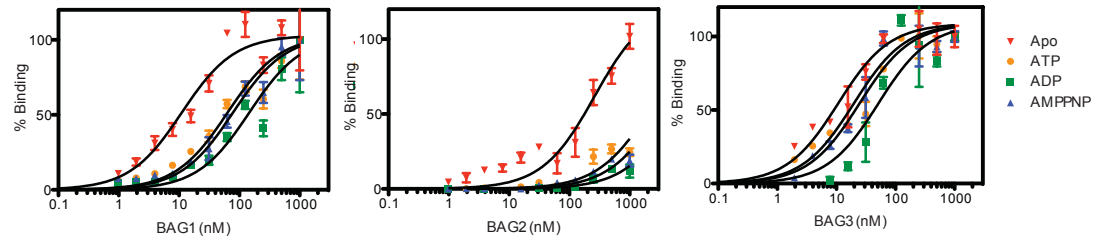

(B) Summary of affinity values

NEF	Apo	ATP	ADP	AMPPNP
BAG1	11 ± 3.0 nM	63 ± 12 nM	150 ± 30 nM	79 ± 15 nM
BAG2	260 ± 90 nM	N/A	N/A	N/A
BAG3	11 ± 3.0 nM	25 ± 6.0 nM	51 ± 13 nM	20 ± 5.0 nM

Figure 2.5. Binding of BAG1-3 to Hsc70 by FCPIA. The binding hierarchy and nucleotide dependence were similar to what was observed with Hsp72 (see Figure 2.1). Results are the average of experiments performed in triplicate and the error bars are SEM

conserved between the major cytoplasmic Hsp70 family members.

2.3.4 BAG proteins cause nucleotide dissociation from Hsp70.

Human BAG1 has been shown to promote release of nucleotide and bound client proteins from Hsp70 [83, 143, 144], but the generality of this model hasn't been tested and these activities have not been compared side-by-side to determine which BAG proteins are the most potent NEFs. Towards that goal, we employed two fluorescence polarization (FP) assays that measure release of fluorescent nucleotide (ATP-FAM) [145] and peptide substrate (HLA-FAM) [35], respectively. First, we confirmed that ATP-FAM binds Hsp72 with an apparent K_D of 1.0 ± 0.1 μM (Figure 2.6A). Using this data, we selected a concentration of Hsp72 (1 μM) and titrated with BAG proteins to determine an EC_{50} for nucleotide release. The results showed that the potency of BAG-induced nucleotide release correlated with the relative affinity values (Figure 2.6B). BAG3 was the most efficient NEF (EC_{50} = 210 ± 60 nM), followed by BAG1 and BAG2 (630 ± 190 and 1040 ± 220 nM, respectively). BAG1C also acted as a NEF (EC_{50} = 470 ± 80 nM), consistent with the importance of the BAG domain (Figure 2.6B). Interestingly, BAG1C was not substantially worse than BAG1 in this context, suggesting that any contacts outside the BAG domain are not relevant for nucleotide release. As controls, we attempted to use unrelated proteins as NEFs and found that none of them: J protein (DnaJA2), a model peptide client (NR peptide) nor bovine serum albumin (BSA) could promote nucleotide release (EC_{50} > 10,000 nM). However, ATP and ADP could compete with ATP-FAM, as expected [145]. These results show that

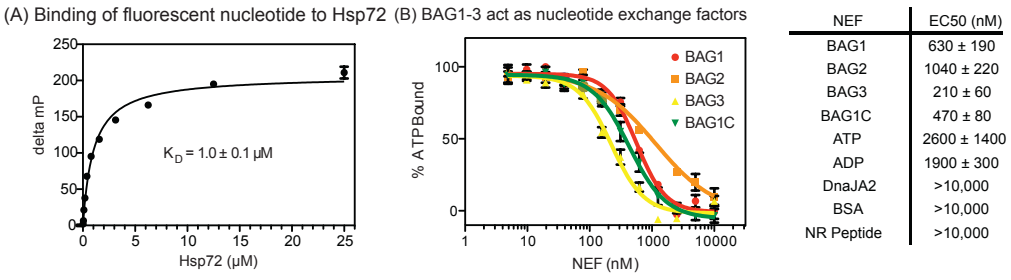

NEF	EC50 (nM)
BAG1	630 ± 190
BAG2	1040 ± 220
BAG3	210 ± 60
BAG1C	470 ± 80
ATP	2600 ± 1400
ADP	1900 ± 300
DnaJA2	>10,000
BSA	>10,000
NR Peptide	>10,000

Figure 2.6 BAG1–3 promote nucleotide release from Hsp72. (A) ATP-FAM binding to Hsp72 as measured by fluorescence polarization. Experiments were performed in triplicate. Error bars represent SEM. (B) BAG1–3 and the BAG1C domain both promote release of ATP-FAM.

BAG proteins indeed function as NEFs for Hsp70, and, in general, their relative potencies seemed to be linked to their affinities for Hsp70.

2.3.5 BAG proteins cause substrate dissociation from Hsp70

To investigate whether the BAG proteins also promote release of peptide substrates from Hsp70, we employed a fluorescently labeled model peptide (HLA-FAM) [11, 38]. Hsp72 bound the probe with a K_D of 3.3 ± 1.6 μM in the absence of added nucleotide and the affinity increased to 0.27 ± 0.05 μM in the presence of excess ADP (1 mM) (Figure 2.7A). As expected, the $Hsp72_{NBD}$ was not able to bind HLA-FAM because it lacks the SBD (Figure 2.7A). Using this platform, we titrated BAG1, BAG2, BAG3 and BAG1C into full length Hsp72 (1 μM, +1 mM ADP) and found that all of them could facilitate peptide release. In general, the relative potency values tracked with their apparent affinity values (Figure 2.7B). However, BAG1C was ~40 fold less efficient than its full-length counterpart, suggesting that regions outside the BAG domain are important for release of HLA-FAM peptide from Hsp72. The control proteins, BSA and CHIP, were unable to accelerate substrate release, whereas NR peptide directly competed with the probe, as expected (Figure 2.7B). Together, these results suggest that the BAG proteins promote release of substrates from Hsp72 and that regions outside the BAG domain might be important for this NEF activity.

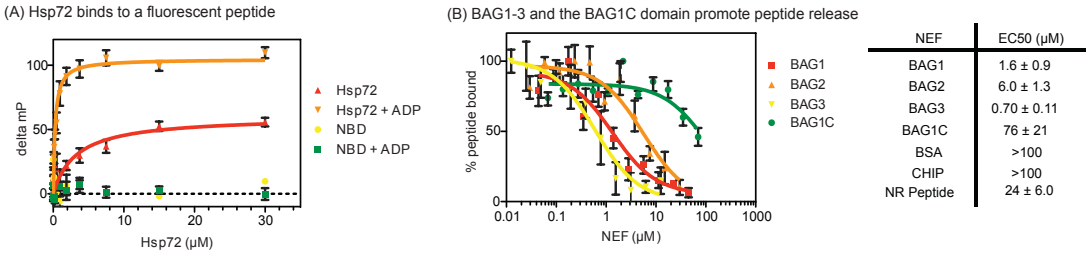

Figure 2.7 BAG1–3 promote release of peptide clients from Hsp72. (A) Binding of an HLA-FAM peptide to Hsp72 is dependent on nucleotide and the presence of the SBD, as measured by fluorescence polarization. Experiments were performed in triplicate. Error bars represent SEM. (B) BAG1–3 and the BAG1C domain stimulate peptide release, with relative potency values (EC_{50}) that mirror their relative affinities.

2.3.6 Specific ratios of BAG proteins and J proteins combine to influence Hsp70 ATPase rates.

Pioneering studies by the Young group showed that Hsp70 is only able to fold denatured luciferase when combined with the J protein, DnaJA2, but not DnaJA1 [80, 133]. These results suggest that some combinations of Hsp70 with its co-chaperones might have discreet biochemical functions *in vitro*, so we wondered how broadly this concept might be applied. The human J proteins are divided into three classes (class A, B and C) [9, 40, 41]. The four major J proteins of the cytosol include two members of class A, DnaJA1 and DnaJA2, and two members of class B, DnaJB1 and DnaJB4 [148]. Thus, to expand on the observations of the Young group, we combined Hsp72, BAG1-3 and DnaJA1, DnaJA2, DnaJB1, or DnaJB4 to generate twelve permutations. These combinations were then tested for their relative activity in functional assays that measure ATP turnover and luciferase refolding. Although there have been extensive studies on the ability of prokaryotic J proteins to promote ATP turnover [131, 149, 150], there is less known about the human J proteins. DnaJA1 and DnaJA2 are known to accelerate nucleotide hydrolysis [13, 42], but this property hasn't been explored for members of the B class and their relative potencies are not yet clear. We found that DnaJA1, DnaJA2, DnaJB1 and DnaJB4 all stimulated the steady-state ATPase activity of Hsp72, as measured by malachite green assays (Figure 2.8). The potencies of all four J proteins were similar, supporting the presumption that

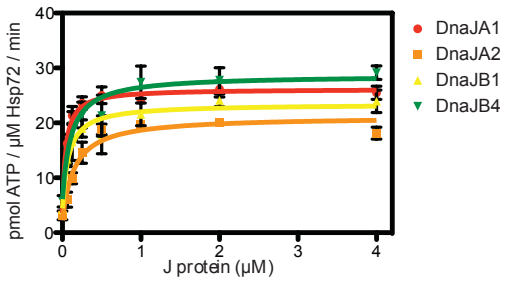

Figure 2.8 J proteins stimulate ATPase rate of Hsp70. All four human J proteins stimulate the ATPase activity of Hsp72, as measured by malachite green ATPase assays. Experiments were performed in independent triplicates and error bars represent SEM.

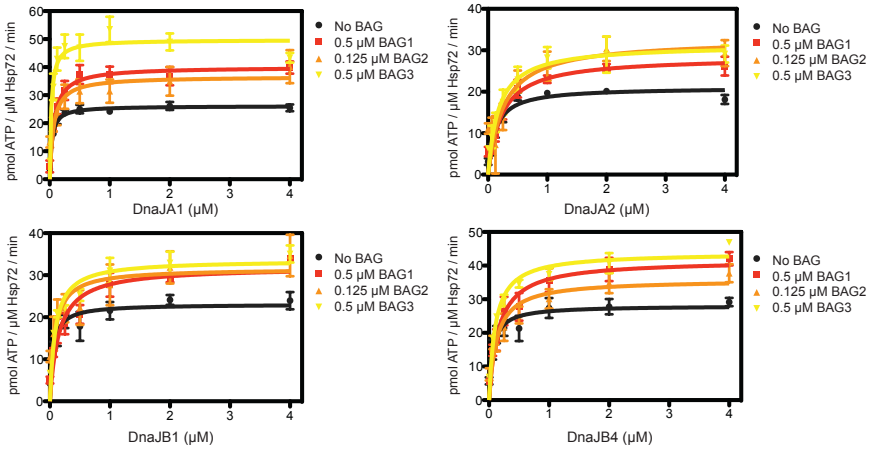

Figure 2.9 BAG proteins stimulated ATP turnover at low levels. Low, substoichiometric levels of BAG proteins promoted the ATPase activity of various Hsp72-J protein pairs. All experiments were performed in independent triplicates. Error bars represent SEM. Only representative BAG concentrations are shown, and the full dataset can be found in Figure 2.11.

they interact with Hsp72 through their highly conserved J domain in a similar manner [32, 43, 44]. None of the BAG proteins strongly stimulated the ATPase rate of Hsp72 in the absence of J protein (Figure 2.11), consistent with previous reports for a subset of these proteins [143, 152, 153]. Using this benchmark, we then titrated Hsp72 (1 µM) with the four J proteins and the three BAG proteins and measured ATP turnover. We found that low, substoichiometric

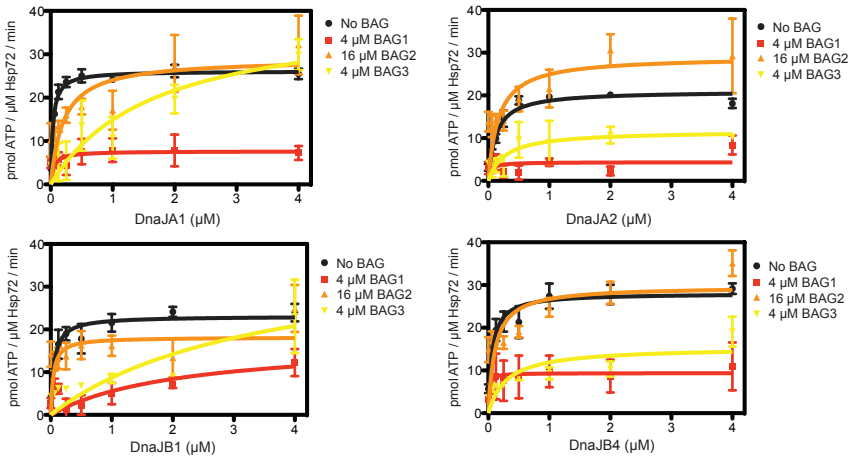

Figure 2.10 BAG proteins inhibited ATP turnover at suprastoichiometric levels. High levels of BAG proteins inhibited the ATPase activity of various Hsp72-J protein pairs. All experiments were performed in independent triplicates. Error bars represent SEM. Only representative BAG concentrations are shown, and the full dataset can be found in Figure 2.11.

concentrations of each BAG (e.g 0.125-0.5 μM BAG) could promote the ATPase activity of each of the Hsp72-J protein pairs (Figure 2.9 and Figure 2.11). Increasing the levels of the BAG proteins (e.g. 4 μM-16 μM BAG) tended to switch this behavior (Figure 2.10 and Figure 2.11). Specifically, high levels of the BAG proteins tended to inhibit ATPase activity, perhaps because they stabilize the apo form of Hsp72. However, in the case of BAG2, the extent of ATPase inhibition was dependent on the identity of the J protein. For example, BAG2 (16 μM) inhibited the ATPase activity of the Hsp72-DnaJA1 system, but it was synergistic with the Hsp72-DnaJA2 pair and it was neutral for the Hsp72-DnaJB4 pair (Figure 2.10). Together (Figure 2.11), these results provide evidence for specific combinations of Hsp72 and its co-chaperones acting as biochemically distinct complexes.

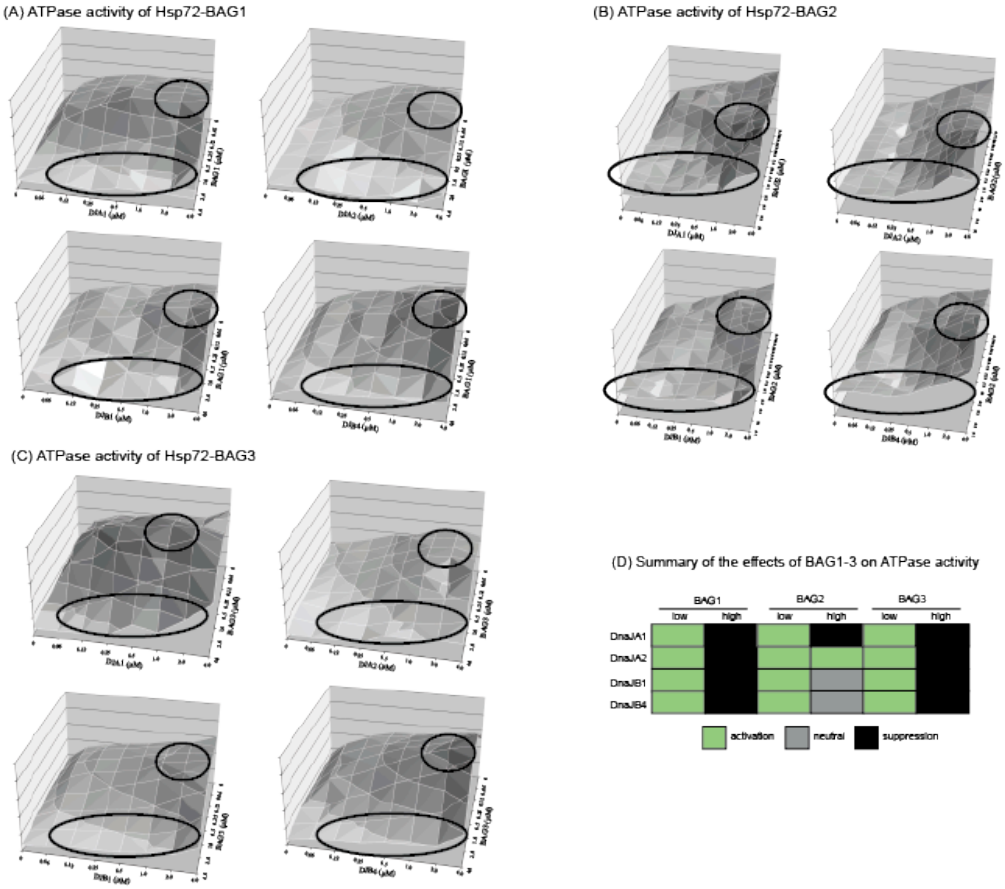

Figure 2.11 Hsp72 and its co-chaperones combine to shape ATPase activity. Hsp72 (1μM) was incubated with J proteins and (A) BAG1, (B) BAG2, or (C) BAG3. All results are the average of independent experiments performed in triplicate. For representative curves (circled regions) and error analysis, see Figure 2.9 and 2.10. The y-axis is pmol ATP/ μM Hsp72 / min. (D) Schematic summary of ATPase results

2.3.7 Combinations of Hsp72, J proteins and BAGs generate complexes with distinct chaperone functions.

The ability of Hsp70 to refold denatured clients, such as firefly luciferase, is a convenient *in vitro* method for estimating chaperone function. Hsp70 typically requires ATP and a J protein for this activity [11, 38] and BAG1 has been shown to inhibit refolding in some studies [80]. However, a systematic approach (in which the identity and stoichiometry of the co-chaperones is varied) has not been reported. Towards that goal, we titrated Hsp72 with J proteins and BAGs and tested the ability of each permutation to rescue denatured firefly luciferase, as measured by recovered luminescence. Consistent with previous reports [46], DnaJA1 was unable to promote luciferase folding by Hsp72 (1 μM) at any concentration tested (Figure 2.12). Addition of BAG proteins was unable to rescue this defect, suggesting that DnaJA1 is not competent for client folding even in the presence of NEFs. DnaJA2 and DnaJB4 both promoted refolding with maximal activity between 0.5 and 1.0 μM (Figure 2.12), while DnaJB1 was slightly less potent (maximal activity at 1.0 to 2.0 μM). Thus, although all of the J proteins are able to stimulate nucleotide hydrolysis to an identical extent, they

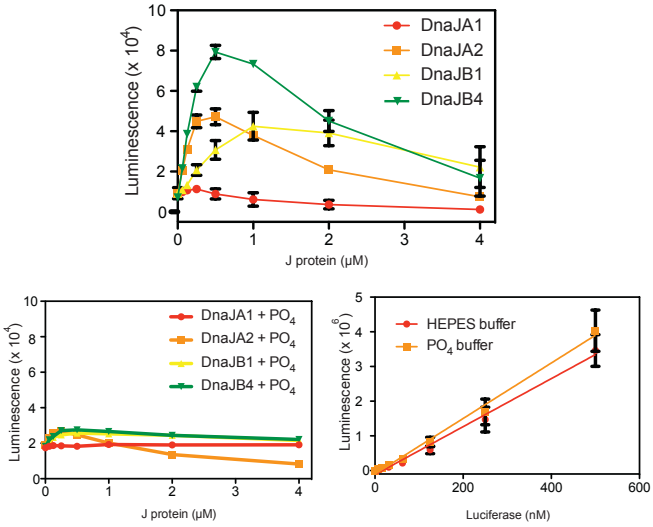

Figure 2.12 J proteins have differing abilities to work with Hsp72 in refolding denatured luciferase. Individual J proteins have different profiles of luciferase refolding that is suppressed in the presence of phosphate (10 mM). The presence of phosphate (10 mM) did not influence the luminescence signal, as shown by the standard curve. Experiments were performed in triplicate. Error bars represent SEM.

vary in their ability to promote folding. This result is consistent with the idea that ATPase rate and the extent of client refolding are not directly linked [46]. At higher concentrations of J proteins, refolding was inhibited, likely because the J proteins bind to luciferase and interfere with the folding process [46]. Previous work has shown that ATPase and refolding rates of the Hsp70 system can be affected by the presence of physiological concentrations of inorganic phosphate (Pi) [46]. Indeed when 10 mM Pi was added to the system we saw a dramatic reduction in the J protein-mediated refolding effect (Figure 2.12), which has been previously attributed to a 5-fold decrease in ADP dissociation [22-28]. When we examined the combined effects of J proteins and BAG1-3 with and without Pi present, we found that each combination was best described by its own, individualized activity profile. For example, in the absence of Pi low levels of BAG1, BAG2 or BAG3 suppressed refolding by the Hsp72-DnaJA2 pair, while these same levels of BAG1 and BAG3 could stimulate the refolding activity of the Hsp72-DnaJB1 pair (Figure 2.13 and Figure 2.14). Thus, certain BAG proteins worked synergistically with some J proteins but not others. In addition, the stoichiometry of the BAG proteins appeared to be important. This result had been suggested by previous work on BAG1 [155] and our results suggest that it is a general property. For example, low concentrations (0.05 to 0.1 μM) of BAG3 enhanced the activity of the Hsp72-DnaJB1 pair, while higher levels of BAG3 (>

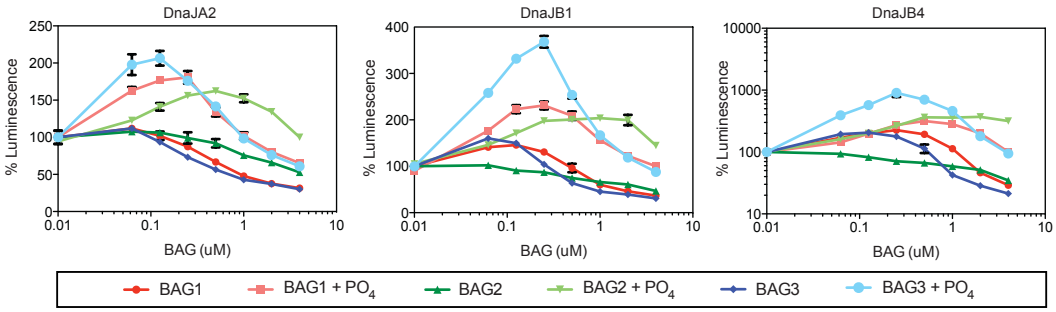

Figure 2.13 BAG1-3 either promote or inhibit luciferase refolding, depending on their concentration, the identity of the J protein, and the presence of Pi. Mixtures of Hsp72, J proteins, and BAG1–3 were used to refold luciferase. See Figure 2.14 for the full results. For clarity, only the effects of varying BAG1–3 in the presence and absence of 10 mM phosphate are shown. J protein concentrations were 0.5 μM DnaJA2, 2 μM DnaJB1, and 1 μM DnaJB4. All experiments were performed in independent triplicates. Error bars represent SEM. The y-axis is normalized so that 100% luminescence is the amount of signal observed in the absence of NEF.

0.5 μM) were strongly inhibitory (Figure. 2.13 and Figure 2.14). In the presence of the correct J protein, BAG3 was a more potent stimulator of refolding than BAG1, while BAG2 was only inhibitory, regardless of the J protein partner (Figure 2.13 and Figure 2.14). Interestingly when the experiments were repeated in the presence of 10 mM Pi the activity profiles of each BAG were even more dramatic. The stimulation of refolding was tremendous, reaching an almost 10-fold increase in refolding for the BAG3-DnaJB4 combination (Figure 2.13). It is important to note that the luminescence values are normalized to lower values in the presence of Pi, since the J-protein stimulation is diminished as previously described above. Together, these results (Figure 2.14) suggest that only some combinations of Hsp72 and its co-chaperones are competent for folding luciferase and the presence of Pi plays an important role in both reducing J-protein mediated effects, as well as enhancing contributions from the NEFs.

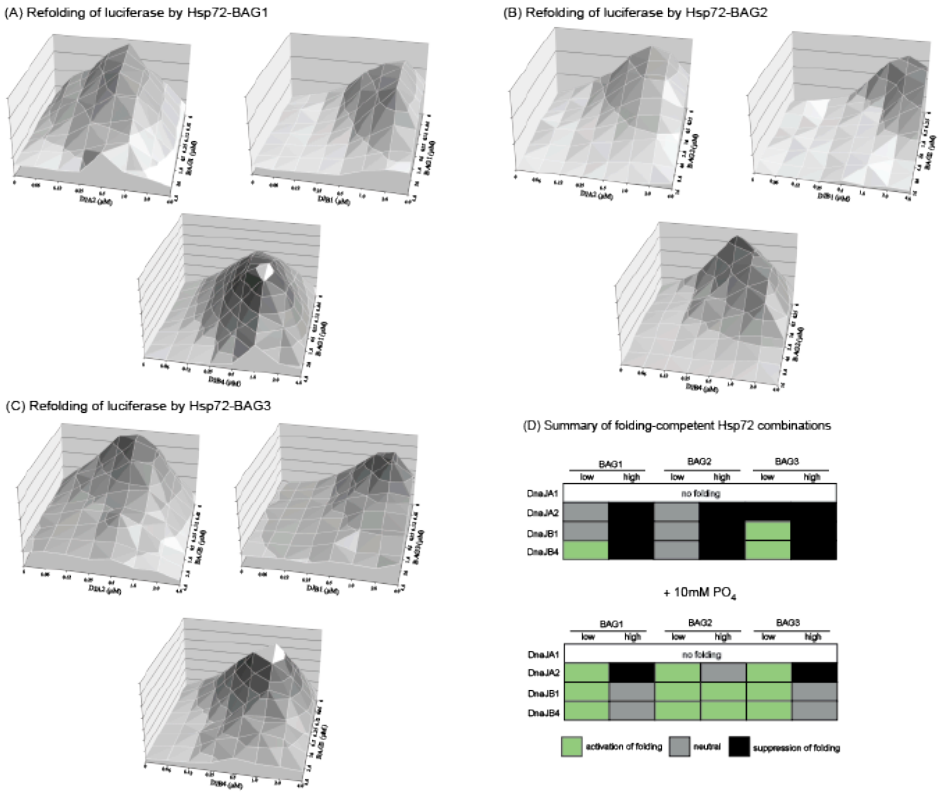

Figure 2.14 Refolding of denatured luciferase by Hsp72 combinations. Luminescence was measured after incubation of denatured luciferase with combinations of Hsp72, J proteins and (A) BAG1, (B) BAG2, or (C) BAG3. Note that DnaJA1 does not permit refolding. All results are the average of independent experiments performed in triplicate. The y-axis is raw luminescence with each tick indicating 10,000 units.

2.3.8 Hsp105 binds Hsp70 and acts as a NEF.

Thus far, we have focused on the BAG family of NEFs because individual members of the family are linked to specific biological pathways, such as cell survival, the proteasome and the autophagy system [34, 90, 91, 101, 106, 108, 139]. The Hsp110 family is an evolutionarily distinct category of eukaryotic NEFs and less is known about their biological roles. These proteins have a structure reminiscent of Hsp70, with an NBD and SBD [50]. The NBD of Hsp110s binds nucleotide [51, 52] and the SBD has affinity for peptide substrates [53]. However, members of the Hsp110 family lack the ability to refold clients [29, 53] and, rather, they have a prominent NEF function on Hsp70s [54]. Recently, human Hsp110 (termed Hsp105) has been shown to help coordinate stabilization of the cystic fibrosis conductance receptor (CFTR) [62], suggesting that this NEF function might be functionally important. However, there is little known about the biochemistry of Hsp105 and its relative position in the hierarchy of eukaryotic NEFs. The structure of a yeast Hsp110 protein (Sse1p) with yeast Hsp70 (Ssa1) shows that the surface involved in the contact is partly overlapping with that used by the BAG proteins [57], however it has yet to be shown whether these NEFs compete. To better understand Hsp105 and compare it to the BAG family of NEFs, we used our battery of assays. In the FCPIA platform, Hsp105 bound

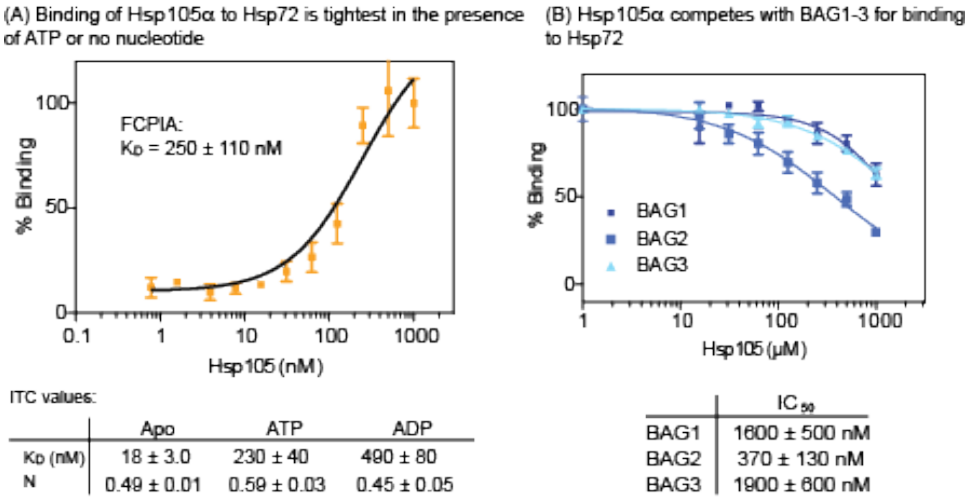

ITC values:

	Apo	ATP	ADP
KD (nM)	18 ± 3.0	230 ± 40	490 ± 80
N	0.49 ± 0.01	0.59 ± 0.03	0.45 ± 0.05

	IC50
BAG1	1600 ± 500 nM
BAG2	370 ± 130 nM
BAG3	1900 ± 600 nM

Figure 2.15 Hsp105α binds Hsp70 and competes with BAG1–3 (A) Alexa Fluor 488-labeled Hsp105α binds to the immobilized ATP-bound form of Hsp72, as measured by FCPIA. The binding to apo-, ADP-, and ATP-bound $Hsp72_{NBD}$ was confirmed by ITC. (B) Hsp105 competes with Alexa Fluor 647-labeled BAG1–3, as measured by FCPIA.

Hsp72 with an affinity of ~ 250 ± 110 nM in the presence of ATP (Figure 2.15A). Consistent with this value, Hsp105 bound ATP-Hsp72$_{NBD}$ with an affinity of 230 ± 40 nM by ITC (Figure 2.15A), suggesting that Hsp105 binds exclusively to the NBD. Similar to what we observed for BAG1-3, Hsp105 had a tighter affinity for the nucleotide free Hsp72$_{NBD}$ (K_D = 18 ± 3 nM) and binding to the ADP-bound form was substantially weaker (K_D = 490 ± 80 nM). The tight binding of Hsp105 to apo-Hsp72 was somewhat unexpected, as binding between the yeast orthologs (Sse1 and Ssa1) has been shown to require nucleotide [59]. However, there are functional differences between human and yeast Hsp105 orthologs [22], so their distinct preferences for nucleotide in Hsp72 might signify broader differences between the orthologs. Our ITC studies also suggested that Hsp105 might bind Hsp72 as a dimer, as the N values were approximately 0.5 under all the nucleotide conditions.

2.3.9 Hsp105 competes with BAG proteins for binding to Hsp70

To test if human Hsp105 could compete with BAG proteins, we immobilized Hsp72 on beads and measured binding to labeled BAG proteins. In this FCPIA platform, Hsp105 competed for binding of Hsp72 to BAG1, BAG2 and BAG3 (Figure 2.15B). Consistent with the hierarchy of binding affinities, Hsp105 was best able to compete for the weakest NEF-Hsp72 interaction (BAG2 IC_{50} 370 ± 130 nM). Like the BAG proteins, Hsp105 accelerated release of HLA-FAM (Figure 2.16A), confirming that it is a *bone fide* NEF. However, Hsp105 had the intrinsic ability to bind ATP-FAM and hydrolyze ATP (Figure 2.16B) [13], so its ability to promote nucleotide release couldn't be reliably tested. Finally, when we combined Hsp105 with Hsp72 and the four J proteins, we found that it was unable to significantly promote nucleotide hydrolysis of any of the Hsp72 combinations (Figure 2.16C), even after correcting for the intrinsic activity of Hsp105. Thus, it seems that Hsp105 accelerated client release without directly promoting ATPase activity. To test its effects in luciferase refolding experiments, we titrated Hsp105 into solutions of Hsp72 and either DnaJA2, DnaJB1 or DnaJB4. Hsp105 lacked intrinsic refolding activity, but it strongly inhibited Hsp72-

mediated refolding (Figure 2.16D) by all three J proteins. These studies show that human Hsp105 is a NEF and that it combines with Hsp70 and its other co-chaperones to expand the diversity of chaperone combinations.

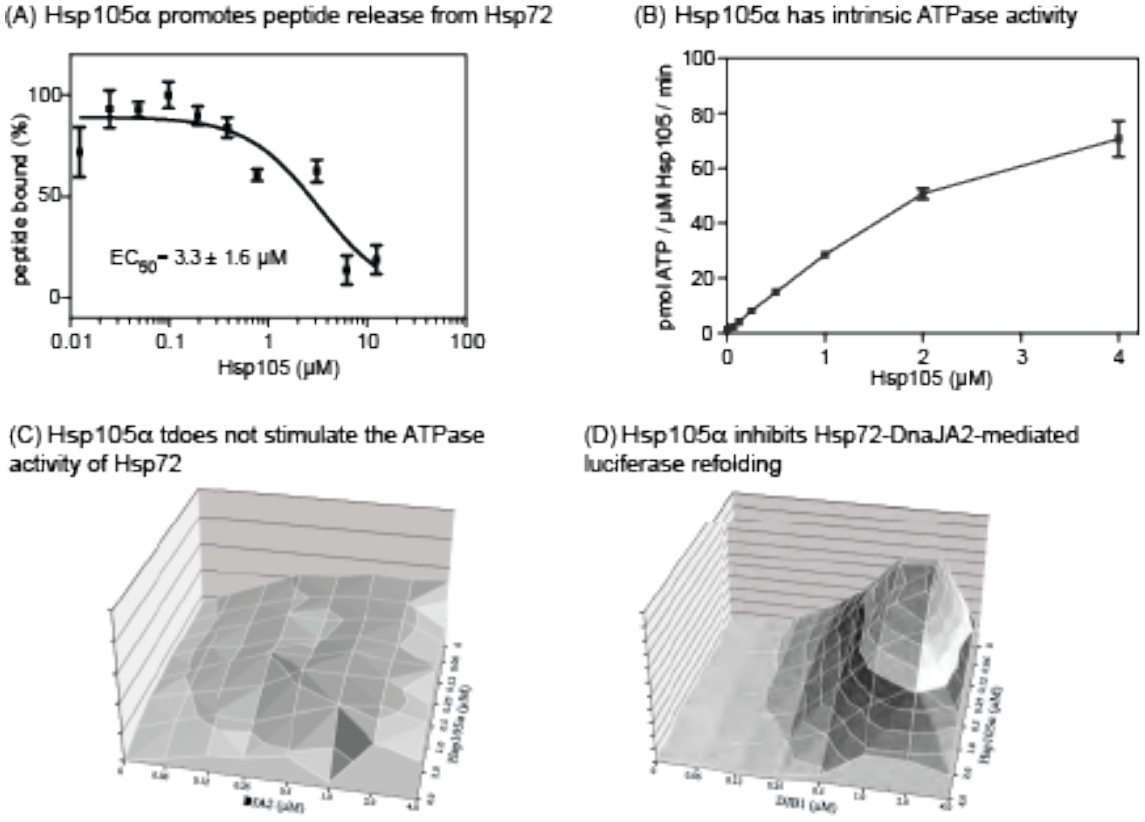

Figure 2.16 Hsp105 acts as a NEF (A) Hsp105 promotes the release of HLA-FAM peptide from Hsp72, as measured by fluorescence polarization. (B) Hsp105 has ATPase activity independently of Hsp72. This intrinsic activity was subtracted from subsequent ATPase studies. (C) Hsp105 does not appear to strongly promote the ATPase activity of Hsp72. The y-axis shows pmol ATP/μM Hsp72/min. (D) Hsp105 strongly inhibits luciferase refolding by Hsp72 and J proteins. The y-axis shows raw luminescence, with each tick representing 10,000 units. The error is ~5–10% of the value.

2.4 Discussion

In eukaryotes, expansion of the number of Hsp70 co-chaperones suggests that these proteins might have evolved specialized functions. Indeed, a number of studies in yeast and other models have supported this general concept. For example, the ER-resident Hsp70, BiP works with a specific J protein (Sec63p) to coordinate translocation of clients into the compartment, but it works with another J protein (Jem1p) to coordinate ER-associated degradation [22-24]. Likewise, the

J proteins Zuo1 and Jjj1 appear to be specialized for ribosome-associated client folding in yeast [135]. Similar to what has been observed with J proteins, NEFs appear to be associated with guiding Hsp70 into specific functional roles. BAG1 is involved in multiple processes, including proteasomal degradation [34, 90, 91], while BAG3 is linked to autophagy [11, 38] and BAG2 coordinates removal of protein aggregates [34]. These observations all suggest that Hsp70 might collaborate with (or "select") specific co-chaperones to extend its functionality in eukaryotes. A handful of studies using purified proteins have also supported the idea that co-chaperones might differentially adjust biochemical properties *in vitro*. The clearest evidence comes from the Young group, in which human DnaJA1, but not the highly related DnaJA2, was found to work with Hsp70 to refold denatured luciferase [60]. Based on these results and our own, an intriguing hypothesis is that Hsp70 complexes might not only have distinct cellular functions, but that their biochemical properties might also differentiate them.

In this study, we first characterized how the BAG1-3 and Hsp105 proteins bound human Hsp72 *in vitro*. These studies revealed a strong hierarchy of binding, with BAG3 being the tightest partner and BAG2 being the weakest. BAG3 is the only stress inducible BAG family member [62], so it is possible that this co-chaperone might effectively out-compete other NEFs under certain cellular conditions. Conversely, BAG2 is the most abundant BAG protein in non-stressed HeLa cells [61], so its concentration might partially compensate for its weaker affinity. We found that Hsp105 competes with the BAG proteins for binding to Hsp70, suggesting that only one NEF (irrespective of which class it belongs to) can bind Hsp70 at one time. Recent studies have shown that Hsp70-interacting protein (HIP) [62], Hsp70 binding protein 1 (HSPBP1) [54] and some chemical Hsp70 inhibitors [63] also converge on this same region of the NBD, suggesting that this surface is a hub for protein-protein and protein-ligand interactions. Co-evolution studies support this notion [54]. HIP binds with an affinity of ~ 8 μM by ITC [63], at least 100 to 1000-fold weaker than BAG3. It will be interesting to understand how the NEFs and other co-chaperones might use secondary interactions (*e.g.*

multivalent contacts with clients or other scaffolding proteins) to better compete for binding to the $Hsp70_{NBD}$, especially if they have relatively poor intrinsic affinities.

All of the NEFs that we tested were able to accelerate release of fluorescent peptide from Hsp72 and the BAG proteins promoted ATP-FAM release, suggesting that all of the human proteins are indeed NEFs *in vitro*. Further, all of the NEFs appeared to use a mechanism that involved stabilization of the nucleotide-free form of Hsp72. Thus, although the co-crystal structures previously suggested that they might help "open" the NBD and release ADP, our results show that all of the NEFs achieve this objective by strongly favoring the apo-form of Hsp70. Given the high levels of ATP in the cytosol of most mammalian cells, it seems possible that NEF release might be mediated, in part, through rebinding of Hsp72 to this nucleotide and subsequent weakening of the NEF-Hsp72 interaction. Indeed, we were able to show through competition with free nucleotide in the FCPIA platform, that ATP and ADP are both able to displace the NEF from Hsp72. These relative affinities provide evidence for an elegant cycle of NEF binding, driven by nucleotide exchange.

In most of our studies, the BAG domain appeared to be critical for interaction with Hsp72 and for mediating NEF activities. However, results with the BAG1C truncation suggested that peptide release, but not nucleotide release, may involve regions outside the BAG domain. Consistent with this idea, full length BAG1 also bound tighter than BAG1C. It is not currently clear how regions outside the BAG domain might interact with Hsp70s or whether other NEFs share this feature.

To study the function of the reconstituted chaperone systems, we titrated Hsp72 with the four NEFs and the four major cytosolic J proteins to generate 16 different systems. Using ATP turnover and luciferase refolding as two representative chaperone activities, we found that the identity and stoichiometry of each

component was important. Some systems, such as Hsp72 plus DnaJA1 and low levels of BAG3, were especially potent ATPase machines, while others, such as combinations of Hsp72 with DnaJA2 and high levels of BAG1, had negligible hydrolysis activity. All of the binary combinations of Hsp72 with J proteins had similar ATPase activity, so it appeared that the NEFs were the major determinant that differentiated the biochemical functions of each system. For example, the ATPase activity of Hsp72-DnaJA2 was activated by high levels of BAG2 and inhibited by BAG3 or Hsp105. However, it cannot be ignored that the identity of the J protein was important in combination with the NEF. For example, high levels of BAG3 were strongly inhibitory to Hsp72-DnaJB4 combinations, but relatively less able to act on the Hsp72-DnaJA1 pair. Thus, it was truly the combination of the chaperone and both co-chaperones that dictated the enzymatic activity of the system. This concept was even more dramatically exemplified by the results of the luciferase refolding studies. While Hsp72 could refold luciferase in collaboration with DnaJA2, DnaJB1 and DnaJB4, the NEFs were all able to suppress this activity at high concentrations. BAG3 is stress inducible, so we speculate that it might be advantageous for this protein to suppress costly refolding activity during conditions of stress. At lower concentrations of NEFs, even more interesting patterns emerged. For example, BAG1 and BAG3 could synergize with the Hsp72-DnaJB1 and Hsp72-DnaJB4 pairs, but not the Hsp72-DnaJA2 combination. When physiological concentrations of Pi were added, the NEF influence on refolding was even more exaggerated, with all NEF/J combinations now showing activation at low concentrations. These results clearly demonstrated that some permutations of Hsp72 and its co-chaperones could fold luciferase, whereas others were less capable or inactive. Thus, some chaperone combinations can indeed be differentiated by their biochemical properties, as well as their cellular functions.

It seems likely that the chaperone systems that we labeled as “inactive” are, instead, specialized for a biochemical activity that was poorly represented by our choice of *in vitro* assays. For example, none of the combinations that included

Hsp105 were able to fold luciferase in our assays, suggesting that it may assist Hsp70 with other functions, such as CFTR trafficking and quality control [64]. Based on this idea, it is intriguing to speculate that an impressive number of permutations might be generated by combinatorial assembly of human co-chaperones. Moreover, some of these systems might have emergent biochemical properties that make them specialized for a subset of Hsp70 functions.

2.5 Methods

2.5.1 Recombinant Protein Production

Human BAG1S (referred to as BAG1 throughout), BAG2 and BAG3 were subcloned into pMCSG7 from cDNA using ligation independent cloning [65] and the sequences confirmed by DNA sequencing at the University of Michigan DNA Sequencing Core. The Hsp105α construct was a kind gift from Xiaodong Wang (U. Toledo), and the BAG1C construct was a gift from Jason Young (McGill). Constructs were transformed into BL21(DE3) cells and single colonies were used to inoculate TB medium containing ampicillin (50 μg/mL). Cultures were grown at 37 °C for 5 hours, cooled to 20 °C and induced overnight with 200 μM IPTG. BAG1S, BAG1C and BAG2-expressing cells were pelleted, re-suspended in His Binding Buffer (50 mM Tris, 300 mM NaCl, 10 mM Imidazole pH 8.0) + protease inhibitor tablets (Roche), and then sonicated. Supernatants were incubated with Ni-NTA resin for 2 hours at 4 °C, washed with Binding Buffer, His Washing Buffer (50 mM Tris, 300 mM NaCl, 30 mM Imidazole pH 8.0) and finally eluted with His Elution Buffer (50 mM Tris, 300 mM NaCl, 300 mM Imidazole pH 8.0). BAG3-expressing cells were pelleted, re-suspended in BAG3 lysis buffer (50 mM Tris, 100 mM NaCl, 1mM EDTA, 15 mM β-ME, pH 8.0), sonicated, fractionated by ammonium sulfate precipitation (0-30% of saturation), re-suspended in His Binding Buffer and then applied to the Ni-NTA resin. After Ni-NTA columns, all proteins were subjected to TEV cleavage overnight and dialyzed into MonoQ Buffer A (20 mM HEPES, 10 mM NaCl, 15 mM β-ME, pH 7.6). Proteins were applied to a MonoQ column (GE Healthcare) and eluted by a linear gradient of

MonoQ Buffer B (Buffer A + 1M NaCl). Fractions were concentrated and applied to a Superdex S200 (GE Healthcare) size exclusion column in BAG buffer (25 mM HEPES, 5 mM MgCl2, 150 mM KCl pH 7.5). DnaJA1, DnaJA2, DnaJB1, and DnaJB4 were purified using a Ni-NTA column, followed by overnight TEV cleavage of the His tag and gel filtration on a Superdex S200. Hsp72, Hsp72NBD and Hsc70 were purified as described elsewhere [36]. Hsp105a was purified using Ni-NTA resin (as described above), the His tag removed by overnight incubation with TEV protease and the protein dialyzed into His Binding Buffer and then subjected to a second Ni-NTA column. The flow-through was concentrated and buffer exchanged into BAG buffer.

To make apo-Hsp72, the protein underwent extensive dialysis; day one (25 mM HEPES, 100 mM NaCl, 5 mM EDTA pH 7.5), day two (25 mM HEPES, 100 mM NaCl, 1 mM EDTA pH 7.5), day three (25 mM HEPES, 5 mM MgCl2, 10 mM KCl pH 7.5). NEFs were labeled with Alexa Fluor® 488 5-SDP ester or Alexa Fluor® 647 NHS ester (Life Technologies) according to the suppliers instructions. Hsp72 was biotinylated using EZ-link NHS-Biotin (Thermo Scientific) according to the supplier instructions. After labeling, the proteins were subjected to gel filtration to remove any unreacted label. Average label incorporation was between 0.5 and 2.0 moles of label per mole of protein, as determined by measuring fluorescence and protein concentration (A_{max} x MW of protein / [protein] x ε_{dye}).

2.5.2 Flow Cytometry Protein Interaction Assay

The assay procedure was adopted from previous reports [66, 67]. Briefly, biotinylated Hsp72 was immobilized (1h at room temperature) on streptavidin coated polystyrene beads (Spherotech), with nucleotide (1 mM) present where indicated. After immobilization, beads were washed to remove any unbound protein and then incubated with labeled NEF protein at indicated concentrations with nucleotide where noted. Binding was detected using an Accuri™ C6 flow cytometer to measure median bead-associated fluorescence. Beads capped with

biocytin were used as a negative control, and non-specific binding to beads was subtracted from signal.

2.5.3 Isothermal Titration Calorimetry.

NEFs and $Hsp72_{NBD}$ were dialyzed overnight against ITC buffer (25 mM HEPES, 5 mM MgCl2, 10 mM KCl pH 7.5). Concentrations were determined using a BCA Assay (Thermo Scientific), and the experiment was performed with a MicroCal VP-ITC (GE Healthcare) at 25 °C. $Hsp72_{NBD}$ (100 µM) in the syringe was titrated into a 5-10 µM cell solution of NEF protein. Calorimetric parameters were calculated using Origin® 7.0 software and fit with a one-site binding model.

2.5.4 Fluorescence Polarization Assays.

A fluorescent ATP analogue, N6-(6-Amino)hexyl-ATP-5-FAM (ATP-FAM) (Jena Bioscience) was used to measure NEF induced nucleotide dissociation from Hsp72. In black, round-bottom, low-volume 384-well plates (Corning), 1 µM Hsp72 and 20 nM ATP-FAM were incubated with varying concentrations of BAG protein for 10 minutes at room temperature in assay buffer (100 mM Tris, 20 mM KCl, 6 mM MgCl2 pH 7.4). After incubation fluorescence polarization was measured (excitation: 485 nm emission: 535 nm) using a SpectraMax M5 plate reader. For substrate binding/dissociation a commercially available fluorescent peptide FAM-HLA (Anaspec), was used as described [146]. Briefly, 1 µM Hsp72 and 25 nM FAM-HLA were incubated with varying concentrations of BAG protein for 30 minutes at room temperature in assay buffer (100 mM Tris, 20 mM KCl, 6 mM MgCl2 pH 7.4). After incubation, fluorescence polarization was measured (excitation: 485 nm emission: 535 nm) using a SpectraMax M5 plate reader.

2.5.5 Malachite Green ATPase Assay.

Experiments were performed according to previous protocols [68]. Briefly, Hsp72 (1µM) and various concentrations of NEF and/or J protein were added to clear 96 well plates and the reactions initiated with the addition of ATP (1 mM). The reactions proceeded for 1 h at 37 °C, developed with Malachite Green Reagent,

quenched with sodium citrate, and plate absorbance was measured at 620nm. A phosphate standard curve was used to calculate pmol ATP/μM Hsp72/min.

2.5.6 Luciferase Refolding Assay.

Experiments were performed as described previously [164]. In brief, luciferase (Promega) was denatured in 6 M GnHCl for 1 h at room temperature, and then diluted into a working solution of Hsp72 in buffer containing an ATP regenerating system (23 mM HEPES, 120 mM KAc, 1.2 mM MgAc, 15 mM DTT, 61 mM creatine phosphate, 35 U/ml creatine kinase, 5 ng/μL BSA pH 7.4). Various concentrations of NEF and J protein were added and the reaction initiated with the addition of ATP (1 mM). When indicated 10mM Pi was included in each well. Assay proceeded for 1 h at 37 °C in white, 96 well plates and luminescence measured using SteadyGlo Luminescence reagent (Promega).

2.6 Notes

A portion of this chapter has been published as **Rauch JN** and Gestwicki JE. *Binding of human nucleotide exchange factors to heat shock protein 70 (Hsp70) generates functionally distinct complexes in vitro*. Journal of Biological Chemistry. 2014; 289(3):1402-14.

2.7 References

1. Hartl, F.U., A. Bracher, and M. Hayer-Hartl, *Molecular chaperones in protein folding and proteostasis.* Nature, 2011. **475**(7356): p. 324-32.
2. Assimon, V.A., et al., *Hsp70 protein complexes as drug targets.* Curr Pharm Des, 2013. **19**(3): p. 404-17.
3. Evans, C.G., L. Chang, and J.E. Gestwicki, *Heat shock protein 70 (hsp70) as an emerging drug target.* J Med Chem, 2010. **53**(12): p. 4585-602.
4. Zhuravleva, A., E.M. Clerico, and L.M. Gierasch, *An interdomain energetic tug-of-war creates the allosterically active state in Hsp70 molecular chaperones.* Cell, 2012. **151**(6): p. 1296-307.
5. Bukau, B. and A.L. Horwich, *The Hsp70 and Hsp60 chaperone machines.* Cell, 1998. **92**(3): p. 351-66.
6. Deuerling, E., et al., *Trigger Factor and DnaK possess overlapping substrate pools and binding specificities.* Mol Microbiol, 2003. **47**(5): p. 1317-28.

7. Ahmad, A., et al., *Heat shock protein 70 kDa chaperone/DnaJ cochaperone complex employs an unusual dynamic interface.* Proceedings of the National Academy of Sciences of the United States of America, 2011. **108**(47): p. 18966-71.
8. Kampinga, H.H. and E.A. Craig, *The HSP70 chaperone machinery: J proteins as drivers of functional specificity.* Nat Rev Mol Cell Biol, 2010. **11**(8): p. 579-92.
9. Laufen, T., et al., *Mechanism of regulation of hsp70 chaperones by DnaJ cochaperones.* Proc Natl Acad Sci U S A, 1999. **96**(10): p. 5452-7.
10. Brehmer, D., et al., *Influence of GrpE on DnaK-substrate interactions.* J Biol Chem, 2004. **279**(27): p. 27957-64.
11. Bhangoo, M.K., et al., *Multiple 40-kDa heat-shock protein chaperones function in Tom70-dependent mitochondrial import.* Mol Biol Cell, 2007. **18**(9): p. 3414-28.
12. Gillies, A.T., R. Taylor, and J.E. Gestwicki, *Synthetic lethal interactions in yeast reveal functional roles of J protein co-chaperones.* Mol Biosyst, 2012. **8**(11): p. 2901-8.
13. Sahi, C. and E.A. Craig, *Network of general and specialty J protein chaperones of the yeast cytosol.* Proc Natl Acad Sci U S A, 2007. **104**(17): p. 7163-8.
14. Vos, M.J., et al., *Structural and functional diversities between members of the human HSPB, HSPH, HSPA, and DNAJ chaperone families.* Biochemistry, 2008. **47**(27): p. 7001-11.
15. Takayama, S., et al., *Cloning and functional analysis of BAG-1: a novel Bcl-2-binding protein with anti-cell death activity.* Cell, 1995. **80**(2): p. 279-84.
16. Kabbage, M. and M.B. Dickman, *The BAG proteins: a ubiquitous family of chaperone regulators.* Cell Mol Life Sci, 2008. **65**(9): p. 1390-402.
17. Zeiner, M. and U. Gehring, *A protein that interacts with members of the nuclear hormone receptor family: identification and cDNA cloning.* Proc Natl Acad Sci U S A, 1995. **92**(25): p. 11465-9.
18. Briknarova, K., et al., *Structural analysis of BAG1 cochaperone and its interactions with Hsc70 heat shock protein.* Nat Struct Biol, 2001. **8**(4): p. 349-52.
19. Sondermann, H., et al., *Structure of a Bag/Hsc70 complex: convergent functional evolution of Hsp70 nucleotide exchange factors.* Science, 2001. **291**(5508): p. 1553-7.
20. Xu, Z., et al., *Structural basis of nucleotide exchange and client binding by the Hsp70 cochaperone Bag2.* Nat Struct Mol Biol, 2008. **15**(12): p. 1309-17.
21. Doong, H., A. Vrailas, and E.C. Kohn, *What's in the 'BAG'?--A functional domain analysis of the BAG-family proteins.* Cancer Lett, 2002. **188**(1-2): p. 25-32.
22. Luders, J., J. Demand, and J. Hohfeld, *The ubiquitin-related BAG-1 provides a link between the molecular chaperones Hsc70/Hsp70 and the proteasome.* J Biol Chem, 2000. **275**(7): p. 4613-7.

23. Tsukahara, F. and Y. Maru, *Bag1 directly routes immature BCR-ABL for proteasomal degradation.* Blood, 2010. **116**(18): p. 3582-92.
24. Carrettiero, D.C., et al., *The cochaperone BAG2 sweeps paired helical filament- insoluble tau from the microtubule.* J Neurosci, 2009. **29**(7): p. 2151-61.
25. Gamerdinger, M., et al., *Protein quality control during aging involves recruitment of the macroautophagy pathway by BAG3.* EMBO J, 2009. **28**(7): p. 889-901.
26. Xu, Z., et al., *14-3-3 protein targets misfolded chaperone-associated proteins to aggresomes.* J Cell Sci, 2013. **126**(Pt 18): p. 4173-86.
27. Carra, S., et al., *HspB8 chaperone activity toward poly(Q)-containing proteins depends on its association with Bag3, a stimulator of macroautophagy.* J Biol Chem, 2008. **283**(3): p. 1437-44.
28. Doong, H., et al., *CAIR-1/BAG-3 forms an EGF-regulated ternary complex with phospholipase C-gamma and Hsp70/Hsc70.* Oncogene, 2000. **19**(38): p. 4385-95.
29. Raviol, H., et al., *Chaperone network in the yeast cytosol: Hsp110 is revealed as an Hsp70 nucleotide exchange factor.* EMBO J, 2006. **25**(11): p. 2510-8.
30. Stuart, J.K., et al., *Characterization of interactions between the anti-apoptotic protein BAG-1 and Hsc70 molecular chaperones.* J Biol Chem, 1998. **273**(35): p. 22506-14.
31. Brive, L., et al., *The carboxyl-terminal lobe of Hsc70 ATPase domain is sufficient for binding to BAG1.* Biochem Biophys Res Commun, 2001. **289**(5): p. 1099-105.
32. Hohfeld, J. and S. Jentsch, *GrpE-like regulation of the hsc70 chaperone by the anti-apoptotic protein BAG-1.* EMBO J, 1997. **16**(20): p. 6209-16.
33. Takayama, S., et al., *BAG-1 modulates the chaperone activity of Hsp70/Hsc70.* EMBO J, 1997. **16**(16): p. 4887-96.
34. Brehmer, D., et al., *Tuning of chaperone activity of Hsp70 proteins by modulation of nucleotide exchange.* Nat Struct Biol, 2001. **8**(5): p. 427-32.
35. Williamson, D.S., et al., *Novel adenosine-derived inhibitors of 70 kDa heat shock protein, discovered through structure-based design.* J Med Chem, 2009. **52**(6): p. 1510-3.
36. Cesa, L.C., et al., *Inhibitors of Difficult Protein-Protein Interactions Identified by High-Throughput Screening of Multiprotein Complexes.* ACS Chem Biol, 2013.
37. Ricci, L. and K.P. Williams, *Development of fluorescence polarization assays for the molecular chaperone Hsp70 family members: Hsp72 and DnaK.* Curr Chem Genomics, 2008. **2**: p. 90-5.
38. Tzankov, S., et al., *Functional divergence between co-chaperones of Hsc70.* J Biol Chem, 2008. **283**(40): p. 27100-9.
39. Hageman, J., et al., *The diverse members of the mammalian HSP70 machine show distinct chaperone-like activities.* Biochem J, 2011. **435**(1): p. 127-42.

40. Wittung-Stafshede, P., et al., *The J-domain of Hsp40 couples ATP hydrolysis to substrate capture in Hsp70.* Biochemistry, 2003. **42**(17): p. 4937-44.
41. Zmijewski, M.A., J.M. Kwiatkowska, and B. Lipinska, *Complementation studies of the DnaK-DnaJ-GrpE chaperone machineries from Vibrio harveyi and Escherichia coli, both in vivo and in vitro.* Arch Microbiol, 2004. **182**(6): p. 436-49.
42. Jiang, J., et al., *Structural basis of J cochaperone binding and regulation of Hsp70.* Mol Cell, 2007. **28**(3): p. 422-33.
43. Luders, J., et al., *Distinct isoforms of the cofactor BAG-1 differentially affect Hsc70 chaperone function.* J Biol Chem, 2000. **275**(20): p. 14817-23.
44. Bimston, D., et al., *BAG-1, a negative regulator of Hsp70 chaperone activity, uncouples nucleotide hydrolysis from substrate release.* EMBO J, 1998. **17**(23): p. 6871-8.
45. Szabo, A., et al., *The ATP hydrolysis-dependent reaction cycle of the Escherichia coli Hsp70 system DnaK, DnaJ, and GrpE.* Proc Natl Acad Sci U S A, 1994. **91**(22): p. 10345-9.
46. Gassler, C.S., et al., *Bag-1M accelerates nucleotide release for human Hsc70 and Hsp70 and can act concentration-dependent as positive and negative cofactor.* J Biol Chem, 2001. **276**(35): p. 32538-44.
47. Srinivasan, S.R., et al., *Molecular chaperones DnaK and DnaJ share predicted binding sites on most proteins in the E. coli proteome.* Mol Biosyst, 2012. **8**(9): p. 2323-33.
48. Easton, D.P., Y. Kaneko, and J.R. Subjeck, *The hsp110 and Grp1 70 stress proteins: newly recognized relatives of the Hsp70s.* Cell Stress Chaperones, 2000. **5**(4): p. 276-90.
49. Oh, H.J., et al., *The chaperoning activity of hsp110. Identification of functional domains by use of targeted deletions.* J Biol Chem, 1999. **274**(22): p. 15712-8.
50. Xu, X., et al., *Unique peptide substrate binding properties of 110-kDa heat-shock protein (Hsp110) determine its distinct chaperone activity.* J Biol Chem, 2012. **287**(8): p. 5661-72.
51. Yamagishi, N., et al., *Modulation of the chaperone activities of Hsc70/Hsp40 by Hsp105alpha and Hsp105beta.* Biochem Biophys Res Commun, 2000. **272**(3): p. 850-5.
52. Shaner, L., et al., *The function of the yeast molecular chaperone Sse1 is mechanistically distinct from the closely related hsp70 family.* J Biol Chem, 2004. **279**(21): p. 21992-2001.
53. Dragovic, Z., et al., *Molecular chaperones of the Hsp110 family act as nucleotide exchange factors of Hsp70s.* EMBO J, 2006. **25**(11): p. 2519-28.
54. Saxena, A., et al., *Human heat shock protein 105/110 kDa (Hsp105/110) regulates biogenesis and quality control of misfolded cystic fibrosis transmembrane conductance regulator at multiple levels.* J Biol Chem, 2012. **287**(23): p. 19158-70.

55. Schuermann, J.P., et al., *Structure of the Hsp110:Hsc70 nucleotide exchange machine.* Mol Cell, 2008. **31**(2): p. 232-43.
56. Polier, S., et al., *Structural basis for the cooperation of Hsp70 and Hsp110 chaperones in protein folding.* Cell, 2008. **133**(6): p. 1068-79.
57. Shaner, L., R. Sousa, and K.A. Morano, *Characterization of Hsp70 binding and nucleotide exchange by the yeast Hsp110 chaperone Sse1.* Biochemistry, 2006. **45**(50): p. 15075-84.
58. Raviol, H., B. Bukau, and M.P. Mayer, *Human and yeast Hsp110 chaperones exhibit functional differences.* FEBS Lett, 2006. **580**(1): p. 168-74.
59. Mattoo, R.U., et al., *Hsp110 is a bona fide chaperone using ATP to unfold stable misfolded polypeptides and reciprocally collaborate with Hsp70 to solubilize protein aggregates.* J Biol Chem, 2013. **288**(29): p. 21399-411.
60. Franceschelli, S., et al., *Bag3 gene expression is regulated by heat shock factor 1.* J Cell Physiol, 2008. **215**(3): p. 575-7.
61. Shomura, Y., et al., *Regulation of Hsp70 function by HspBP1: structural analysis reveals an alternate mechanism for Hsp70 nucleotide exchange.* Mol Cell, 2005. **17**(3): p. 367-79.
62. Chang, L., et al., *Chemical screens against a reconstituted multiprotein complex: myricetin blocks DnaJ regulation of DnaK through an allosteric mechanism.* Chem Biol, 2011. **18**(2): p. 210-21.
63. Eschenfeldt, W.H., et al., *A family of LIC vectors for high-throughput cloning and purification of proteins.* Methods Mol Biol, 2009. **498**: p. 105-15.
64. Thompson, A.D., et al., *Analysis of the tau-associated proteome reveals that exchange of Hsp70 for Hsp90 is involved in tau degradation.* ACS Chem Biol, 2012. **7**(10): p. 1677-86.
65. Blazer, L.L., et al., *Use of flow cytometric methods to quantify protein-protein interactions.* Curr Protoc Cytom, 2010. **Chapter 13**: p. Unit 13 11 1-15.
66. Chang, L., et al., *High-throughput screen for small molecules that modulate the ATPase activity of the molecular chaperone DnaK.* Anal Biochem, 2008. **372**(2): p. 167-76.
67. Miyata, Y., et al., *High-throughput screen for Escherichia coli heat shock protein 70 (Hsp70/DnaK): ATPase assay in low volume by exploiting energy transfer.* J Biomol Screen, 2010. **15**(10): p. 1211-9.
68. Wisen, S. and J.E. Gestwicki, *Identification of small molecules that modify the protein folding activity of heat shock protein 70.* Anal Biochem, 2008. **374**(2): p. 371-7.

Chapter 3

Development of a Capillary Electrophoresis Platform for Identifying Inhibitors of Hsp70-BAG3 Interactions

3.1 Abstract

To better understand the cellular functions of Hsp70-BAG complexes that were characterized in Chapter 2, we sought to identify chemical inhibitors. However, methods for identifying inhibitors of protein-protein interactions (PPIs) are often prone to the discovery of false positives, particularly those caused by molecules that induce protein aggregation. Thus, there is interest in developing new platforms that might allow earlier identification of these problematic compounds. For these reasons, we evaluated capillary electrophoresis (CE) as a method to screen for PPI inhibitors using the challenging system of Hsp70 interacting with its co-chaperone BAG3. In the method, Hsp70 is labeled with a fluorophore, mixed with BAG3, and the resulting bound and free Hsp70 separated and detected by CE with laser-induced fluorescence detection. The method used a modified CE capillary to prevent protein adsorption. Inhibitors of the Hsp70-BAG3 interaction were detected by observing a reduction in the bound to free ratio. The method was used to screen a library of 3,443 compounds and results compared to those from a flow cytometry protein interaction assay. CE was found to produce a lower hit rate with more compounds that reconfirmed in subsequent testing suggesting greater specificity. This finding was primarily attributed to two features: use of electropherograms to detect artifacts such as aggregators and differences in the way that the target proteins were modified. Increases in throughput are required to make the CE method suitable for larger primary

screens but it is attractive as a secondary screen to test hits found by higher throughput methods.

3.2 Introduction

Protein-protein interactions (PPIs) are involved in key cellular processes [165-167] and enthusiasm is growing for developing chemical inhibitors of these contacts [6]. PPIs were previously considered to be intractable drug targets, but recent successes have demonstrated that potent and selective inhibitors can indeed be found [6]. More than 100 inhibitors of PPIs have now been reported in the literature and some of these molecules have low nanomolar potency [6-9]. Interestingly, a recent analysis of known PPI inhibitors suggests that the most tractable PPI targets feature a relatively small contact area, with clear energetic "hotspots" [73]. Conversely, other PPIs have been more difficult to target, likely because they involve large, relatively flat surface areas and/or because the interactions are relatively weak [73, 170-172]. Despite these challenges, a handful of inhibitors of difficult PPIs have also been reported and it seems likely that emerging discovery methods, such as fragment-based screening, will continue to expand the categories of PPIs that are considered "druggable" [9].

Often, high throughput screening (HTS) [11] plays a critical role in the discovery of chemical PPI inhibitors. The assay platforms used for PPI targets can be divided into two general classes: those that measure binding of test molecules to one of the proteins and those that directly measure disruption of the protein-protein contact. The first class of methods relies on the idea that binding of a small molecule might potentially disrupt PPIs involving the protein target. The techniques used in this type of search include NMR, surface plasmon resonance (SPR), differential scanning fluorimetry (DSF), and *in silico* approaches. These strategies have been successful in yielding PPI inhibitors [12-18]. The alternative approach is to measure the PPI itself and then screen for compounds that inhibit the contact. Methods such as FRET, AlphaLisa, fluorescence polarization (FP) and flow cytometry protein interaction assay (FCPIA) are commonly used in this

type of paradigm. While these technologies are powerful, they suffer from high false positive rates, often from the presence of “aggregator” molecules [174]. Such compounds bind and denature a protein target causing it to aggregate. These artifacts are particularly problematic in screens of difficult PPIs because flat, poorly soluble molecules tend to interact with the relatively shallow topologies of protein-protein contacts. Likewise, intrinsically fluorescent compounds are widespread in most commercial compound libraries and fluorescent artifacts often need to be carefully removed in secondary screens. However, indiscriminate removal of all fluorescent compounds necessarily removes molecules with true potential as inhibitors (*e.g.* false negatives).

In principle capillary electrophoresis (CE) could be used to screen for modulators of PPI. A variety of CE methods have been successfully used to probe non-covalent interactions *in vitro* [175-181]. We have explored affinity probe CE (APCE) [17, 21] for this purpose. In this method, binding partners are mixed together and the mixture separated fast enough by CE that the non-covalent complex and free partners can be detected as separate peaks. Typically one of the binding partners is fluorescently labeled to allow sensitive detection by laser-

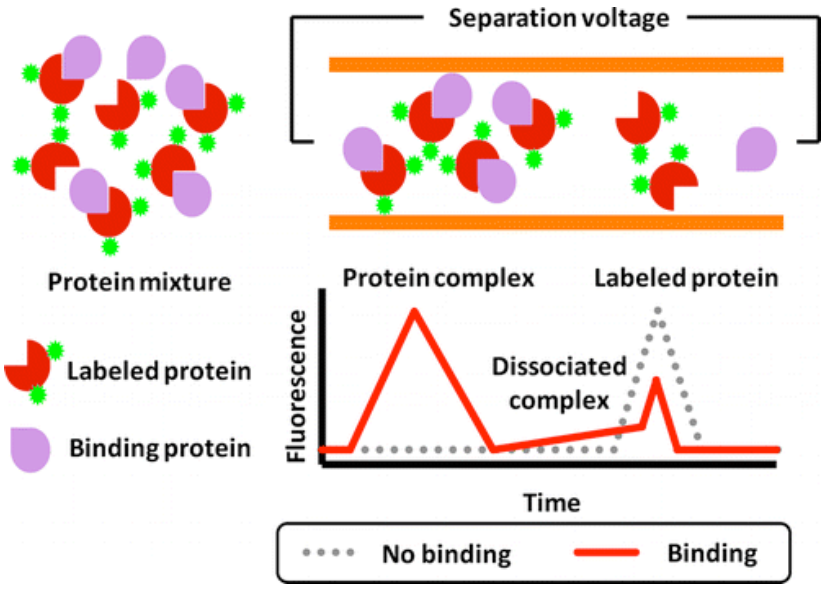

Figure 3.1 Schematic for using APCE to detect PPIs. In this method, one protein partner is fluorescently labeled, mixed with its binding partner and then separated by CE. The protein complex and free protein are distinguished by their electrophoretic mobility.

induced fluorescence (LIF) (Figure 3.1). This approach has been used in immunoassays [22-24], aptamer assays [185-187], and to detect protein aggregation [15, 27], protein-DNA [189] , protein-saccharide [18], protein-protein [181], protein-peptide interactions [189, 191, 192]. Binding inhibitors added to mixtures can be detected by observing the shift in bound to free peak areas that result in electropherograms. This has been used for competitive immunoassays [32, 33] and to detect inhibitors in small scale screens of protein-peptide interactions [194], *e.g*. SH2 domains binding to short phosphorylated peptides. Extending this approach to interactions of full proteins is of interest because many proteins do not have well-defined, linear peptide binding targets and allosteric modulation may be an important mode of interaction.

As a screening tool for the discovery of PPI inhibitors, CE has a number of potential advantages over currently used screening methods. Namely, this method might allow detection of aggregators, based on the appearance of peaks different from the complex and free affinity probe. Moreover, CE would allow separation of fluorescent test compounds from the complex to prevent interference in binding detection. This feature has the potential to identify and possibly “rescue” false negatives. CE, especially in microchip format, is also compatible with scale up to HTS based on its low sample consumption (~4 nL), fast separation speed, high degree of automation and straight forward quantification [124, 195]. Indeed, commercial systems are available that use microchip electrophoresis for screening enzymatic reactions, *e.g.* Caliper LabChip EZ reader.

The potential application of CE for screening PPIs requires addressing a number of specific technical challenges, such as the tendency of some proteins to adsorb to CE columns and difficulties with obtaining adequate resolution of bound and free protein under non-denaturing conditions. Moreover, this method has yet to be tested head-to-head with existing HTS platforms to rigorously uncover whether it has any demonstrable advantages. Finally, we consider it important to

attempt pilot studies on challenging and physiologically meaningful PPIs to meet the goal of adding CE to the arsenal of methods for meeting the specific and emerging challenges of difficult PPIs.

Here, we report the first use of CE as a PPI screening platform. As a target, we selected the PPI between heat shock protein 70 (Hsp70) and Bcl2-associated anthanogene 3 (BAG3). As discussed in Chapters 1, Hsp70 is a molecular chaperone that cooperates with BAG3 to regulate protein quality control [124]. The BAG3-Hsp70 complex stabilizes a number of key oncogenes, making it a promising anti-cancer target [116-120, 195]. However, this complex has a large predicted contact interface (>1800 $Å^2$) and work in Chapter 2 showed that it has a relatively high affinity, placing it in the category of a challenging PPI [40]. In this research, we used APCE to detect formation of the Hsp70-BAG3 complex by labeling the Hsp70 with a fluorophore. Further, by modifying the CE column we limited undesirable adsorption of Hsp70 and enabled screening of a pilot collection of 3,443 small molecules against this target. Concurrently, we screened the same library using FCPIA. A comparison between the results of these parallel screens revealed strengths and weaknesses of the HTS methods. From these studies, we conclude that CE is a promising method for finding inhibitors of PPIs and a significant advantage is that it enables early detection of aggregators.

3.3 Results

3.3.1 Development of a CE-based assay for Hsp70 binding to BAG3.

In APCE, one of the binding partners is normally labeled to allow sensitive detection of the complex by LIF. For these experiments we labeled recombinant, human Hsp70 (HSPA1A) with Alexa-488, such that there was an average of 0.5 fluorophores per protein. This modification did not affect the activity of Hsp70 as measured by comparing the ATPase activity of unmodified and labeled samples (Figure 3.2).

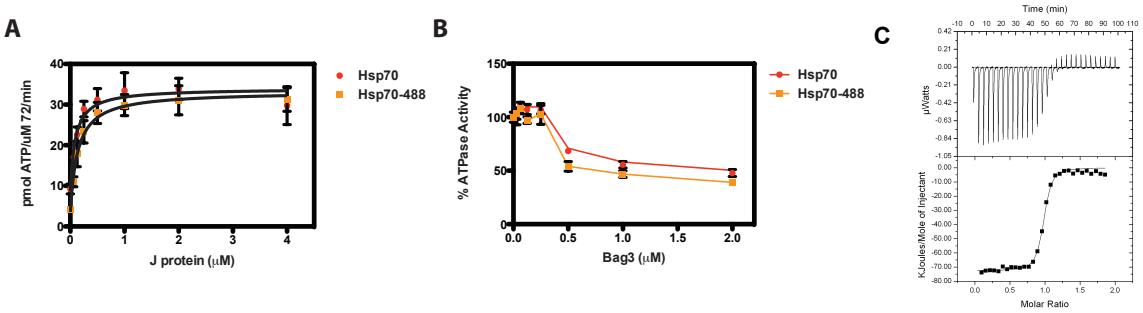

Figure 3.2 ATPase stimulation and binding to Hsp70 is unaffected by labeling. (A) ATPase stimulation by the Hsp70 co-chaperone J protein. (B) Bag3 effect on Hsp70/J protein ATPase stimulation. (C) Binding to BAG3 is unaffected by label

Initial experiments were directed at identifying separation conditions that would allow detection of Hsp70-488 and its complex with BAG3. Samples containing 0.5 μM Hsp70-488 or Hsp70-488 and BAG3 mixed at a 1:1 ratio (0.5 μM each) were analyzed by APCE. In this stage of the study, we found that the biggest challenge was BAG3 adsorption. For example, when using unmodified fused silica for the CE capillary, the Hsp70-488 peak was detected and it decreased upon addition of BAG3; however, no complex peak was detected (Figure 3.4A). To prevent adsorption, the capillary surface was modified using a perfluorinated silane and 0.01% (w/v) Tween-20 was added to the electrophoresis buffer [41] (Figure 3.3). Using these modifications, the mixture of labeled Hsp70 and unlabeled BAG3 was readily observed as two individual bands with migration

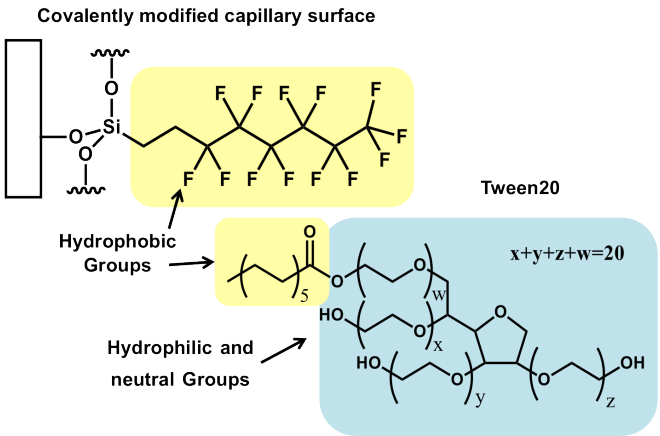

Figure 3.3 Modification of capillary surface. The capillary surface was modified with perfluorinated silane to prevent BAG3 absorption. Tween-20 (0.01%) was also added to the electrophoresis buffer.

times of 96 and 122 s, corresponding to the complex and the free Hsp70 respectively (Figure 3.4B). A “bridge” is observed between the complex and free peak, which is attributed to Hsp70-488 that dissociated during separation (Figure 3.4B).

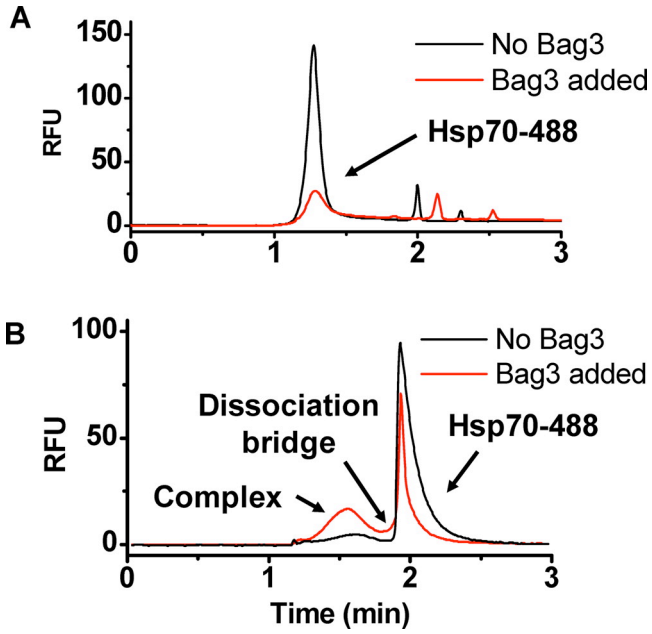

Figure 3.4 Electropherograms of Hsp70-488 with and without BAG3 added using (A) bare silica capillary; (B) PFOTCS modified capillary. Free Hsp70-488 decreases with added Bag3 in (A), but no complex peak is detected suggesting adsorption induced by BAG3. A complex peak with dissociation, forming a bridge to the free Hsp70-488, is observed with the modified capillary. Separations were performed at 500 V/cm through 10 cm effective length. 0.5 psi was applied to drive flow and decrease analysis time.

To evaluate whether this method could faithfully recapitulate the known affinity of the Hsp70-BAG3 complex, we titrated BAG3 into Hsp70-488 and measured formation of the complex by CE. The peak area of complex plus “bridge” increased as a function of BAG3 concentration (Figure 3.5A). Plotting this peak area against BAG3 concentration and using a non-linear regression yielded a binding constant of 23 ± 8 nM (Figure 3.5B), which is in good agreement with affinities obtained in Chapter 2, as well as the ~15 nM KD obtained from isothermal titration calorimetry (ITC) (Figure 3.2C).

To confirm that the peak attributed to complex was in fact Hsp70-BAG3 and demonstrate that we could detect inhibition of this complex, we performed

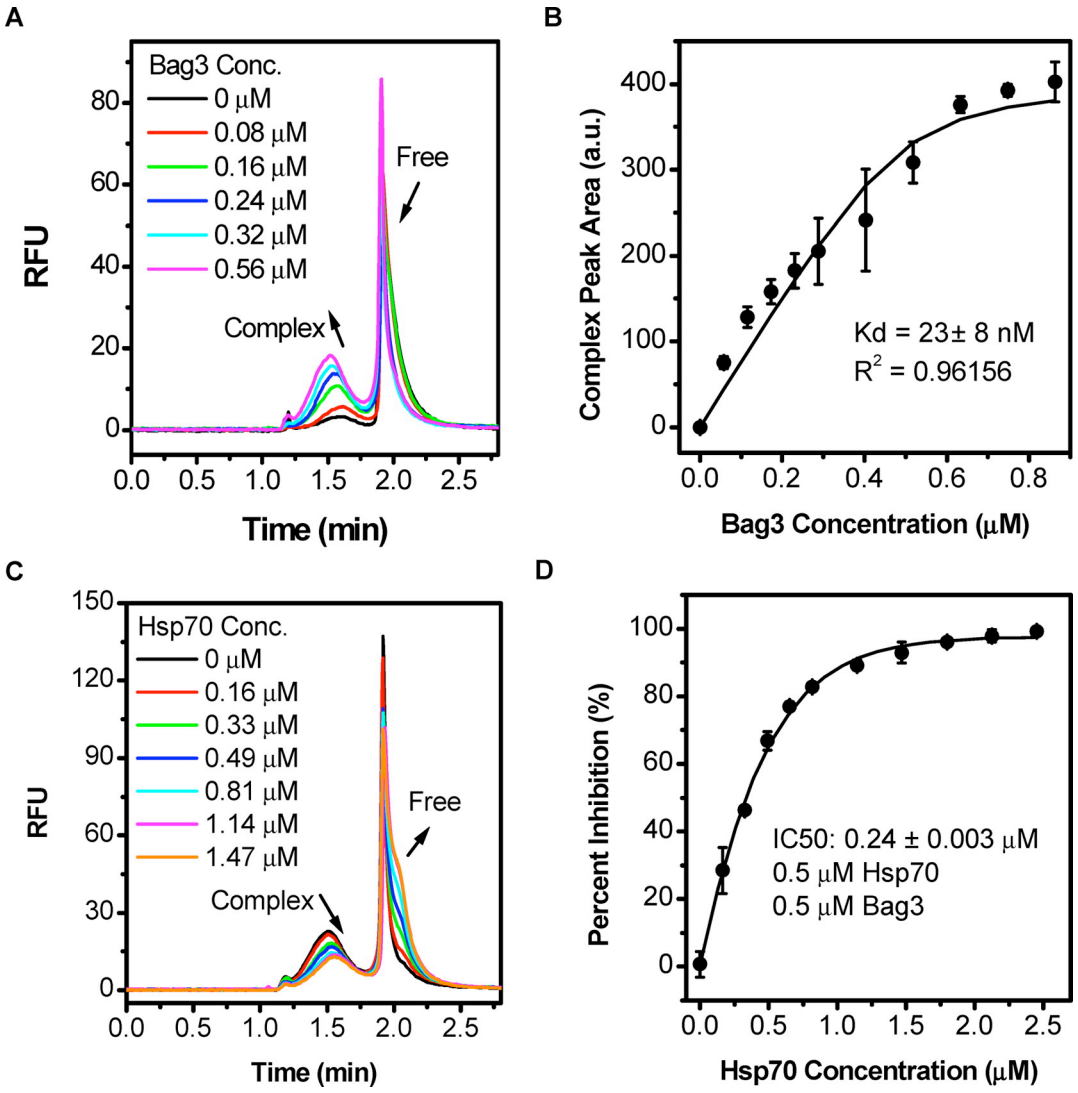

Figure 3.5 Determination of dissociation constant (K_d) and IC_{50} of binding by CE-LIF. (A) Electropherograms of 0.5 μM Hsp70 with increasing concentrations of BAG3; (B) Saturation curve from the titration experiments in Figure 3.4 by plotting the peak area of complex and dissociation bridge against BAG3 concentration. Non-linear regression determined the K_d to be 23 ± 8 nM. (C) Electropherograms of 0.5 μM Hsp70 and BAG3 with increasing concentration of unlabeled Hsp70. (D) Peak area ratio (bound to free)'s response to increasing Hsp70 concentration. IC_{50} can be determined for unlabeled Hsp70 to be 0.240 ± 0.003 μM.

competition experiments in which unlabeled Hsp70 was added at different concentrations to the Hsp70-488 and BAG3 mixture. These experiments showed that the complex peak decreased with added Hsp70, confirming the identity of the peak. Analysis of the data yielded an IC_{50} of 0.24 μM (Figure 3.5D), suggesting that the PPI was specific and that detection of bound to free ratios could be used to detect an inhibitor.

3.3.2 Adapting CE to a Screening Format.

After validating the CE method as an effective platform for monitoring the Hsp70-BAG3 interaction, we evaluated its potential for screening using automated analysis from 96-well microtiter plates. Each CE assay required ~ 6.5 min to complete, including 1 min rinsing, 5 s injection and 3 min separation. This protocol allowed us to screen 220 samples per day. Thus, while the method is not yet practical for screening large (*e.g.* 100,000) chemical libraries, it is suitable for proof-of-principle pilot screens.

The robustness of the CE platform was tested by performing a sequence of control assays from a 96-well plate. Each sample contained Hsp70-488 (0.5 μM) mixed with BAG3 (0.5 μM). Half of the samples were positive controls (2 μM unlabeled Hsp70 added) and half were negative controls (only 1% DMSO added). The calculated *Z*-factor for this experiment was 0.78, well above the suggested minimum for HTS (~0.50) [42]. We also tested the robustness of using our FCPIA platform (established in Chapter 2) as an HTS method for this PPI. Briefly, Hsp70 was biotinylated and immobilized on streptavidin coated polystyrene beads, while BAG3 was fluorescently labeled with Alexa-Fluor 488. The two partners were then incubated together and analyzed using an Accuri flow cytometer to measure bead-associated fluorescence [43]. This platform yielded a *Z*-factor of 0.86. Together, these experiments established two platforms for screening of the Hsp70-BAG3 complex.

3.3.3 Screening and Selection of PPI inhibitors.

Using these conditions, we screened a pilot library of 3,443 compounds by CE using the workflow shown in Figure 3.6. A comparable workflow was used for a FPCIA screen. In the CE screen, each well produced an electropherogram which was then integrated and the peak area ratios (bound Hsp70-488 to free Hsp70-488) were used to identify putative inhibitors [42]. Ratios were used instead of single peak areas to minimize artifacts from variations in injection volume, light source instability or sample evaporation effects. This approach also allowed the

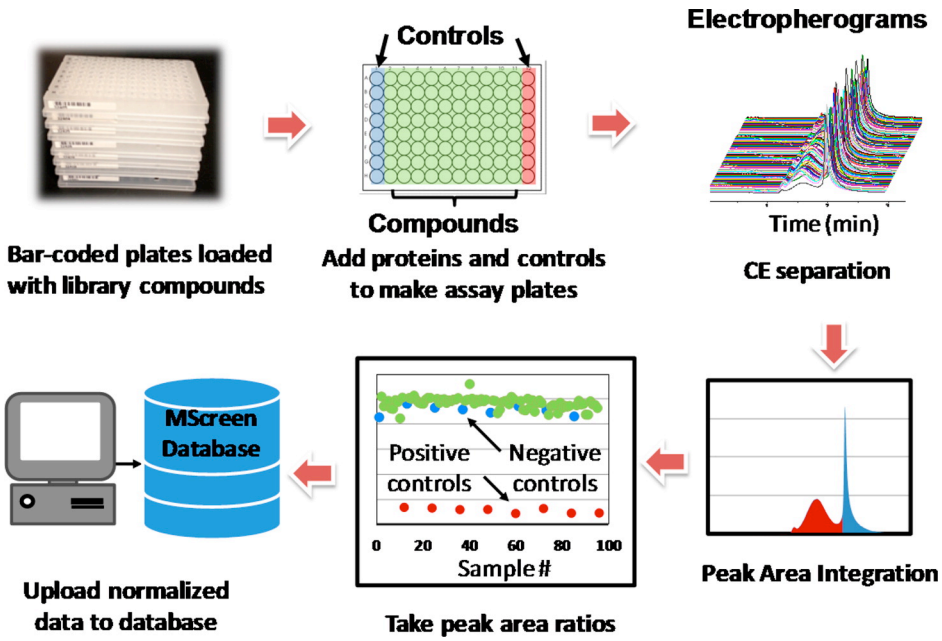

Figure 3.6 Illustration of workflow for the CE screen. Library compounds were placed in 96 well plates along with controls. After CE separation, peaks were integrated and bound:free ratio for Hsp70-488 was measured. Hits were defined as those compounds that perturbed the ratio by more than 3 standard deviations.

results from each individual microtiter well to be submitted to the screening database as a convenient single point data; however, the full electropherograms were stored and could also be retrieved. Test compounds in both the CE and FCPIA screens were screened at a single concentration (20 μM) and those that blocked the PPI with a percentage of inhibition that was ≥ 3 standard deviations (SD) from the negative controls were considered “hits”. Using this criterion, CE identified 79 primary hits (2.3%), while FCPIA identified 117 (3.4%) as shown in Figure 3.7. Active molecules from the CE screen were further triaged based on visual inspection of the raw electropherograms. This analysis readily identified aggregator molecules and compounds with high intrinsic fluorescence because of irregular electropherograms (see Figure 3.9). Removing these artifacts reduced the number of putative inhibitors to 48 (1.4%). Interestingly, only 6 primary hits were common between the two assays, suggesting a large number of false positives and/or negatives.

Select compounds from both lists of confirmed inhibitors were then repurchased from commercial sources: 14 compounds from the CE screen and 18 from the

FCPIA screen including 2 shared inhibitors. Only hits that were available from different commercial sources and were deemed to have potential for further development as drugs or chemical probes were selected for retesting. Repurchased compounds were tested by dose response curves (DRC) in the original screening platforms, and eight were reconfirmed from each list. These

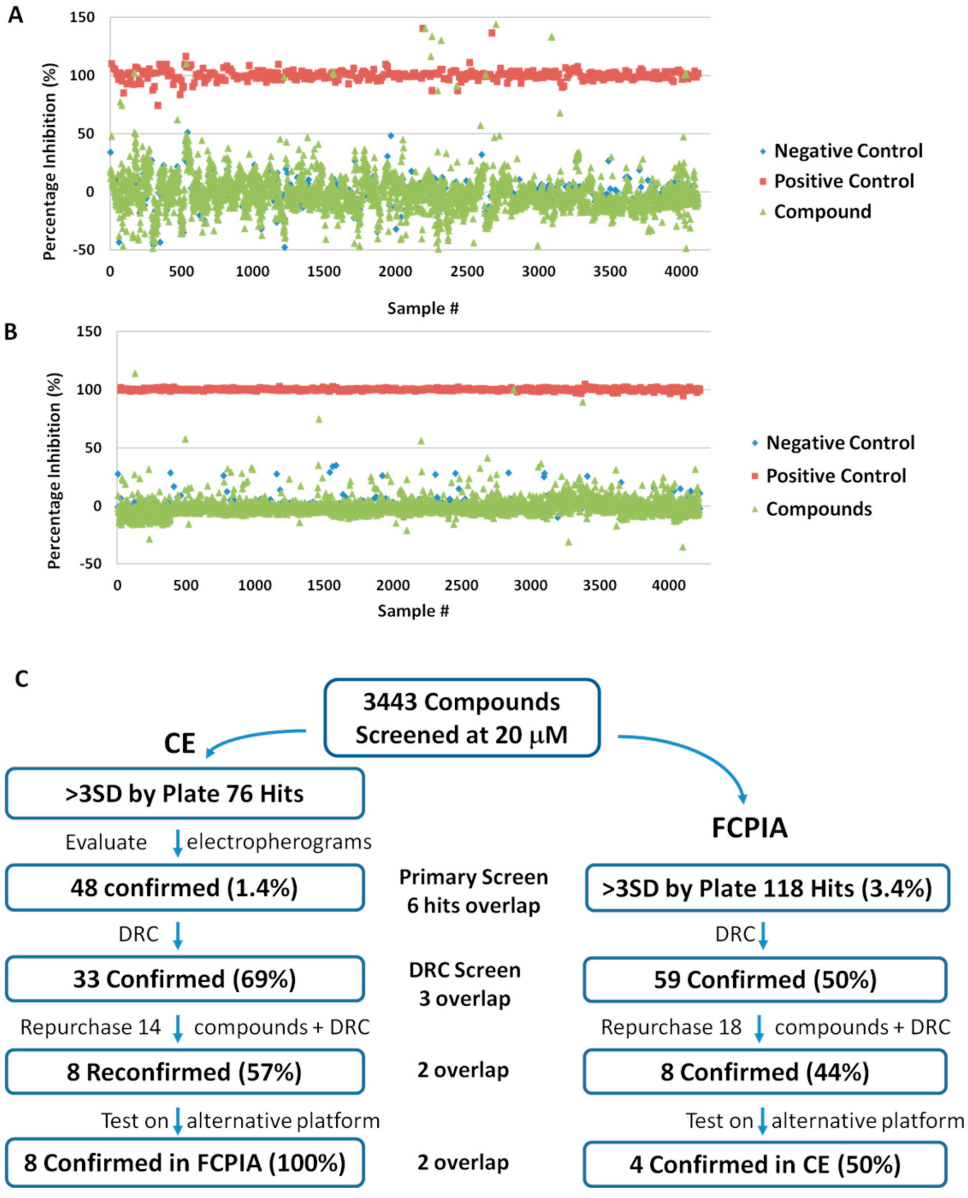

Figure 3.7 Results from screens of 3,443 compounds using CE and FCPIA. (A) Campaign view of CE screen. Negative controls (DMSO) are shown in blue, positive controls (4μM Hsp70) are shown in red, and compound wells are shown in green. Average plate Z' score was 0.58. (B) Campaign view of FCPIA screen. Negative controls (DMSO) are shown in blue, positive controls (1μM Hsp70) are shown in red, and compound wells are shown in green. Average plate Z' score was 0.86. (C) Summary of triage and confirmation of hits for CE and FCPIA HTS.

results suggest that some of the hits are due to degraded compounds or other artifacts from the library, a common observation in screening.

The eight confirmed hits from each assay were tested by DRC on the other assay. Interestingly, all (8/8) repurchased compounds that reconfirmed in CE were also confirmed in FCPIA; however, only 50% (4/8) of the compounds that showed activity in FCPIA were considered inhibitors in the CE platform. (DRC from cross testing are shown in Figure 3.8.)

Of the 4 compounds found by FCPIA that reconfirmed by CE, two were detected and two were missed in the original CE screen. The two inhibitors overlooked by CE were confirmed at a concentration 5 times higher than the concentration used for the screen. The use of lower concentrations during the screen combined with lower Z-factor of the CE assay led to their being missed in the original screen. Of

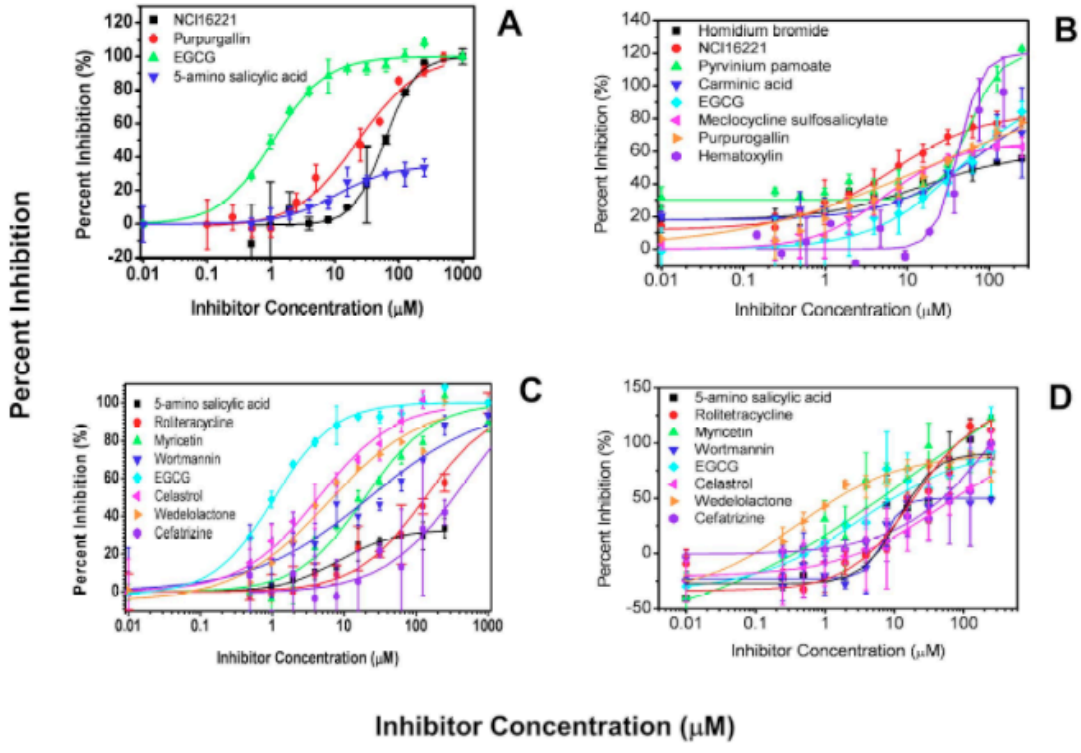

Figure 3.8 DRCs of confirmed FCPIA hits using (A) CE, (B) FCPIA and CE hits using (C) CE, (D) FCPIA. Only 4 compounds are shown (A) because other FCIPIA hits showed no activity at 100 ⌈M in the CE assay. Error bars are the range for two replicates.

the 8 compounds found by CE that reconfirmed by FCPIA, 6 were missed in the original FCPIA screen. Two of these, celastrol [43] and myricetin [42], are known modulators of Hsp70. These results suggest that CE gave fewer false negatives. Nevertheless, it is apparent that the screens complement each other.

3.3.4 Evaluation of the CE Platform and Opportunities for Further Optimization.

Compared to the standard screen by FCPIA, CE produced lower hit rates with a higher percentage of compounds that were eventually confirmed by retesting using multiple techniques. We suspect that the enhanced reproducibility and specificity of CE might derive from the use of the electropherogram to triage molecules, which allowed streamlining of the hit selection process at multiple stages. For example, molecules that induce Hsp70-488 aggregation were readily identified by the appearance of sharp spikes corresponding to insoluble particulates (Figure 3.9B). Removal of these aggregators from future consideration greatly streamlined the subsequent confirmation steps. CE also allowed direct detection of intrinsically fluorescent compounds, which might

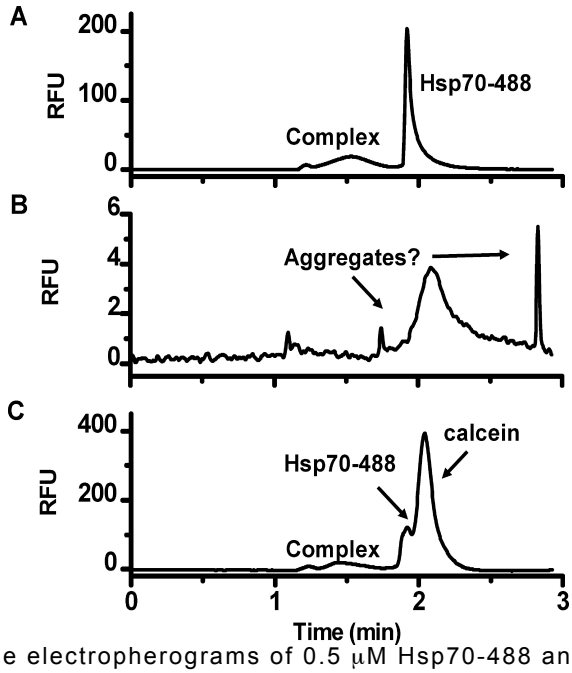

Figure 3.9 Sample electropherograms of 0.5 μM Hsp70-488 and 0.5 μM Bag3 with (A) 15 μM Epigallocatechin gallate (EGCG), a confirmed PPI inhibitor; (B) 20 μM haematoxylin, identified as an aggregator; (C) 20 μM calcein added, identified as a fluorescent compound that interferes with detection of free Hsp70-488.

otherwise give false positives in a fluorescent screening assay and require secondary screens for their removal (Figure 3.9C). In principle, these compounds could be further evaluated in screens by CE.

Another difference between the assays is that the CE assay used labeled Hsp70 and allowed interaction in free solution. In contrast, the FPCIA used labeled BAG3 and immobilized Hsp70. This difference may have also yielded some differences in the results such as the 4 hits confirmed by FPCIA but not detected by CE and the rank order of IC50s. A label or surface immobilization may yield subtle changes in protein conformation, affect access to the binding site or inhibit allosteric mechanisms. Thus, in principle the lower degree of protein modification required by CE would be advantageous.

3.4 Discussion

Despite these advantages, the application of CE to screening PPI is still in its infancy and several issues need to be addressed. We observed that peak area ratios began to drift after about 500 injections. This was attributed to deterioration of the surface coating because switching to a new capillary restored the original bound to free ratio. This effect may have contributed to the lower Z-factor of the CE method and it might have caused us to overlook some active compounds. More stable coatings are likely to help this effect. Of course, not all proteins will require coatings. Another limitation is the current requirement for covalent labeling with fluorophores, which has the potential to interfere with the PPI itself depending on the system. Use of post-column derivatization, native protein fluorescence, and/or label-free detection methods are alternatives that may eliminate this requirement.

At the throughput enabled by a commercial CE instrument, this assay is best suited as a secondary screen to test hits found by higher throughput methods. Use of novel microchip systems [43, 44] or adoption to commercial microchip

electrophoresis, *e.g.* Caliper LabChip EZ reader, will be required to make this a tool suitable for screens of larger chemical collections.

Recent interest in PPI inhibitors has driven a search for new methodologies that are suitable for HTS. In particular, HTS methods that permit screening of relatively weak or transient interactions are becoming an area of need. The experiments with CE described here provide a framework for development of this method as a robust tool for the discovery of new inhibitors of PPIs that complements existing techniques.

In terms of Hsp70-BAG3 biology, this method provides an initial set of molecules that could be optimized to generate chemical probes. As part of the broader goal of this thesis work, it would be important to identify molecules that disrupt binding of Hsp70 to BAG3. While this work was being performed, studies by other members of the Gestwicki laboratory identified a promising scaffold for this purpose [28]. Using FCPIA we were able to determine that these molecules inhibit Hsp70-NEF interactions [45, 46], and this platform has become critical for driving structure-activity relationships (SAR) in this series. Furthermore, this compound series has provided valuable insight into Hsp70-BAG3 biology, specifically in the context of cancer signaling networks. Future work expanding on these compounds will be discussed in Chapter 5.

3.5 Methods

3.5.1 Protein Purification and Labeling.

Human Hsp70 (HSPA1) was purified as previously described [47] using a N-terminal 6xHis tag and Ni-NTA column, followed by overnight TEV Protease cleavage of the His tag and lastly an ATP-agarose affinity column. Human N-terminal 6xHis-tagged BAG3 was purified based on previous reports [49]. Briefly, BAG3 was purified by ammonium sulfate (0-30% of saturation) followed by a Ni-NTA column and overnight TEV cleavage of the His tag. BAG3 was dialyzed overnight into Buffer A (25 mM HEPES, 10 mM NaCl, 15 mM β-mercaptoethanol,

0.1mM EDTA, pH 7.6) and subjected to ion-exchange chromatography on a Mono-Q HR 16/10 column (GE Healthcare). Finally, BAG3 was subjected to size exclusion chromatography on a Superdex 200 gel filtration column (GE Healthcare). Hsp70 and BAG3 were labeled with Alexa Fluor® 488 5-SDP ester (Life Technologies) according to the suppliers instructions. Hsp70 was biotinylated using EZ-link NHS-Biotin (Thermo Scientific) according to the supplier instructions. After labeling, the proteins were subjected to gel filtration to remove any unreacted label.

3.5.2 Capillary Surface Modification.

The inner surface of a 30 cm long fused silica capillary (Polymicro Technologies; Phoenix, AZ) with 50 μm inner diameter and 360 μm outer diameter was activated for derivatization by pumping the following through the capillary at 30 psi for 1 h each: 1) methanol at room temperature; 2) RCA solution (NH_4OH:H_2O_2:H_2O v:v:v = 1:1:5) at 120 °C; 3) 0.1 M HCl at 90°C. Temperature was maintained by an oil bath. After activation, the residual liquid was purged out of the capillary and the capillary inner surface was dried under dry nitrogen flow at 165 °C overnight. 10% (volume percent) 1H, 1H, 2H, 2H-perfluorooctyltrichlorosilane (sigma, St. Louise, MO) in toluene was continuously infused for 3 h at 120 °C. The derivatized capillary was rinsed with toluene and methanol before purging with nitrogen and drying in an oven at 80 °C overnight.

3.5.3 Capillary Electrophoresis.

A Beckman Coulter MDQ/PACE was used for CE experiments unless otherwise noted. The capillary was mounted to have a separation length of 10 cm. Capillary temperature was kept at 25 °C for all experiments. Separation buffer was 10 mM sodium phosphate adjusted to pH 7.5 with 0.01% Tween 20 (w:v). All separation buffers were made fresh every day from 5X stock solution. All buffer solutions were made using water purified and deionized to 18 MΩ resistivity using a Series 1090 E-pure system (Barnstead Thermolyne Cooperation, Dubuque, IA) and then filtered through a 0.2 μm pore size membrane (Whatman, GE). The

separation method consisted of three steps: 1) 1 min rinsing using with separation buffer; 2) pressure injection at 0.3 p.s.i. for 5 s; 3) separation at 500 V/cm with normal polarity resulting in current of 14.0 μA. 0.5 p.s.i. pressure was applied during separation to generate flow in the same direction of EOF to decrease separation time to 3 min. LIF detection was accomplished using a 20 mW optically pumped semiconductor Sapphire laser (Coherent, Santa Clara, CA) coupled to the Beckman Coulter MDQ/PACE LIF detection module through an optical fiber. The LIF was equipped with $\lambda_{ex}/\lambda_{em}$ filters of 488 nm/520 nm. All data were collected by 32 Karat software and exported as ASCII files, which were further processed using software written in house [45, 48].

3.5.4 Small Molecule Libraries.

The chemical library of 3,443 distinct compounds was assembled at the University of Michigan's Center for Chemical Genetics (CCG) from several small libraries. The MicroSource MS2000 library contains 2000 bioactive compounds with a minimum of 95% purity. The collection contains 958 known therapeutic drugs, 629 natural products and natural product derivatives, 343 compounds with reported experimental biological activities and 70 compounds approved for agricultural use. The CCG Focused collection includes ~1000 small molecules that target specific activities (e.g., Wnt Pathway) and natural products. The CCG Biofocus NCC library is an NIH Clinical collection that contains ~450 small molecules that have a history of use in human clinical trials including some FDA approved drugs. The activity of promising compounds was confirmed with repurchased samples from commercial sources including Sigma-Aldrich, Enzo Life Sciences, Cayman Chemical, Acros Organics, Alfa Aesar, and MP Biomedicals.

3.5.5 Screening by Capillary Electrophoresis.

Binding reactions were performed in 96-well conical bottom PCR plates (ISC BIoexpress). A stock solution of Alexa Fluor® 488 labeled Hsp70 (Hsp70-488) and unlabeled BAG3 was prepared fresh daily in assay buffer (25 mM HEPES,

10 mM KCl, 5 mM $MgCl_2$, 0.3% Tween-20 pH 7.5) so that the final concentration of both proteins was 500 nM in the assay. Compounds and DMSO were dry spotted in plates prior to protein addition using a Mosquito liquid handler (TTP Labtech). Assay buffer (5 µL) was added to each well except for positive control wells that received 5 µL of unlabeled Hsp70. Hsp70-BAG3 solution (10 µL) was then added to each well. All additions were added using a Matrix Electronic Multichannel pipette (Thermo Scientific). Plates were incubated for at least 15 min and then analyzed on the CE system.

3.5.6 High-throughput Flow Cytometry Protein Interaction Assay.

The assay procedure was adopted from previous reports[162]. In brief, biotinylated Hsp70 was incubated with streptavidin coated polystyrene beads (Spherotech) for one hour prior to assay for immobilization. A stock solution of Alexa Fluor® 488 labeled BAG3 was prepared in assay buffer (25 mM HEPES, 10 mM KCl, 5 mM $MgCl_2$, 0.3% Tween-20 pH 7.5) so that the final concentration of BAG3 was 30 nM in the assay. Assay buffer (5 µL) was added to each well of a black 384 well plate (Thermo Scientific), followed by compound or DMSO addition (0.2 µL) using a Biomek HDR (Beckman). Positive control wells received 5 µL unlabeled Hsp70 instead of assay buffer. BAG3 solution (10µL) was then added to each well, followed by Hsp70-bead addition (5 µL). All components other than compounds were added using a Multidrop dispenser (Thermo Fisher Scientific). Plates were incubated for 15 min then analyzed using a Hypercyt liquid sampling unit in line with an Accuri® C6 Flow Cytometer. Median bead associated fluorescence was calculated using Hyperview software for each well and data was uploaded to the Mscreen database.

3.5.7 Malachite Green ATPase Assay.

Assay was performed as described previously [1]. All assays used 1µM Hsp70 and 0.25µM DJA2 was added for BAG3 ATPase activity. Plates were incubated for 1 hour at 37°C and inorganic phosphate was detected using Malachite Green reagent.

3.5.8 Isothermal Titration Calorimetry.

BAG3 and Hsp70 were dialyzed against 25mM HEPES, 5mM MgCl2, 10mM KCl pH 7.5 (ITC Buffer). The experiment was performed with a MicroCal VP-ITC at 25°C by titrating 5μL injects of Hsp70 (85μM) into a 5μM solution of Bag3. Calorimetric parameters were calculated using Origin® 7.0 software and fit with a one-site binding model.

3.6 Notes

A portion of this chapter has been published as **Rauch JN***, Nie J*, Buchholz TJ, Gestwicki JE, Kennedy RT. *Development of a capillary electrophoresis platform for identifying inhibitors of protein-protein interactions*. Analytical Chemistry. 2013; 85(20):9824-31. (*co-first authors)

3.7 References

1. Rual, J.F., et al., *Towards a proteome-scale map of the human protein-protein interaction network.* Nature, 2005. **437**(7062): p. 1173-8.
2. Stelzl, U., et al., *A human protein-protein interaction network: a resource for annotating the proteome.* Cell, 2005. **122**(6): p. 957-68.
3. Bonsor, D.A. and E.J. Sundberg, *Dissecting protein-protein interactions using directed evolution.* Biochemistry, 2011. **50**(13): p. 2394-402.
4. Vidal, M., M.E. Cusick, and A.L. Barabasi, *Interactome networks and human disease.* Cell, 2011. **144**(6): p. 986-98.
5. Powers, E.T., et al., *Biological and chemical approaches to diseases of proteostasis deficiency.* Annu Rev Biochem, 2009. **78**: p. 959-91.
6. Wells, J.A. and C.L. McClendon, *Reaching for high-hanging fruit in drug discovery at protein-protein interfaces.* Nature, 2007. **450**(7172): p. 1001-9.
7. Smith, M.C. and J.E. Gestwicki, *Features of protein-protein interactions that translate into potent inhibitors: topology, surface area and affinity.* Expert Rev Mol Med, 2012. **14**: p. e16.
8. Thompson, A.D., et al., *Fine-tuning multiprotein complexes using small molecules.* ACS Chem Biol, 2012. **7**(8): p. 1311-20.
9. Makley, L.N. and J.E. Gestwicki, *Expanding the number of 'druggable' targets: non-enzymes and protein-protein interactions.* Chem Biol Drug Des, 2013. **81**(1): p. 22-32.
10. Arkin, M.R. and A. Whitty, *The road less traveled: modulating signal transduction enzymes by inhibiting their protein-protein interactions.* Curr Opin Chem Biol, 2009. **13**(3): p. 284-90.

11. Thorne, N., D.S. Auld, and J. Inglese, *Apparent activity in high-throughput screening: origins of compound-dependent assay interference.* Curr Opin Chem Biol, 2010. **14**(3): p. 315-24.
12. Schou, C. and N.H.H. Heegaard, *Recent applications of affinity interactions in capillary electrophoresis.* Electrophoresis, 2006. **27**(1): p. 44-59.
13. Sun, Y., et al., *Capillary Electrophoresis Frontal Analysis for Characterization of αvβ3 Integrin Binding Interactions.* Analytical Chemistry, 2008. **80**(9): p. 3105-3111.
14. Shimura, K., et al., *Mobility moment analysis of molecular interactions by capillary electrophoresis.* Analytical Chemistry, 2005. **77**(2): p. 564-572.
15. Chu, Y.H., et al., *Affinity capillary electrophoresis mass spectrometry for screening combinatorial libraries.* Journal of the American Chemical Society, 1996. **118**(33): p. 7827-7835.
16. Shimura, K. and B.L. Karger, *AFFINITY PROBE CAPILLARY ELECTROPHORESIS - ANALYSIS OF RECOMBINANT HUMAN GROWTH-HORMONE WITH A FLUORESCENT-LABELED ANTIBODY FRAGMENT.* Analytical Chemistry, 1994. **66**(1): p. 9-15.
17. Picou, R.A., et al., *Separation and detection of individual A beta aggregates by capillary electrophoresis with laser-induced fluorescence detection.* Analytical Biochemistry, 2012. **425**(2): p. 104-112.
18. Schultz, N.M. and R.T. Kennedy, *Rapid immunoassays using capillary electrophoresis with fluorescence detection.* Analytical Chemistry, 1993. **65**(21): p. 3161-3165.
19. German, I., D.D. Buchanan, and R.T. Kennedy, *Aptamers as ligands in affinity probe capillary electrophoresis.* Analytical Chemistry, 1998. **70**(21): p. 4540-4545.
20. Buchanan, D.D., et al., *Effect of buffer, electric field, and separation time on detection of aptamer-ligand complexes for affinity probe capillary electrophoresis.* Electrophoresis, 2003. **24**(9): p. 1375-1382.
21. Zhang, H., X.-F. Li, and X.C. Le, *Tunable Aptamer Capillary Electrophoresis and Its Application to Protein Analysis.* Journal of the American Chemical Society, 2007. **130**(1): p. 34-35.
22. Stebbins, M.A., et al., *Design and optimization of a capillary electrophoretic mobility shift assay involving trp repressor-DNA complexes.* Journal of Chromatography B-Biomedical Applications, 1996. **683**(1): p. 77-84.
23. Shimura, K. and K. Kasai, *DETERMINATION OF THE AFFINITY CONSTANTS OF CONCANAVALIN-A FOR MONOSACCHARIDES BY FLUORESCENCE AFFINITY PROBE CAPILLARY ELECTROPHORESIS.* Analytical Biochemistry, 1995. **227**(1): p. 186-194.
24. Shimura, K., et al., *Determination of the affinity constants of recombinant human galectin-1 and-3 for simple saccharides by capillary affinophoresis.* Journal of Chromatography B-Analytical Technologies in the Biomedical and Life Sciences, 2002. **768**(1): p. 199-210.

25. Shimura, K., et al., *Analysis of protein-protein interactions with a multi-capillary electrophoresis instrument.* Electrophoresis, 2006. **27**(10): p. 1886-1894.
26. Yang, P.L., et al., *Multiplexed detection of protein-peptide interaction and inhibition using capillary electrophoresis.* Analytical Chemistry, 2007. **79**(4): p. 1690-1695.
27. Lyubarskaya, Y.V., et al., *Screening for High-Affinity Ligands to the Src SH2 Domain Using Capillary Isoelectric Focusing-Electrospray Ionization Ion Trap Mass Spectrometry.* Analytical Chemistry, 1998. **70**(22): p. 4761-4770.
28. Kennedy, R.T., et al., *Fast analytical-scale separations by capillary electrophoresis and liquid chromatography.* Chemical Reviews, 1999. **99**(10): p. 3081-+.
29. Simpson, P.C., et al., *High-throughput genetic analysis using microfabricated 96-sample capillary array electrophoresis microplates.* Proceedings of the National Academy of Sciences of the United States of America, 1998. **95**(5): p. 2256-2261.
30. He, Y. and E.S. Yeung, *High-throughput screening of kinase inhibitors by multiplex capillary electrophoresis with UV absorption detection.* Electrophoresis, 2003. **24**(1-2): p. 101-108.
31. Pei, J., J. Nie, and R.T. Kennedy, *Parallel Electrophoretic Analysis of Segmented Samples On Chip for High-Throughput Determination of Enzyme Activities.* Analytical Chemistry, 2010. **82**(22): p. 9261-9267.
32. Assimon, V.A., et al., *Hsp70 protein complexes as drug targets.* Curr Pharm Des, 2013. **19**(3): p. 404-17.
33. Boiani, M., et al., *The Stress Protein BAG3 Stabilizes Mcl-1 Protein and Promotes Survival of Cancer Cells and Resistance to Antagonist ABT-737.* J Biol Chem, 2013. **288**(10): p. 6980-90.
34. Chiappetta, G., et al., *The antiapoptotic protein BAG3 is expressed in thyroid carcinomas and modulates apoptosis mediated by tumor necrosis factor-related apoptosis-inducing ligand.* J Clin Endocrinol Metab, 2007. **92**(3): p. 1159-63.
35. Jacobs, A.T. and L.J. Marnett, *HSF1-mediated BAG3 expression attenuates apoptosis in 4-hydroxynonenal-treated colon cancer cells via stabilization of anti-apoptotic Bcl-2 proteins.* J Biol Chem, 2009. **284**(14): p. 9176-83.
36. Wang, H.Q., et al., *Inhibition of the JNK signalling pathway enhances proteasome inhibitor-induced apoptosis of kidney cancer cells by suppression of BAG3 expression.* Br J Pharmacol, 2009. **158**(5): p. 1405-12.
37. Festa, M., et al., *BAG3 protein is overexpressed in human glioblastoma and is a potential target for therapy.* Am J Pathol, 2011. **178**(6): p. 2504-12.
38. Liu, P., et al., *BAG3 gene silencing sensitizes leukemic cells to Bortezomib-induced apoptosis.* FEBS Lett, 2009. **583**(2): p. 401-6.

39. Westerheide, S.D., et al., *Celastrols as inducers of the heat shock response and cytoprotection.* Journal of Biological Chemistry, 2004. **279**(53): p. 56053-56060.
40. Chang, L., et al., *Chemical Screens against a Reconstituted Multiprotein Complex: Myricetin Blocks DnaJ Regulation of DnaK through an Allosteric Mechanism.* Chemistry & Biology, 2011. **18**(2): p. 210-221.
41. Pei, J., et al., *Microfabricated channel array electrophoresis for characterization and screening of enzymes using RGS-G protein interactions as a model system.* Analytical Chemistry, 2008. **80**(13): p. 5225-5231.
42. Rousaki, A., et al., *Allosteric drugs: the interaction of antitumor compound MKT-077 with human Hsp70 chaperones.* J Mol Biol, 2011. **411**(3): p. 614-32.
43. Colvin, T.A., et al., *Hsp70-Bag3 interactions regulate cancer-related signaling networks.* Cancer Res, 2014. **74**(17): p. 4731-40.
44. Li, X., et al., *Validation of the Hsp70-Bag3 Protein-Protein Interaction as a Potential Therapeutic Target in Cancer.* Mol Cancer Ther, 2015.
45. Chang, L., et al., *Mutagenesis reveals the complex relationships between ATPase rate and the chaperone activities of Escherichia coli heat shock protein 70 (Hsp70/DnaK).* J Biol Chem, 2010. **285**(28): p. 21282-91.
46. Miyata, Y., et al., *High-throughput screen for Escherichia coli heat shock protein 70 (Hsp70/DnaK): ATPase assay in low volume by exploiting energy transfer.* J Biomol Screen, 2010. **15**(10): p. 1211-9.
47. Shemetov, A.A. and N.B. Gusev, *Biochemical characterization of small heat shock protein HspB8 (Hsp22)-Bag3 interaction.* Arch Biochem Biophys, 2011. **513**(1): p. 1-9.
48. Chang, L., et al., *High-throughput screen for small molecules that modulate the ATPase activity of the molecular chaperone DnaK.* Anal Biochem, 2008. **372**(2): p. 167-76.
49. Blazer, L.L., et al., *Use of flow cytometric methods to quantify protein-protein interactions.* Curr Protoc Cytom, 2010. **Chapter 13**: p. Unit 13 11 1-15.

Chapter 4

BAG3 is a modular scaffolding protein that links the molecular chaperone Hsp70 to the sHsp system

4.1 Abstract

BAG3 is a multi-functional protein implicated in many cellular processes. In Chapter 2, we examined the role of BAG3 as a nucleotide exchange factor (NEF) for Hsp70 and in Chapter 3 we screened for small molecules that could disrupt the BAG3-Hsp70 interaction. In this Chapter, we assess the role of BAG3 as a modular scaffolding protein that links Hsp70 to the small heat shock protein (sHsp) system. Previous work had identified that BAG3 contains two IPV motifs that can interact with different sHsps, however the full scope of these interactions was unknown and their implications on sHsp structure was uncertain. In this work we show that BAG3 binds a large range of human sHsps, using both of its IPV motifs to form a 2:1 stoichiometric complex (sHsp:BAG3). BAG3 is competitive with sHsp-sHsp self-self interactions and can reduce sHsp oligomer size. Furthermore, we go on to show that BAG3 uses its BAG domain to interact with Hsp70 and that it can bridge a ternary complex between sHsps and Hsp70. All together, this data indicates that BAG3 is situated at the interface of the Hsp70 and sHsp systems, and could potentially regulate client transfer between them.

4.2 Introduction

As introduced in Chapter 1, Bcl-2 Associated Anthanogene-3 (BAG3) is an Hsp70 co-chaperone that has gained attention for its ever-growing roles in disease [3-5]. BAG3 is a relatively large protein that, on top of its established activity as a NEF for Hsp70, also contains many additional protein-protein

interaction (PPI) motifs. In its N-terminus, BAG3 has a WW domain (see Figure 4.4A) that has been shown to be important for binding PPxY motif proteins, such as RAPGEF6 [6] and SYNPO2 [7]. The PXXP region of BAG3 has been implicated in interactions with various SH3 domain-containing proteins, such as Src [5] and PLC-γ [8]. Finally, BAG3 contains two IPV motifs separated by ~100 amino acids. IPV or IXI/V motifs are known to be important for binding small heat shock proteins (sHsps) [9-11] and have been reported to be important for linking BAG3 to various sHsps [12].

Together, these PPI motifs in BAG3 allow it to act as a scaffolding protein that might link Hsp70 to important pathways. Indeed, mass spectrometry studies have estimated the BAG3 “interactome” to include >300 proteins [13]. This implicates BAG3 in a diverse range of cellular processes such as signal transduction [14], transcription [7], apoptosis [15, 16], and autophagy [17, 18]. However, it isn’t yet clear how BAG3 supports the assembly of these multi-protein complexes.

The interaction between BAG3 and sHsps was particularly interesting to us, because sHsps are a large and enigmatic class of molecular chaperones. In humans, there are ten members of the sHsp family, denoted HSPB1 through HSPB10 [19]. Unlike Hsp70, sHsps do not possess any enzymatic function; instead, sHsps function as “holdases”, binding to denatured or non-native protein folds and preventing their aggregation [20, 21]. sHsp expression is induced by stress, and they are thought to act as a first line of defense in suppressing protein aggregation.

Individual sHsps range in size from 12 to 43 kDa and they are defined by the presence of a conserved α-crystallin domain that is flanked by variable, disordered N- and C-terminal domains (Figure 4.1). The structure of the α-crystallin domain of Hsp27 has been solved by NMR and it features an anti-parallel beta-sheet that mediates stable dimerization (Figure 4.1) [22, 23]. In addition, the α-crystallin domain contains two highly conserved beta sheets,

termed β4-β8, that form a hydrophobic groove. In some sHsps, such as Hsp27 and αB crystallin, an IXI motif in the C-terminus binds to this groove and stabilizes higher order oligomers (Figure 4.1) [1, 24] [9, 11]. This groove can even support hetero-oligomers between different sHsp family members [25]. The oligomers are typically polydisperse and range in size from 12 to 40 dimer subunits [25, 26].

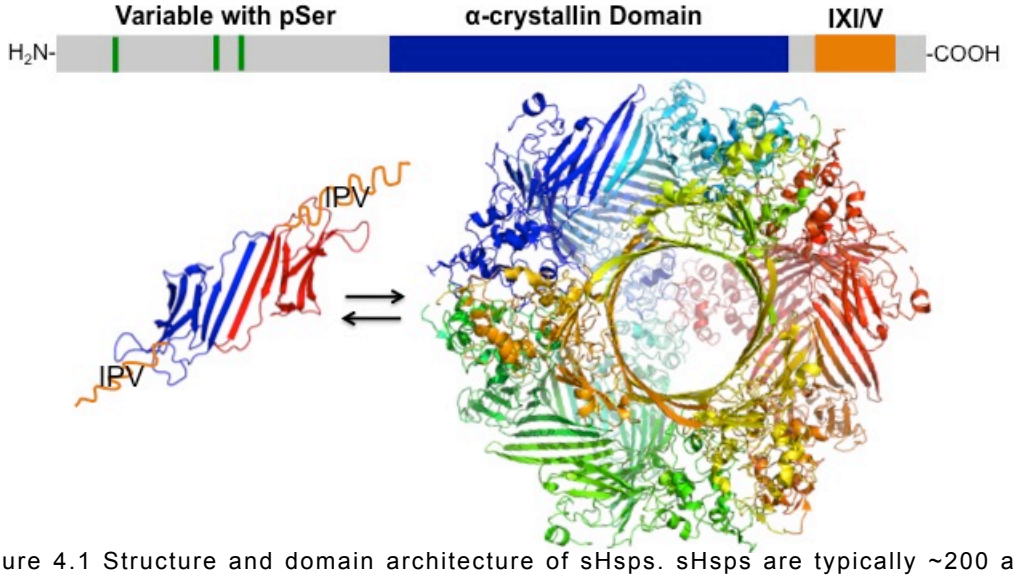

Figure 4.1 Structure and domain architecture of sHsps. sHsps are typically ~200 amino acids in length, composed of an N-terminal domain containing 3 phosphorylation sites, an α-crystallin domain, and an IXI/V motif in the C-terminus. The α-crystallin domain creates the dimer interface, and the IXI/V motifs allow dimers to stack up into oligomers. Solution NMR structure of the dimer is courtesy of the Klevit lab, and the 24-mer model is from [1, 2].

While it is well accepted that sHsps bind unfolded proteins and prevent their aggregation, it is not yet clear how they interact with clients. Moreover, it isn't clear how they cooperate with other members of the molecular chaperone network. One attractive model suggests that the sHsp oligomers dissociates in the presence of clients, and then re-form into a new oligomeric form containing bound client [27, 28]. This idea is supported by electron microscopy [29] and mass spectrometry studies [30] analyzing sHsp-substrate complexes. Furthermore, it has been suggested that smaller oligomeric forms of sHsp are more potent holdases *in vitro* [31]. All of this data suggests a model wherein sHsps stabilize a reservoir of denatured proteins that can then be passed on to a

refolding system like Hsp70. This is an exciting model because it would suggest the first direct link between two major “arms” of the protein homeostasis network. However, the mechanisms and requirements for this “hand-off” mechanism are entirely unknown.

In Chapter 2, I characterized the interaction between BAG3 and Hsp70 and determined that the BAG domain is likely primarily responsible for the interaction. BAG3 has been proposed to interact with sHsps through its IXI motifs [12, 32, 33], mimicking the intra-molecular interactions that normally occur in the β4-β8 grooves. Based on these findings, we hypothesized that BAG3 could potentially be a scaffolding protein that links Hsp70 with the sHsp system. To test this model, we generated a suite of BAG3 constructs with individual PPI domains mutated or deleted. We found that BAG3 interacts with multiple sHsps through its IPV motifs. Interestingly, we found that BAG3 preferred binding to smaller oligomers and that binding reduced oligomer size. This finding is exciting because it suggests that BAG3 is not only a scaffolding factor for sHsps, but that it actively remodels them. Lastly, we were able to show that indeed BAG3 can bridge sHsps and Hsp70, perhaps providing the missing link for substrate hand-off between these major players of the proteostasis network.

4.3 Results

4.3.1 BAG3 binds multiple sHsps

To study the interactions with BAG3, we selected four members of the sHsp family that are ubiquitously expressed in all human tissues [19]: Hsp27 (HSPB1), αB crystallin (HSPB5), Hsp20 (HSPB6), and Hsp22 (HSPB8). Of these proteins, Hsp20, Hsp22 and αB crystallin have been reported to interact with BAG3 by pulldown studies [12, 33], however, the affinities and stoichiometries of these interactions were not known. Therefore we employed a flow cytometry protein interaction assay (FCPIA) to assess binding of sHsps to BAG3. FCPIA was introduced in Chapter 2 as a workhorse method for studying protein-protein interactions. Briefly, sHsp was biotinylated and immobilized on streptavidin

coated polystyrene beads. Binding was then detected using fluorescently labeled BAG3. Using this platform, we found that BAG3 bound to Hsp27, Hsp20, Hsp22 and αB crystallin with affinity constants in the low- to mid-nanomolar range (Figure 4.2A). We next asked how oliogomerization affects binding to BAG3 using two additional Hsp27 variants. Hsp27-3D is a phospho-mimetic mutant that is reported to form smaller oligomers in solution [31]. Hsp27c is a truncated form that contains only the core α-crystallin domain and exists as a dimer in solution [34]. Using the FCPIA platform, we found that Hsp27c bound with the lowest

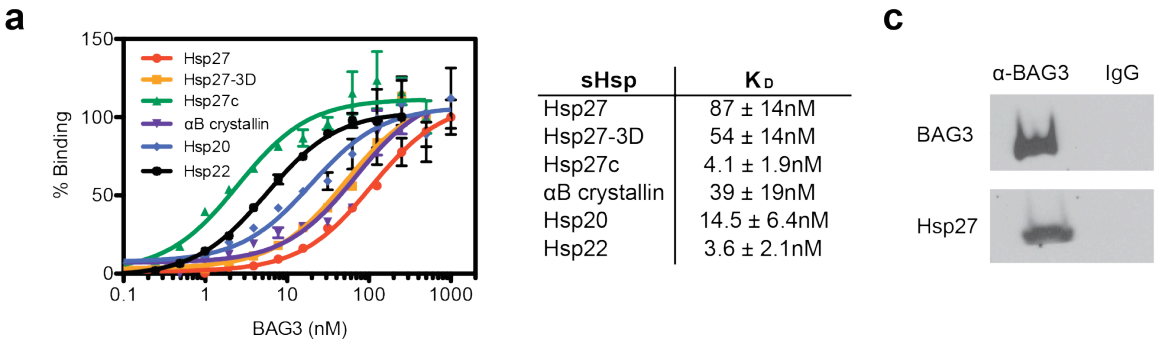

sHsp	K_D
Hsp27	87 ± 14nM
Hsp27-3D	54 ± 14nM
Hsp27c	4.1 ± 1.9nM
αB crystallin	39 ± 19nM
Hsp20	14.5 ± 6.4nM
Hsp22	3.6 ± 2.1nM

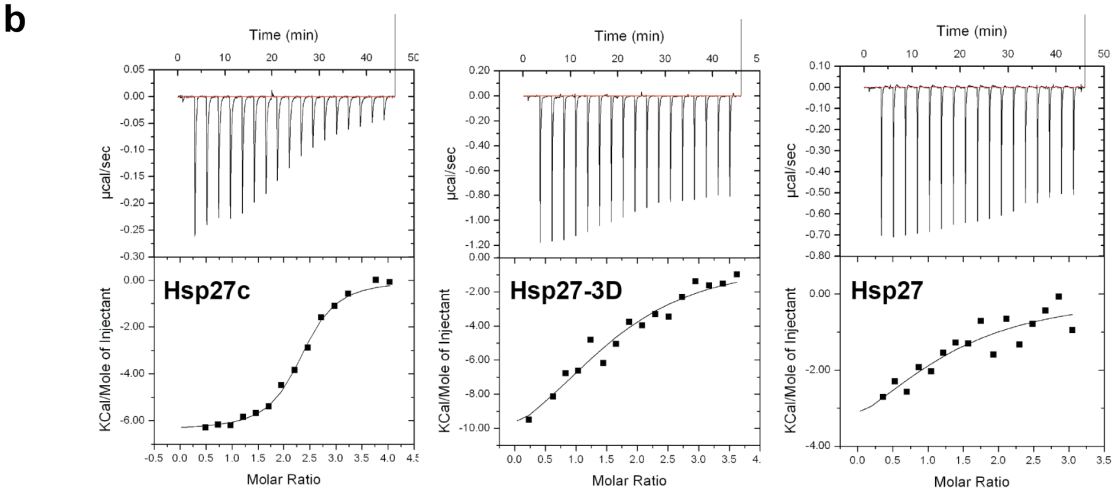

	Hsp27	Hsp27-3D	Hsp27c	αB crystallin	Hsp20	Hsp22
K_D	8.7 ± 2.2µM	3.5 ± 1.7µM	490 ± 60nM	5.0 ± 0.6µM	1.2 ± 0.7µM	1.2 ± 0.3µM
N	1.7 ± 0.2	1.9 ± 0.2	2.0 ± 0.1	1.8 ± 0.1	1.9 ± 0.2	2.0 ± 0.05

Figure 4.2 BAG3 binds multiple sHsps. (a) FCPIA of BAG3 and various sHsps. sHsps were immobilized on beads and binding was detected using fluorescently labeled BAG3. Non-specific binding of BAG3 to control beads was subtracted. Curves were fit with a non-linear regression with affinities reported in the table. Experiments were performed in triplicate and the error reported is SEM. (b) Representative ITC graphs of BAG3 titrated with different Hsp27 constructs. Experiments were performed in duplicate, affinities are reported in the table and the error is SEM. Representative graphs for the other sHsp can be found in Figure 4.3. (c) Co-IP of Hsp27 and BAG3 from HEK293 cells.

affinity (K_D ~ 4 nM), followed by Hsp27-3D, and then Hsp27. These results suggest that larger oligomers have the weakest affinity for BAG3, at least in the case of Hsp27.

To confirm these results, we also tested binding by Isothermal Titration Calorimetry (ITC). The affinities of the PPIs were similar to those obtained by FCPIA, although the values tended to be higher in this solution-based platform (Figure 4.2B and Figure 4.3C). This difference is not unusual and likely reflects differences in affinity from fluorophore labeling and multivalency effects at the bead surface. Nevertheless, the overall rank ordering of affinities were consistent between the two platforms. ITC also revealed the stoichiometry of the sHsp:BAG3 interaction as 2:1. This was an intriguing result because BAG3 contains two IPV motifs, so it could potentially interact across the dimer interface engaging both β4-β8 grooves.

The interaction with Hsp27 was slightly surprising, because a previous report using co-imunoprecipitation had suggested that BAG3 does not bind to Hsp27 in HeLa cells [35]. When we repeated the pull-downs in HEK293 cells with endogenous protein, we found that Hsp27 co-immunoprecipitated with BAG3 (Figure 4.2C). Furthermore, we were able to use NMR on our Hsp27c construct to show that BAG3 interacts specifically with the β4-β8 groove of Hsp27c (Figure 4.3A), as has been previously reported for other sHsps [12]. These results are consistent with the high conservation of the β4-β8 binding groove (Figure 4.3B).

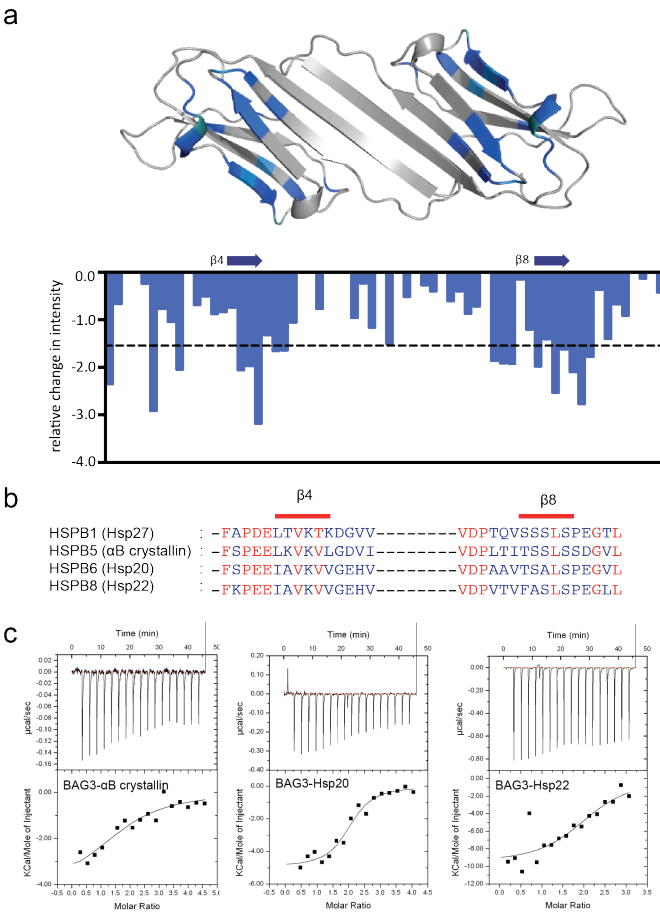

Figure 4.3 BAG3 interacts with β4-β8 groove of Hsp27c (a) Interaction surface for full length BAG3 binding to Hsp27c. The changes in backbone amide peak intensities exceeding 2 standard deviations (dotted line in histogram) are plotted onto the cartoon representation of Hsp27c in blue. Intensity changes between 1.5 and 2 standard deviations are plotted in marine. Locations of the β4 and β8 strands are indicated above the histogram. (b) Alignment of β4 and β8 sheets from indicated sHsps using COBALT (c) Representative ITC graphs for αB crystallin, Hsp20 and Hsp22. Affinities are reported in Figure 4.2.

4.3.2 BAG3 uses IPV motifs to interact with sHsp

It had been proposed that BAG3's IPV motifs are critical for sHsp interactions, but the effects of IPV mutations or deletions had not been quantitatively measured. To address this question, we generated BAG3 variants in which individual domains were systematically deleted: ΔWW, Δ87-101, Δ200-213, Δ87-101&Δ200-213, ΔPXXP, ΔBAG and BAG3C (Figure 4.4A). We assayed these proteins for binding to Hsp27c using FCPIA and ITC and found that deletion of the WW, PXXP, or BAG domain had no effect on binding affinity. The BAG3C

construct also showed no interaction (Figure 4.4B), as expected. Deletion of individual IPV motifs (Δ87-101, Δ200-213) or mutation of either IPV motif (IPV to GPG), reduced affinity by 2- to 5-fold (Figure 4.4C & 4.4F). When both IPV motifs were deleted (Δ87-101&Δ200-213) or mutated (IPV1&2) the affinity was reduced dramatically (Figure 4.4C & 4.4F). These results were further amplified in the ITC platform, where no binding could be detected for the double IPV

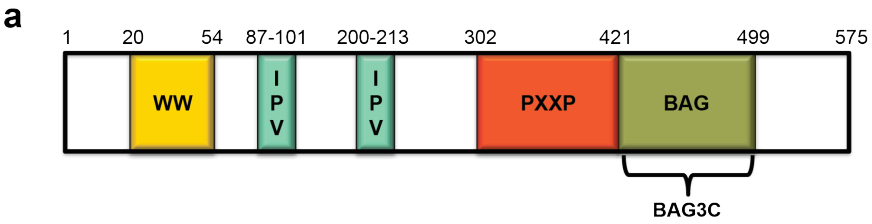

b

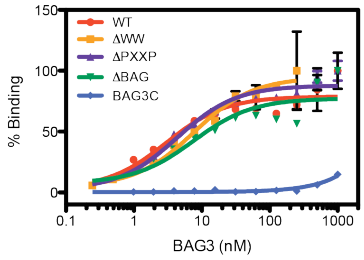

d

BAG3	Hsp27c	
	K_D	N
WT	490 ± 60nM	2.0 ± 0.1
IPV1	1030 ± 30nM	1.15 ± 0.02
IPV2	710 ± 140nM	1.21 ± 0.09
IPV1&2	No binding	No binding
Δ87-101	1100 ± 190nM	1.1 ± 0.2
Δ200-213	1990 ± 750nM	0.8 ± 0.2
Δ87-101 & Δ200-213	No binding	No binding
ΔWW	600 ± 250nM	2.0 ± 0.2
ΔPXXP	680 ± 160nM	1.8 ± 0.1
ΔBAG	730 ± 180nM	2.05 ± 0.08
BAG3C	No binding	No binding

c

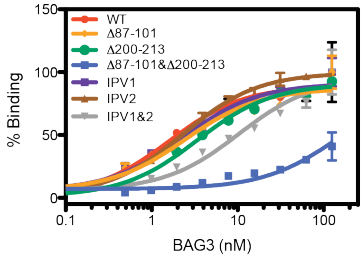

e

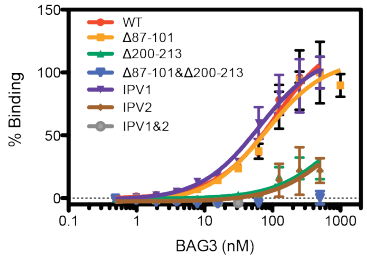

f

BAG3	Hsp27	Hsp273D	Hsp27c	αB crystallin	Hsp20	Hsp22
WT	87 ± 14nM	54 ± 14nM	4.1 ± 1.9nM	39 ± 19nM	14.5 ± 6.4nM	3.6 ± 2.1nM
Δ87-101	2x	1.3x	2x	1.9x	1.1x	2x
Δ200-213	No Binding	4x	5x	1.8x	2.7x	2x
Δ87-101 & Δ200-213	No Binding	No Binding	25x	No Binding	No Binding	50x
IPV1	3x	1.7x	3.5x	1.9x	1x	3x
IPV2	No Binding	8x	2x	1.6x	1x	5x
IPV1&2	No Binding	No Binding	7x	No Binding	3x	7x

Figure 4.4 Deletion/mutation of IPV motifs affect binding to sHsps. (a) Schematic of BAG3 domain architecture. (b) Domain deletions outside IPV motifs do not affect binding to Hsp27c as measured by FCPIA. (c) Deletion of both IPV motifs drastically reduces binding of BAG3 to Hsp27c (d) ITC results show that mutation/deletion of individual IPV motifs reduces stoichiometry from 2:1 to 1:1 (Hsp27c:BAG3) (e) IPV mutations/deletions affect binding to Hsp27 as measured by FCPIA. (f) Full table of FCPIA results for all sHsp and IPV constructs with fold loss in affinity indicated. All experiments were performed in triplicate and the error reported is SEM.

deletions/mutations (Figure 4.4D). Interestingly, when individual IPV motifs were removed, the stoichiometry of the interaction was reduced from 2:1 to 1:1 (Hsp27c:BAG3), suggesting that BAG3 uses both of its IPV motifs to engage an Hsp27c dimer.

We next generated IPV mutations and deletions in full-length sHsp proteins. Consistent with the results from the Hsp27c model system, we found that double IPV deletion profoundly disrupted binding to BAG3 (Figure 4.4F). Interestingly, Hsp27 seemed to show a preference for the second IPV motif over the first, because mutation/deletion of the second motif had a more dramatic effect than mutation or deletion of the first (Figure 4.4E & 4.4F). This result perhaps indicates co-operativity of IPV motifs when binding Hsp27. However, other sHsp, such as Hsp20, showed no motif preference and were only substantially affected by double mutation/deletions (Figure 4.4F).

4.3.3 BAG3 reduces oligomeric size of Hsp27

Knowing that BAG3 uses its IPV motifs to interact with sHsps and that sHsps also use these same motifs to regulate their oligomer size, we wondered if BAG3 in fact could influence sHsp oligomerization. To test this hypothesis, we used size exclusion chromatography with multi-angle light scattering (SEC-MALS). This technique allows absolute molecular weight determination of a sample based on the intensity of light scattering as a function of angle. SEC-MALS can differentiate samples from 200Da to 1GDa, making it appealing for use in studying sHsp oligomers. Injection of Hsp27 (30 μM) alone yielded an SEC-MALS trace with a suggested mass of 402 ± 15 kDa (Figure 4.5), indicating an average of 18 monomeric subunits that is consistent with literature values [36]. In addition, the Hsp27 peak was broad, suggesting a polydisperse ensemble of oligomers that has been observed previously [37]. To dissect the role of BAG3 in oligomerization, we added increasing amount of BAG3ΔPXXP to a constant concentration of Hsp27. BAG3ΔPXXP was used in these experiments because we had previously determined that it showed no binding deficits to sHsps (Figure

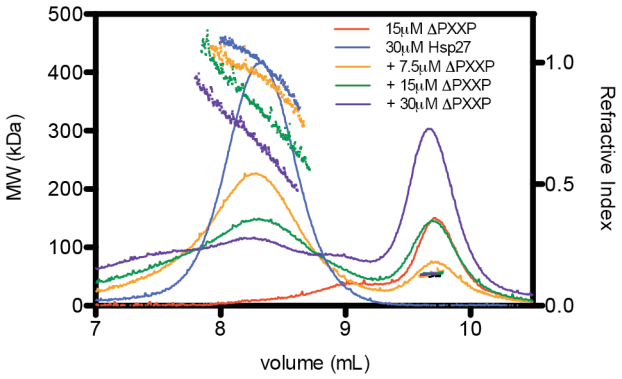

	MW (kDa)	Subunits
15μM ΔPXXP	51.6 ± 1.2	1
30μM Hsp27	402 ± 15	18
30μM Hsp27 + 7.5μM ΔPXXP	387 ± 5	17
30μM Hsp27 + 15μM ΔPXXP	356 ± 18	16
30μM Hsp27 + 30μM ΔPXXP	301 ± 6	13

Figure 4.5 BAG3 reduces oligomer size of Hsp27. Hsp27 was incubated with increasing concentrations of BAG3ΔPXXP and analyzed by SEC-MALS. Increasing amounts of BAG3ΔPXXP reduced the average molecular weight of the Hsp27 peak and increased the polydispersity of the sample. Experiments were repeated in duplicate and average MW is reported with SEM and the average number of subunits reported.

4.4) and it was well behaved in the SEC-MALS system (Figure 4.5). Increasing the concentrations of BAG3ΔPXXP effectively reduced oligomeric size of Hsp27 from 402 kDa to 301 kDa. This represents a drop in average subunit size from 18 monomers to 13 monomers. This estimate is conservative because it is likely that the new peaks contain BAG3ΔPXXP protein as well. Another striking feature was the increase in polydispersity of the sample after treatment with BAG3ΔPXXP (Figure 4.5). This result supports the hypothesis that BAG3 can disassemble oligomers of Hsp27, likely by competing with the intra-molecular IPV motifs that normally hold together the oligomers.

4.3.4 BAG domain is essential for Hsp70 NEF function

In Chapter 2, we performed a detailed characterization of Hsp70 interactions with its various NEFs. We found that, of the human NEFs, BAG3 has the tightest interaction with Hsp70 (K_D ~10 nM) and that it was a potent stimulator of ADP and client release. However, we had not previously explored whether regions

outside the BAG domain might contribute to Hsp70 binding. Our results with BAG1 had suggested that while the BAG domain was sufficient for nucleotide release, alternate contacts might contribute to affinity and substrate release (Chapter 2). To explore this idea for BAG3, we measured binding of the BAG3 deletion mutants to Hsp70. Using FCPIA and ITC we first confirmed that the BAG domain is essential for binding to Hsp70 (Figure 4.6A & 4.6B). Much like BAG1, we found that the BAG domain alone bound weaker than the full-length protein, with an affinity ~3 fold lower (Figure 4.6A & 4.6B). These results suggest that, although the majority of the binding energy originates from the BAG domain-Hsp70 interaction, there are additional contacts in other regions.

a

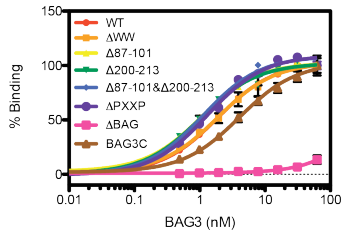

b

BAG3	NBDL	
	KD	N
WT	12.8 ± 4.3 nM	0.9 ± 0.01
ΔWW	10.0 ± 6.0 nM	0.88 ± 0.01
Δ87-101	5.9 ± 3.0 nM	1.0 ± 0.01
Δ200-213	7.5 ± 2.0 nM	0.92 ± 0.004
Δ87-101 & Δ200-213	23 ± 11 nM	0.91 ± 0.02
ΔPXXP	28 ± 13 nM	0.93 ± 0.04
ΔBAG	No Binding	No Binding
BAG3C	32 ± 12 nM	1.05 ± 0.02

c

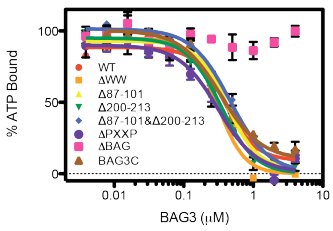

Figure 4.6 BAG3 deletions do not affect Hsp70 interactions. (a) Deletion of domains outside of the BAG domain do not affect binding to Hsp70 as measured by FCPIA. (b) ITC results confirm that only deletion of the BAG domain affects binding to Hsp70. (c) All BAG3 deletions can release nucleotide from Hsp70, except for ΔBAG as measured by fluorescence polarization. All experiments were performed in triplicate and error reported is SEM.

To test the functional importance of these interactions, we turned to the ATP release assay introduced in Chapter 2. We found that all of the domain deletion constructs were capable of releasing nucleotide from Hsp70 (Figure 4.6C), with the exception of the ΔBAG construct. Likewise, ATPase and luciferase refolding activities did not appear to be affected by any deletions outside of the BAG domain (Figure 4.7). Again, the BAG3C construct was less potent than its full-length counterpart (Figure 4.7A & 4.7C), suggesting that regions outside the BAG domain might be important. The Gestwicki laboratory is working with Professor Erik Zuiderweg to further explore the structural basis for these secondary contacts.

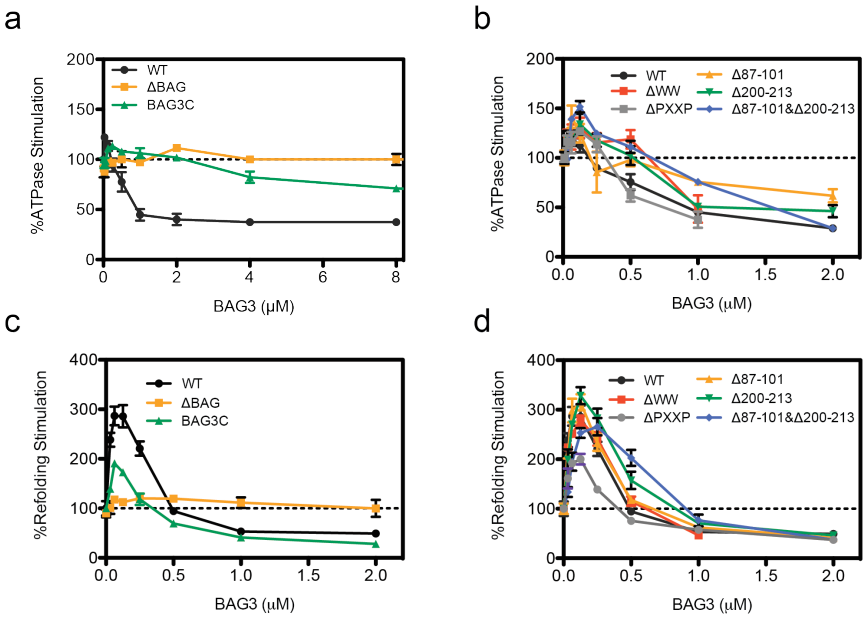

Figure 4.7 BAG3 deletions do not affect Hsp70 NEF function. (a) BAG3 stimulates ATP hydrolysis at low concentrations and inhibits ATP hydrolysis at high concentrations. BAG domain alone shows reduced activity and ΔBAG has no activity (b) Deletions outside of the BAG domain have no effect on ATPase activity. (c) BAG3 stimulates refolding of luciferase at low concentrations and inhibits at high concentrations. BAG domain alone shows reduced activity and ΔBAG has no activity (d) Deletions outside of the BAG domain have no effect on refolding activity. All experiments were performed in triplicate. Error is SEM.

4.3.5 Hsp70-BAG3-sHsp form a ternary complex

After characterizing the individual, binary interactions between BAG3-sHsp and BAG3-Hsp70, we set out to determine if a ternary Hsp70-BAG3-sHsp complex could be formed. The results of the binding studies thus far suggested that BAG3 is a highly modular scaffolding protein, leading to the prediction that binding to Hsp70 would not impact binding to sHsp and *vice versa*. To ask this question, we immobilized sHsps on streptavidin beads, incubated with a constant concentration (50 nM) of Alexa Fluor 647 (AF647) labeled BAG3, and then added increasing amounts of Alexa Fluor 488 (AF488) labeled Hsp70 (Figure 4.8B). If Hsp70 could compete with sHsp for binding to BAG3, we would expect to see a decrease in AF647 signal upon titration. However, we observed no decrease in AF647 fluorescence in the presence of Hsp70 (Figure 4.8A). Moreover, since we labeled BAG3 and Hsp70 with different fluorophores, we were also able to confirm both proteins were bound at the same time. Finally, the affinity of the

Hsp70 interaction was unchanged compared to the binary interaction (15 ± 3 nM), suggesting that sHsp does not interfere with (or promote) binding (Figure 4.6, also see Chapter 2 and Chapter 3). In control studies, we found that Hsp70 and sHsp did not bind to each other in the absence of BAG3 (Figure 4.8A). Thus, BAG3 appears to be a modular scaffolding protein for these two chaperones. To confirm this idea, we used size exclusion chromatography and SDS-PAGE (Figure 4.8C). In ongoing work, the Gestwicki laboratory is collaborating with the Southworth and Andrews laboratories to visualize this complex by electron microscopy and map the interactions by crosslinking and mass spectrometry.

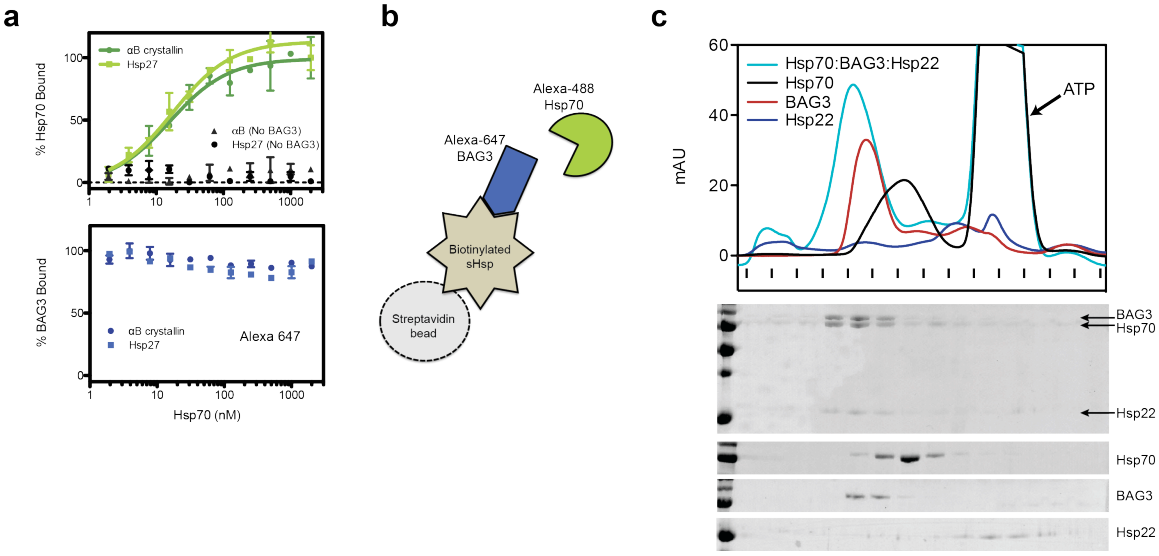

Figure 4.8 Hsp70-BAG3-sHsp form a ternary complex. (a) Alexa Fluor 488-labeled Hsp70 NBD was titrated against a solution of Alexa Fluor 647-labeled BAG3 in the presence of sHsp coated beads. Binding was detected using a flow cytometer. Experiments were performed in triplicate and error is SEM. (b) Schematic of binding experiment in (a). (c) SEC and SDS-PAGE gel analysis of Hsp22-BAG3-Hsp70 (12μM:6μM:6μM) in complex and as individual traces.

4.4 Discussion

Hsp70 and the sHsps constitute an ancient system for protecting unfolding proteins under conditions of proteotoxic stress. To understand the links between these important chaperone machines, we wanted to probe their structure, dynamics, and physical interactions. sHsps are capable of binding and stabilizing unfolded/denatured proteins in refolding competent forms [21]. Due to their lack of intrinsic refolding ability, sHsp must collaborate with refolding machineries, like

the Hsp70 system, to restore proper proteostasis [38]. Indeed, it has been shown both *in vitro* and *in vivo* that sHsp substrates can be refolded by the Hsp70 chaperone system [39-42]. However, a mechanistic understanding of how sHsps communicate with the Hsp70 system has been elusive, until now.

In order to examine the link between sHsps and the Hsp70 system, we focused our efforts on the Hsp70 NEF, BAG3. BAG3 had been reported to interact with sHsp [32, 33], but regulation of these interactions was not well understood. In this study, we first examined which sHsps could interact with BAG3. We found that all of the sHsp tested bound to BAG3 and formed a 2:1 (sHsp:BAG3) stoichiometric complex. This data (combined with the mutational analysis on BAG3's IPV motifs) allows us to propose that BAG3 uses both of its IPV motifs to engage the two β4-β8 grooves present in the obligate sHsp dimer, especially in the case of the dimeric Hsp27c. In the case of full length sHsps, which are known to form higher ordered oligomers, this does not rule out the possibility of 4:2, 8:4 or even 16:8 complexes, only that an overall ratio of 2:1 is likely to persist.

Affinity for smaller oligomeric sizes was evident in both binding platforms tested. Hsp20 and Hsp22 both lack their own IPV motifs and have reported to form smaller oligomers in solution [32, 43], and of the full length constructs tested displayed the highest affinity for BAG3. In the case of Hsp27, BAG3 preferred binding to Hsp27c, followed by Hsp27-3D and finally Hsp27. Again, pointing to oligomeric size, and overall accessibility of binding site as a main determinant for affinity. To further explore this point, we accessed the BAG3-Hsp27 complex size using SEC-MALS. As expected, incubation of full length Hsp27 with increasing amounts of BAG3 lead to an overall decrease in oligomeric size as well as increased the overall polydispersity of the complex.

To understand individual domain contributions we made a large suite of mutants and deletion constructs within the BAG3 sequence. We found that the IPV motifs provided the complete interaction surface for sHsps, and in some cases mutation

of four single residues (IPV to GPG in both motifs), was sufficient to completely kill binding. On the Hsp70 side, only deletion of the BAG domain affected BAG3's Hsp70 dependent activities. Like our previous work on BAG1, we observed reduced affinity with our BAG3C construct. Future work will be needed to determine if alternative contact sites on Hsp70 exist. Finally, since we had determined that BAG3 uses non-overlapping regions to interact with both proteins we asked if we could visualize a ternary complex. Using both FPCIA and SEC we saw that all three proteins can interact in one complex, and that this complex is indeed mediated by BAG3.

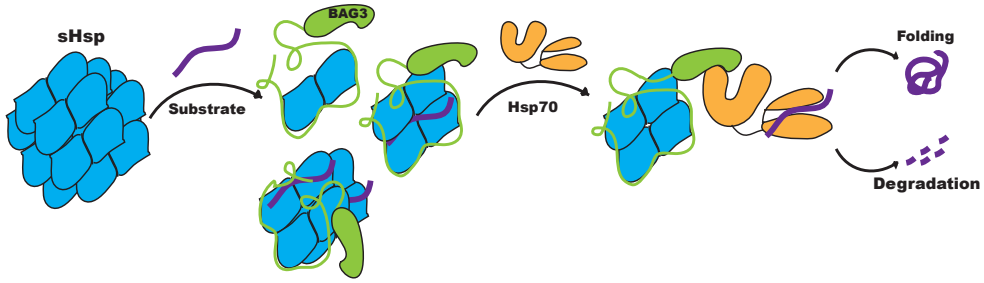

Figure 4.9 Model for BAG3 regulation of sHsp-Hsp70 substrate hand off. sHsps exist in large oligomeric ensembles in the cell. Under times of stress, sHsps can dissociate and bind unfolded substrates, protecting them from aggregation. BAG3 can promote small chaperone active forms of sHsps. When stress subsides BAG3 actively scaffolds sHsp-substrate complex with Hsp70 to promote active refolding of client proteins or promote autophagic clearance of terminally misfolded clients.

All of this data leads us to propose a model for substrate client hand off between the sHsp and Hsp70 chaperone systems. Under stress conditions when substrate proteins are destabilized and begin to unfold, sHsps are able to bind these partially or completely unfolded substrates and keep them in a folding competent state. The physiologic ensemble of sHsp oligomers are activated by a shift to a higher content of smaller oligomeric species. Upregulation of BAG3 and Hsp70 expression, then allows association of sHsp with BAG3 and an active pass to the Hsp70 chaperone system. Substrates can then under go cycles of concerted refolding or can be targeted for autophagic clearance via BAG3's association with dynein.

4.5 Methods

4.5.1 Cloning and Recombinant Protein Production.

All domain deletion constructs were subcloned from the BAG3 pMCSG7 parent vector using appropriate primers and confirmed with DNA sequencing. Mutations were constructed using standard mutagenesis protocols. Constructs for Hsp27, Hsp27c, Hsp27-3D, and αB crystallin were all received from the Klevit laboratory. Hsp22 was a kind gift from Jean-Marc Fontaine, and Hsp20 was received from the Conklin laboratory and subsequently cloned into the pMCSG7 vector.

All constructs were transformed into BL21(DE3) cells and single colonies were used to inoculate TB medium containing ampicillin (50 μg/mL). Cultures were grown at 37 °C for 5 hours, cooled to 20 °C and induced overnight with 200 μM IPTG. BAG3 full length and IPV mutants were purified as previously described [44]. BAG3 deletion constructs were pelleted and re-suspended in His Binding Buffer (50mM Tris, 300mM NaCl, 10mM imidazole, pH 8.0) + 3M Urea. Samples were sonicated and then applied to the Ni-NTA resin. After Ni-NTA columns, all proteins were subjected to TEV cleavage overnight, concentrated and applied to a Superdex S200 (GE Healthcare) size exclusion column in BAG buffer (25 mM HEPES, 5 mM $MgCl_2$, 150 mM KCl pH 7.5). Hsp72 and $Hsp72_{NBD}$ were purified as described elsewhere [45]. sHsp in plasmids containing an N-terminal His tag (Hsp27-3D, αB crystallin, Hsp22, and Hsp20) were all purified using a His column and subsequent SEC on a Superdex S200 in BAG buffer or PBS. Hsp27 and Hsp27c were in tagless vectors, so they were purified using a two step ammonium sulfate precipitation followed by MonoQ and SEC. Briefly, ammonium sulfate was added to a final concentration of 16.9% (w/v), centrifuged, pellet discarded, and then an additional 16.9% (w/v) ammonium sulfate was added to the supernatant to precipitate the protein from solution. Precipitated protein was brought up and dialyzed into MonoQ Buffer A (20mM Tris, pH 8.0) overnight, followed by a MonoQ column (0-1M NaCl gradient), and finally an SEC on a Superdex S75 (Hsp27c) or Superdex S200 (GE Healthcare) equilibrated in 50mM NaPi, 100mM NaCl, pH 7.5 buffer.

Proteins were labeled with Alexa Fluor® 488 5-SDP ester or Alexa Fluor® 647 NHS ester (Life Technologies) according to the suppliers instructions. Hsp70 and sHsp were biotinylated using EZ-link NHS-Biotin (Thermo Scientific) according to the supplier instructions. After labeling, the proteins were subjected to gel filtration to remove any unreacted label.

4.5.2 Flow Cytometry Protein Interaction Assay (FCPIA)

The assay procedure was adopted from previous reports. Briefly, biotinylated sHsp or Hsp70 was immobilized (1h at room temperature) on streptavidin coated polystyrene beads (Spherotech). After immobilization, beads were washed to remove any unbound protein and then incubated with labeled BAG3 protein at indicated concentrations. Binding was detected using an Accuri™ C6 flow cytometer to measure median bead-associated fluorescence. Beads capped with biocytin were used as a negative control, and non-specific binding to beads was subtracted from signal.

For ternary complex formation experiments, sHsps were immobilized on beads with constant concentration (50nM) of Alexa Fluor 647-labeled BAG3 present. Increasing concentrations of Alexa Fluor 488-labeled Hsp72 NBD were titrated against the sHsp-BAG3 solution and fluorescence was measured using an Accuri™ C6 flow cytometer. Again, beads capped with biocytin were used as a negative control, and non-specific binding to beads was subtracted from signal.

4.5.3 Isothermal Titration Calorimetry (ITC)

BAG3 constructs, $Hsp72_{NBD}$ and sHsps were dialyzed overnight against ITC buffer (25 mM HEPES, 5 mM MgCl2, 100 mM KCl pH 7.5). Concentrations were determined using a BCA Assay (Thermo Scientific), and the experiment was performed with a MicroCal VP-ITC (GE Healthcare) at 25 °C. $Hsp72_{NBD}$ (100 µM) or indicated sHsp (200 µM) in the syringe was titrated into a 10 µM cell solution

of BAG3 protein. Calorimetric parameters were calculated using Origin® 7.0 software and fit with a one-site binding model.

4.5.4 Co-immunoprecipitation

HEK293 cell extracts were prepared in M-PER lysis buffer (Thermo Scientific) and adjusted to 5mg of total protein in 1mL of extract. Equal 500µL samples were incubated with either a mouse monoclonal α-BAG3 (Santa Cruz sc-136467) or Goat IgG (Santa Cruz sc-2028). Samples were gently rotated overnight at 4°C, followed by a 4 h incubation with protein A/G-Sepharose Beads (Santa Cruz). The immunocomplexes were centrifuged at 1000 x g, washed 3 times with PBS pH 7.4, and eluted with SDS loading dye. Samples were run on a 4-15% Tris-Tricine gel (Bio-rad) and transferred to nitrocellulose membrane. The membranes were blocked in nonfat milk (5% milk in TBS, 0.1% Tween) for 1 h, incubated with primary antibodies for Hsp27 (Santa Cruz sc-59562) and BAG3 (Santa Cruz sc-136467) overnight at 4°C, washed, and then incubated with a horseradish peroxidase-conjugated secondary antibody (Anaspec) for 1 h. Finally, membranes were developed using chemiluminescence (Thermo Scientific, Supersignal® West Pico).

4.5.5 Nucleotide Release Assay

A fluorescent ATP analogue, N6-(6-Amino)hexyl-ATP-5-FAM (ATP-FAM) (Jena Bioscience) was used to measure BAG3 induced nucleotide dissociation from Hsp72. In black, round-bottom, low-volume 384-well plates (Corning), 1 µM Hsp72 and 20 nM ATP-FAM were incubated with varying concentrations of BAG3 protein for 10 minutes at room temperature in assay buffer (100 mM Tris, 20 mM KCl, 6 mM $MgCl_2$ pH 7.4). After incubation fluorescence polarization was measured (excitation: 485 nm emission: 535 nm) using a SpectraMax M5 plate reader.

4.5.6 Size Exclusion Chromotography

Solutions of BAG3 (6μM), Hsp72 (6μM), Hsp22 (12μM), and BAG3-Hsp72-Hsp22 (6μM:6μM:12μM) were examined using a Superdex S200 (GE Healthcare) size exclusion column. Indicated fractions were collected and analyzed using SDS-PAGE gel analysis. Samples were run on a 4-15% Tris-Tricine gel (Bio-rad) and stained with Coomassie Blue Reagent. Image color was changed to B&W to provide clarity.

4.5.7 Nuclear Magnetic Resonance (NMR)

HSQC spectra were acquired at 30C on a Bruker DRX500 with a QCl Z-axis gradient cryoprobe, running Topspin version 1.3. Spectra were acquired on samples containing 150-200μM Hsp27c in 50mM NaPi, 100mM NaCl, pH 7.5. Processing and spectral visualization was performed using rNMR [46] and Sparky.

4.5.8 SEC-MALS

Samples were resolved by analytical size exclusion chromatography on a Shodex 804 column on an Ettan LC (GE Healthcare). Molecular weights were determined by multiangle laser light scattering using an in-line DAWN HELEOS detector and an Optilab rEX differential refractive index detector (Wyatt Technology Corporation). The column was equilibrated overnight in BAG buffer prior to analysis. Samples were run at the indicated concentrations.

4.5.9 ATPase/Refolding Assay

Experiments were performed according to previous protocols [47, 48]. Briefly, Hsp72 (1μM) and J protein (DnaJB4, 0.25 μM) and various concentrations of BAG3 protein were added to clear 96 well plates and the reactions initiated with the addition of ATP (1 mM). The reactions proceeded for 1 h at 37 °C, developed with Malachite Green Reagent, quenched with sodium citrate, and plate absorbance was measured at 620nm. A phosphate standard curve was used to calculate pmol ATP/μM Hsp72/min.

4.5.10 Luciferase Refolding Assay.

Experiments were performed as described previously [49]. In brief, luciferase (Promega) was denatured in 6 M GnHCl for 1 h at room temperature, and then diluted into a working solution of Hsp72 (1μM) and DJB4 (0.5μM) in buffer containing an ATP regenerating system (23 mM HEPES, 120 mM KAc, 10mM Pi, 1.2 mM MgAc, 15 mM DTT, 61 mM creatine phosphate, 35 U/ml creatine kinase, 5 ng/μL BSA pH 7.4). Various concentrations of BAG3 were added and the reaction initiated with the addition of ATP (1 mM). Assay proceeded for 1 h at 37°C in white, 96 well plates and luminescence measured using SteadyGlo Luminescence reagent (Promega).

4.6 Notes

The work described here was done in collaboration with Leah Makley and Rebecca Freilich of the Gestwicki Laboratory. Likewise, future work determining the structure of sHsp-BAG3-Hsp70 complexes is being completed in collaboration with Eric Tse from the Southworth Laboratory.

4.7 References

1. Braun, N., et al., *Multiple molecular architectures of the eye lens chaperone alphaB-crystallin elucidated by a triple hybrid approach.* Proc Natl Acad Sci U S A, 2011. **108**(51): p. 20491-6.
2. Papadopoulos, J.S. and R. Agarwala, *COBALT: constraint-based alignment tool for multiple protein sequences.* Bioinformatics, 2007. **23**(9): p. 1073-9.
3. Zhu, H., et al., *Overexpressed BAG3 is a potential therapeutic target in chronic lymphocytic leukemia.* Ann Hematol, 2014. **93**(3): p. 425-35.
4. Franaszczyk, M., et al., *The BAG3 gene variants in Polish patients with dilated cardiomyopathy: four novel mutations and a genotype-phenotype correlation.* J Transl Med, 2014. **12**: p. 192.
5. Colvin, T.A., et al., *Hsp70-Bag3 interactions regulate cancer-related signaling networks.* Cancer Res, 2014. **74**(17): p. 4731-40.
6. Iwasaki, M., et al., *BAG3 directly associates with guanine nucleotide exchange factor of Rap1, PDZGEF2, and regulates cell adhesion.* Biochem Biophys Res Commun, 2010. **400**(3): p. 413-8.
7. Ulbricht, A., et al., *Cellular mechanotransduction relies on tension-induced and chaperone-assisted autophagy.* Curr Biol, 2013. **23**(5): p. 430-5.

8. Doong, H., et al., *CAIR-1/BAG-3 forms an EGF-regulated ternary complex with phospholipase C-gamma and Hsp70/Hsc70.* Oncogene, 2000. **19**(38): p. 4385-95.
9. Studer, S., et al., *A critical motif for oligomerization and chaperone activity of bacterial alpha-heat shock proteins.* Eur J Biochem, 2002. **269**(14): p. 3578-86.
10. Saji, H., et al., *Role of the IXI/V motif in oligomer assembly and function of StHsp14.0, a small heat shock protein from the acidothermophilic archaeon, Sulfolobus tokodaii strain 7.* Proteins, 2008. **71**(2): p. 771-82.
11. Pasta, S.Y., et al., *The IXI/V motif in the C-terminal extension of alpha-crystallins: alternative interactions and oligomeric assemblies.* Mol Vis, 2004. **10**: p. 655-62.
12. Fuchs, M., et al., *Identification of the key structural motifs involved in HspB8/HspB6-Bag3 interaction.* Biochem J, 2010. **425**(1): p. 245-55.
13. Chen, Y., et al., *Bcl2-associated athanogene 3 interactome analysis reveals a new role in modulating proteasome activity.* Mol Cell Proteomics, 2013. **12**(10): p. 2804-19.
14. Kassis, J.N., et al., *CAIR-1/BAG-3 modulates cell adhesion and migration by downregulating activity of focal adhesion proteins.* Exp Cell Res, 2006. **312**(15): p. 2962-71.
15. Boiani, M., et al., *The Stress Protein BAG3 Stabilizes Mcl-1 Protein and Promotes Survival of Cancer Cells and Resistance to Antagonist ABT-737.* J Biol Chem, 2013. **288**(10): p. 6980-90.
16. Virador, V.M., et al., *The anti-apoptotic activity of BAG3 is restricted by caspases and the proteasome.* PLoS One, 2009. **4**(4): p. e5136.
17. Gamerdinger, M., et al., *Protein quality control during aging involves recruitment of the macroautophagy pathway by BAG3.* EMBO J, 2009. **28**(7): p. 889-901.
18. Gamerdinger, M., et al., *BAG3 mediates chaperone-based aggresome-targeting and selective autophagy of misfolded proteins.* EMBO Rep, 2011. **12**(2): p. 149-56.
19. Kappe, G., et al., *The human genome encodes 10 alpha-crystallin-related small heat shock proteins: HspB1-10.* Cell Stress Chaperones, 2003. **8**(1): p. 53-61.
20. Basha, E., et al., *Chaperone activity of cytosolic small heat shock proteins from wheat.* Eur J Biochem, 2004. **271**(8): p. 1426-36.
21. Kakkar, V., et al., *Barcoding heat shock proteins to human diseases: looking beyond the heat shock response.* Dis Model Mech, 2014. **7**(4): p. 421-34.
22. Kim, K.K., R. Kim, and S.H. Kim, *Crystal structure of a small heat-shock protein.* Nature, 1998. **394**(6693): p. 595-9.
23. van Montfort, R.L., et al., *Crystal structure and assembly of a eukaryotic small heat shock protein.* Nat Struct Biol, 2001. **8**(12): p. 1025-30.
24. Jehle, S., et al., *N-terminal domain of alphaB-crystallin provides a conformational switch for multimerization and structural heterogeneity.* Proc Natl Acad Sci U S A, 2011. **108**(16): p. 6409-14.

25. Arrigo, A.P., *Human small heat shock proteins: protein interactomes of homo- and hetero-oligomeric complexes: an update.* FEBS Lett, 2013. **587**(13): p. 1959-69.
26. Aquilina, J.A., et al., *Polydispersity of a mammalian chaperone: mass spectrometry reveals the population of oligomers in alphaB-crystallin.* Proc Natl Acad Sci U S A, 2003. **100**(19): p. 10611-6.
27. Shashidharamurthy, R., et al., *Mechanism of chaperone function in small heat shock proteins: dissociation of the HSP27 oligomer is required for recognition and binding of destabilized T4 lysozyme.* J Biol Chem, 2005. **280**(7): p. 5281-9.
28. Giese, K.C. and E. Vierling, *Changes in oligomerization are essential for the chaperone activity of a small heat shock protein in vivo and in vitro.* J Biol Chem, 2002. **277**(48): p. 46310-8.
29. Stromer, T., et al., *Analysis of the interaction of small heat shock proteins with unfolding proteins.* J Biol Chem, 2003. **278**(20): p. 18015-21.
30. Sobott, F., et al., *Subunit exchange of multimeric protein complexes. Real-time monitoring of subunit exchange between small heat shock proteins by using electrospray mass spectrometry.* J Biol Chem, 2002. **277**(41): p. 38921-9.
31. Jovcevski, B., et al., *Phosphomimics destabilize hsp27 oligomeric assemblies and enhance chaperone activity.* Chem Biol, 2015. **22**(2): p. 186-95.
32. Carra, S., S.J. Seguin, and J. Landry, *HspB8 and Bag3: a new chaperone complex targeting misfolded proteins to macroautophagy.* Autophagy, 2008. **4**(2): p. 237-9.
33. Hishiya, A., et al., *BAG3 directly interacts with mutated alphaB-crystallin to suppress its aggregation and toxicity.* PLoS One, 2011. **6**(3): p. e16828.
34. Hochberg, G.K., et al., *The structured core domain of alphaB-crystallin can prevent amyloid fibrillation and associated toxicity.* Proc Natl Acad Sci U S A, 2014. **111**(16): p. E1562-70.
35. Carra, S., et al., *HspB8 chaperone activity toward poly(Q)-containing proteins depends on its association with Bag3, a stimulator of macroautophagy.* J Biol Chem, 2008. **283**(3): p. 1437-44.
36. Theriault, J.R., et al., *Essential role of the NH2-terminal WD/EPF motif in the phosphorylation-activated protective function of mammalian Hsp27.* J Biol Chem, 2004. **279**(22): p. 23463-71.
37. Aquilina, J.A., et al., *Subunit exchange of polydisperse proteins: mass spectrometry reveals consequences of alphaA-crystallin truncation.* J Biol Chem, 2005. **280**(15): p. 14485-91.
38. Haslbeck, M., et al., *Some like it hot: the structure and function of small heat-shock proteins.* Nat Struct Mol Biol, 2005. **12**(10): p. 842-6.
39. Mogk, A., et al., *Small heat shock proteins, ClpB and the DnaK system form a functional triade in reversing protein aggregation.* Mol Microbiol, 2003. **50**(2): p. 585-95.

40. Lee, G.J., et al., *A small heat shock protein stably binds heat-denatured model substrates and can maintain a substrate in a folding-competent state.* EMBO J, 1997. **16**(3): p. 659-71.
41. Ehrnsperger, M., et al., *Binding of non-native protein to Hsp25 during heat shock creates a reservoir of folding intermediates for reactivation.* EMBO J, 1997. **16**(2): p. 221-9.
42. Lee, G.J. and E. Vierling, *A small heat shock protein cooperates with heat shock protein 70 systems to reactivate a heat-denatured protein.* Plant Physiol, 2000. **122**(1): p. 189-98.
43. van de Klundert, F.A., et al., *The mammalian small heat-shock protein Hsp20 forms dimers and is a poor chaperone.* Eur J Biochem, 1998. **258**(3): p. 1014-21.
44. Rauch, J.N. and J.E. Gestwicki, *Binding of human nucleotide exchange factors to heat shock protein 70 (Hsp70) generates functionally distinct complexes in vitro.* J Biol Chem, 2014. **289**(3): p. 1402-14.
45. Thompson, A.D., et al., *Analysis of the tau-associated proteome reveals that exchange of Hsp70 for Hsp90 is involved in tau degradation.* ACS Chem Biol, 2012. **7**(10): p. 1677-86.
46. Lewis, I.A., S.C. Schommer, and J.L. Markley, *rNMR: open source software for identifying and quantifying metabolites in NMR spectra.* Magn Reson Chem, 2009. **47 Suppl 1**: p. S123-6.
47. Chang, L., et al., *High-throughput screen for small molecules that modulate the ATPase activity of the molecular chaperone DnaK.* Anal Biochem, 2008. **372**(2): p. 167-76.
48. Miyata, Y., et al., *High-throughput screen for Escherichia coli heat shock protein 70 (Hsp70/DnaK): ATPase assay in low volume by exploiting energy transfer.* J Biomol Screen, 2010. **15**(10): p. 1211-9.
49. Wisen, S. and J.E. Gestwicki, *Identification of small molecules that modify the protein folding activity of heat shock protein 70.* Anal Biochem, 2008. **374**(2): p. 371-7.

Chapter 5
Conclusions and Future Directions

5.1 Conclusions

Nucleotide exchange factors (NEFs) of Hsp70 are an interesting and diverse class of co-chaperone proteins. Human Hsp70 NEFs are involved in diverse biological pathways and the literature suggests their roles in a number of diseases [1-4]. As introduced in Chapter 1, there are three families of NEFs: HspBP1, Hsp110, and the BAG family. This thesis has focused on examining the biochemistry and function of the Hsp110 and BAG families. In choosing this topic for my thesis work, I wanted to better understand how the NEFs bind Hsp70, how they regulate chaperone function and how they might link Hsp70 to other pathways in the cell.

In Chapter 2, we showed how Hsp105 and the BAG family of NEFs regulate Hsp70 functions *in vitro*. Previous work had provided scattered examples of affinity constants and roles in Hsp70's ATPase and refolding activities. However, I wanted to take a systematic approach, allowing side-by-side comparisons of these NEFs. From my results, we identified a hierarchy of binding affinities, especially between BAG family members, indicates a striking layer of regulation that is likely exploited to promote specific Hsp70-NEF complexes in cells. The full diversity of Hsp70 chaperone function is further expanded with addition of the J protein co-chaperones. We have shown that individual complexes of Hsp70-NEF-J protein, can lead to distinct biochemical functions (*i.e*. ATPase stimulation, refolding activity). Thus, not all co-chaperones are created equal. Genetic studies (*e.g*. knockdowns, etc.) had suggested individual roles of specific co-chaperones in Hsp70 biology, but my results show that these functional differences are

manifested *in vitro* as well. An important implication of this paradigm is the prediction that chemical interruption of specific co-chaperones could provide discrete phenotypes that could be beneficial in treating disease. Further, the different biochemical properties of the complex might be helpful in identifying such molecules and/or optimizing their selectivity.

In Chapter 3, we expanded on this idea by screening for small molecules that could disrupt Hsp70-BAG3 complexes. Protein-protein interactions (PPIs) are notoriously hard to inhibit, so we developed a novel-screening platform, Capillary Electrophoresis (CE), that proved to be robust in PPI inhibitor detection. We used CE and a parallel screening platform, FCPIA, to identify molecules that were potent Hsp70-BAG3 inhibitors. Future work in the lab will likely explore these molecules as starting points for Hsp70-NEF modulators (see below). In addition, the CE method is expected to provide a powerful platform for studying additional PPIs and larger, multi-protein complexes.

Finally, in Chapter 4 we tackled an important question in NEF function; namely, by describing how BAG3 links Hsp70 to the small heat shock proteins (sHsps). Using BAG3 mutants and truncations, we were able to identify the specific regions that interact with sHsps and Hsp70. Beyond just passively binding to these partners, we found that BAG3 is an active member of the ternary complex. BAG3 is a potent NEF for Hsp70, regulating its ATPase and substrate binding activities. Moreover, we found that BAG3 can also regulate sHsp oligomer size, preferring smaller and presumably more active forms. Together, this data suggests that BAG3 bridges the Hsp70 and sHsps systems, potentially mediating client transfer between them and acting to activate both chaperones. These are exciting results that provide new insight into how different cellular chaperone systems communicate.

Overall, this thesis has advanced our understanding of human Hsp70 NEFs. This work has revealed important aspects of the chaperone system that were

previously unknown, including the first link between Hsp70 and the sHsps. Further, this work helped launch the first chemical inhibitors of the Hsp70-BAG3 PPI, generating powerful chemical probes for future studies.

5.2 Future Directions

5.2.1 Role of Hsp70-NEF complexes in disease

As summarized in Chapter 1, NEFs are involved in many human diseases. Some of the most striking examples include the overexpression of BAG3 and Hsp105 in multiple cancer types [5-8], the dual regulation of tau by BAG1 and BAG2 [9, 10], and genetic evidence that BAG3 mutations causing various myopathies [11, 12]. In most of these cases Hsp70 involvement is essential for disease manifestation, however, some of these functions may be independent. Future work should focus on elucidating which NEF functions are dependent on Hsp70. This knowledge will be important in understanding when and where to deploy inhibitors of Hsp70-BAG PPIs. Likewise, function of NEFs that are independent of Hsp70 might provide new opportunities for targeting PPIs between BAGs and other factors. An intriguing example of this is exemplified by BAG3. BAG3 has been reported to promote autophagic clearance of proteins, even in the absence of its BAG domain [13]. This activity seems to be dependent on specific phosphorylation events and interactions with 14-3-3 proteins/dynein [14]. Therefore, further work exploring this interaction, particularly which kinases are responsible for phosphorylating BAG3, may be an interesting route to understand BAG3 dependent autophagy. The hope is that the methods, ideas and framework provided here will accelerate these discoveries.

5.2.2 Future development of the CE platform to identify Hsp70-NEF inhibitors

In Chapter 3, we used two parallel high throughput screens to find molecules that could disrupt BAG3-Hsp70 interactions. We focused on a handful of the most active molecules, but further work is needed to fully characterize these molecules. Using Differential Scanning Fluorimetry (DSF), I found that some of these active molecules bound Hsp70 (Figure 5.1A). Additionally, they appeared to inhibit all of the major BAG and Hsp105 proteins with similar potency (Figure 5.1B). These studies suggest that the compounds from that screen act similarly to MKT-077 analogs to block Hsp70-NEF interactions (see below). However, future work will be needed to increase their potency and understand whether they are allosteric or orthosteric inhibitors. Another future direction for this project is the discovery of inhibitors that act on specific NEFs and not others. For example, a BAG3-selective inhibitor would be a useful tool for chemically disrupting this PPI. Although the screen in Chapter 3 did not achieve this goal, the CE platform appears to be well suited for asking this question. I propose that BAG1, BAG2 and BAG3 could be labeled with individual fluorophores and that their independent binding to Hsp70 could be monitored. Then, small molecules that preferentially disrupt one Hsp70-NEF complex, but not others could be selected as actives. This approach would require a multi-color CE instrument and considerable optimization of the conditions to allow all three complexes to form.

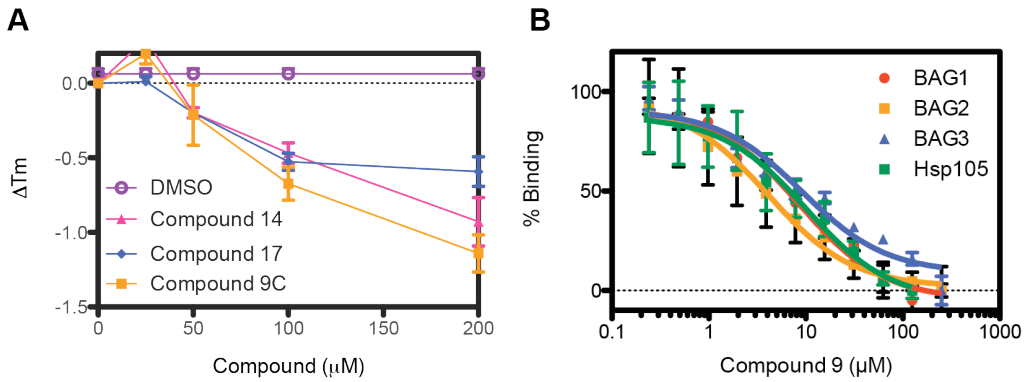

Figure 5.1 Hit compounds from Chapter 3 HTS are pan NEF-inhibitors. (A) Thermafluor experiments with Hsp70 and compound displayed a dose dependent decrease in melting temperature (Tm) compared to a DMSO control. This suggests that compounds bind and destabilize Hsp70. (B) FCPIA experiments showed that hit compounds were capable of inhibiting various Hsp70-NEF complexes. One representative compound is shown. Experiments were performed in triplicate and error is SEM.

However, it is a feasible concept and the Gestwicki laboratory is actively working towards this objective with the Kennedy group.

5.2.3 Use of the FCPIA platform to characterize Hsp70-NEF inhibitors.

In a series of papers published by our lab we have found that analogs of the MKT-077 molecule are potent NEF inhibitors (Figure 5.2A). This molecule (and its analogs) stabilize Hsp70 in an ADP-like state [15]; prolonging interactions with Hsp70 substrates, and inhibiting NEF induced substrate release/nucleotide turnover (Figure 5.2B). These molecules do not show selectivity among different NEF family members (Figure 5.2A). However, they have promising activity in a variety of disease models [16-19]. For example, the MKT-077 analog, YM-01 inhibits NEF interactions in cells (Figure 5.2C). In collaboration with Michael Sherman's group (Boston University), we have used YM-01 to show that Hsp70-BAG3 is a promising new cancer target because this complex is required for stability of multiple oncogenes, including FoxM1 and survivin [20]. YM-01 was

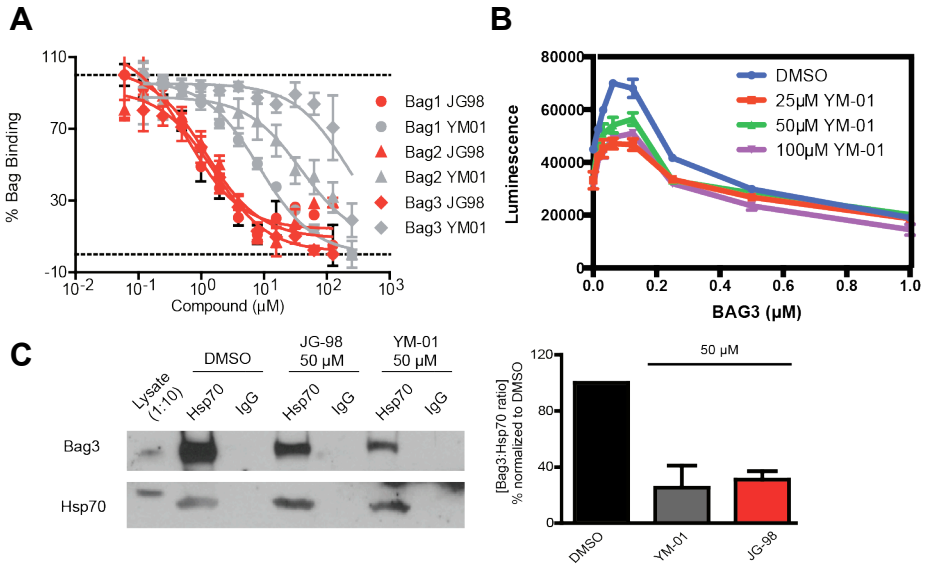

Figure 5.2 MKT-077 Analogs inhibit Hsp70-NEF interactions. A) YM-01 and JG-98 efficiently compete various Hsp70-NEF interactions in an *in vitro* FCPIA assay. Experiments were performed in triplicate over three independent experiments, which were normalized and combined; the error bars represent the SEM. B) YM-01 reduces BAG3 effects in an *in vitro* luciferase refolding assay. Experiments were performed in triplicate and the error bars represent SEM C) Co-immunoprecipitation assays of Hsp70 in HeLa lysate show that YM-01 and JG98 decrease the amount of Hsp70-BAG3 complex formed. Experiments were repeated in triplicate, with a representative gel shown. Quantitation of all experiments is shown to the right.

toxic to MDA-MB-231 and MCF7 breast cancer cells, with an EC_{50} around 4 μM. These results are interesting because the same molecules are not cytotoxic to normal fibroblasts (EC_{50} > 50 μM). Thus, cancer cells seem to be particularly "addicted" to the Hsp70-BAG3 complex. All of this data suggests that NEF inhibition may be a viable therapeutic approach in some disease indications. More broadly, the methods developed in this thesis provide a way to test, optimize and advance this chemical series. Hao Shao, a current postdoctoral fellow in the Gestwicki group, is pursuing this avenue.

Work towards Hsp70 inhibitors with new scaffolds is an active program in the Gestwicki laboratory (Figure 5.3B). In addition to the molecules found in Chapter 3 and the MKT-077 scaffold described above, work in the lab has also focused on new chemical matter. In all of these studies, the FCPIA assay is proving to be a workhorse method for rank-ordering compounds. Additionally, the fundamental binding constants and structural information in this thesis is helping guide decisions about which scaffolds to pursue. For example, Hao Shao and Izzy Taylor in the group have recently developed compounds JG2-10 and compound R and used the FCPIA platform to test their ability to inhibit the Hsp70-BAG1 interaction (Figure 5.3). Similarly, Hao Shao is using peptides derived from BAG1 as potential inhibitors (Figure 5.3), with the eventual goal of building

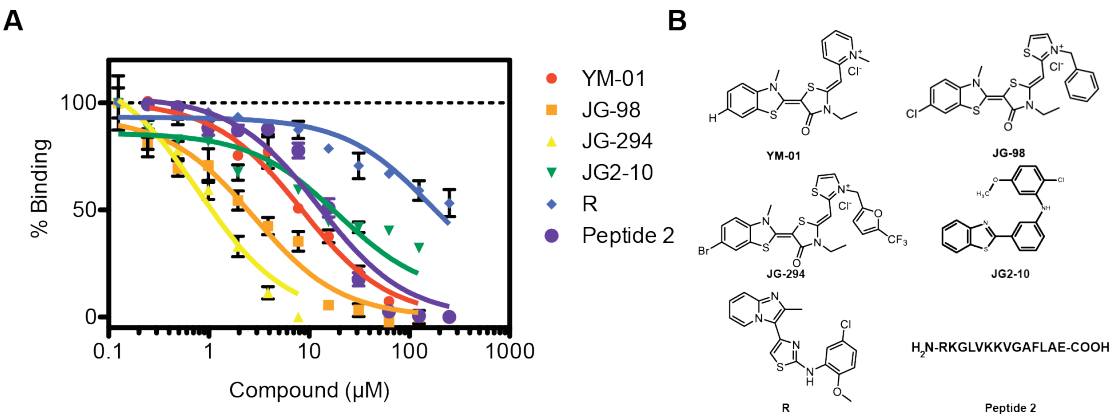

Figure 5.3 Various scaffolds inhibit BAG-Hsp70 interactions. (A) FCPIA shows that various small molecules and BAG1 derived peptides can inhibit Hsp70-BAG1 interactions. (B) Chemical structures of small molecules in (A).

peptidomimetics. While these peptides are still weak inhibitors, they may eventually progress to be useful probes. Additionally, they may provide a starting point for a fluorescence polarization (FP)-based high throughput screening effort. Our lab has used FP as a screening platform before [21], and while screening Hsp70 with BAG1 peptides might not lead to BAG1 specific inhibitors it could provide new chemical scaffolds worth pursuing.

5.2.3 Mutational analysis of BAG proteins suggest hotspots for targeting specific BAG-Hsp70 interactions

Structural information on BAG1-Hsp70 and BAG2-Hsp70 interactions has provided great starting points for mutational analysis of the BAG-Hsp70 complex. We have made a large suite of mutations on both the Hsp70 and BAG interfaces (Figure 5.4A) that disrupt or hinder binding. All residues on Hsc70 that we've analyzed can inhibit binding across the BAG family (Figure 5.4B – residues in red). However, overlaying the crystal structures of BAG1 and BAG2, we can highlight specific regions that may be key to developing BAG1/2 specific inhibitors (Figure 5.4B – yellow:BAG1 purple:BAG2). While both BAG1 and BAG2 share similar regions of binding on Hsc70 (red), alternative secondary interaction sites could be targeted to provide specificity. We have already shown that a peptide derived from the secondary BAG1 interaction site (Peptide 4), can

A

Hsc70	BAG2
N57A	Q156A
M61A	I160A
R,R 258,262 A,A	Q167A
E283D	
E,D 283,292 A,A	BAG3
	E455A
BAG1	E455K
E168A	R477A
R190A	R477H
R,K 193,194 A,A	R,R 480,481 A,A
Q201A	Q488A
D208A	E495A

B

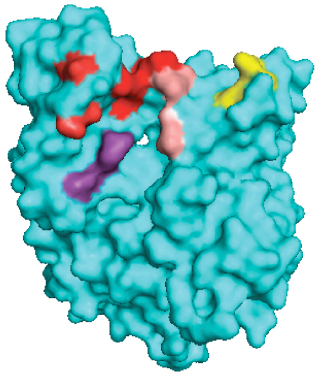

C

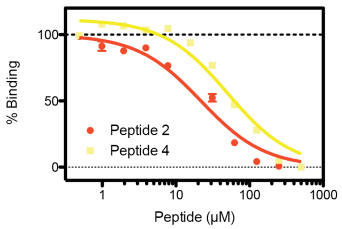

Figure 5.4 Mutagenesis and peptides provide clues on selective inhibition. (A) Table of various mutations that have been made in Hsc70 & BAG1-3. The shade of red indicates degree of inhibition with the darkest red indicating complete loss in binding and light pink with little to no loss in affinity. (B) Crystal structure of Hsp70 (PDB: 3AY9) with residues from (A) shown in red. Secondary sites of interaction for BAG1 (yellow) and BAG2 (purple) provide potential sites for selectivity. (C) BAG1 derived Peptide 4 can inhibit BAG1-Hsc70 interactions. Peptide 2 is composed of residues that bind in the red region of (B) and Peptide 4 is composed of residues that bind in the yellow region of (B)

indeed inhibit the BAG1-Hsc70 interaction (Figure 5.4C), albeit not as potent as the primary site (Peptide 2). Further testing will be needed to see if Peptide 4 is unable to compete a BAG2-Hsc70 interaction, whereas Peptide 2 would be predicted to be just as effective. Likewise, slightly below the primary binding site of both BAG proteins, lies an interaction surface that BAG2 seems to take advantage of, but is untouched in the BAG1 crystal structure. Mutagenesis of this site will be needed to test this hypothesis.

5.2.4 Targeting BAG proteins themselves

While targeting of Hsp70 is a proven strategy, another useful approach may be to target binding sites on NEFs instead. Within the BAG family, BAG2 shares very little sequence conservation among family members and as previously mentioned interacts down the backside of lobe II, instead of across the top of the NBD like BAG1. On top of this lack of conservation, attempts at making a functional BAG2 BAG domain have fallen short. Suggesting that unlike BAG1 and BAG3, BAG2 NEF activity may be dependent on regions outside of its BAG domain. This data, compiled with the inherent weak affinity of BAG2, implies that BAG2 may be the lowest hanging fruit on the Hsp70-NEF tree. Chemical matter that could specifically target a BAG2 would be useful as a chemical probe, since, in spite of being the most highly expressed BAG protein, very little research has focused on understanding BAG2's role in the cell.

5.2.5 Targeting BAG3 disease relevant mutants as therapies for cardiomyopathies

In Chapter 4 we performed a dissection of individual PPI domains in BAG3. BAG3 is a very interesting BAG protein due to its numerous roles outside of its basic NEF function. Site-specific mutations in BAG3, especially within various PPI regions, provide genetic support for targeting BAG3. One specific mutation that our lab has explored is BAG3P209L. This mutant causes a severe dominant myofibrillar myopathy [22]. Interestingly, this disease mutation occurs in the second IPV motif responsible for sHsp binding. Characterization of this mutant,

showed that while P209L shows no loss in Hsp70 binding affinity, sHsp stoichiometry drops and binding is dramatically affected (Figure 5.5A). Mutational scanning of this residue showed that while mutation to a hydrophobic at this position was detrimental, hydrophilic or neutral changes only showed modest losses in affinity with no stoichiometric change in binding (Figure 5.5B). Further analysis determined that a hydrophobic mutation was likely to cause β-sheet character in this region, and likely provided an interface for oligomer formation. This is in well agreement with previous work, noticing BAG3 positive puncta formation in BAG3P209L cells [23]. Our work, and others [24], would suggest that a monomeric version of BAG3P209L could still be functional in a cellular context. Now that we understand the biophysical properties of this mutant, it is possible that we could find chemical matter that could stabilize and promote monomerization.

A

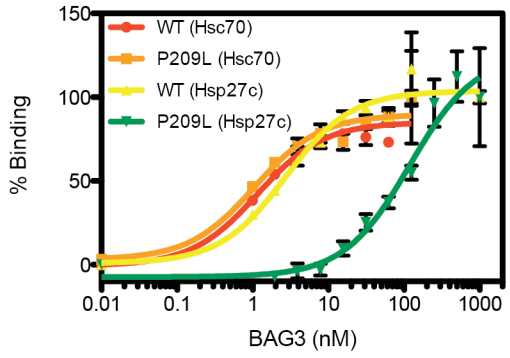

B

	ITC	
MUTANT	AVG FOLD CHANGE	N
P209A	2.0	1.98
P209D	1.9	1.93
P209G	1.9	1.84
P209K	2.6	2.03
P209I	3.6	0.91
P209L	3.7	1.07
P209W	2.8	1.33
P99L	5.2	1.15

Figure 5.5 Hydrophobic mutations in IPV motifs of BAG3 reduce affinity and stoichiometry of sHsp binding. (A) BAG3P209L shows reduced binding to Hsp27c, but no deficits in binding to Hsc70 as determined by FCPIA. (B) ITC results show that hydrophobic mutations result in loss in affinity as well as a drop in stoichiometry, while non-hydrophobic mutations are able to retain a 2:1 stoichiometry.

5.2.6 Structural and functional analysis of sHsp-BAG3-Hsp70 complex

In Chapter 4 we laid out a potential model for substrate hand off between the sHsp and Hsp70 chaperone systems. Further work will be needed to explicitly test this model. In particular, electron microscopy (EM) will be essential for understanding spatial constraints on a ternary complex of sHsp-BAG3-Hsp70.

Understanding how these proteins are oriented in respect to one another in the presence and absence of substrates will continue to drive our knowledge forward. Currently, we are collaborating with Eric Tse in the Southworth Laboratory to address these questions.

Likewise, developing a functional biochemical or cellular assay to study client handoff will be necessary. The Gestwicki laboratory is actively pursuing multiple avenues including, collaboration with the Conklin Laboratory at UCSF to look at BAG3's role in cardiomyocyte development, as well as exploring the microtubule associated protein tau as a potential client. Sue-Ann Mok and Rebecca Freilich are leading efforts to understand tau's association with both sHsp and Hsp70 using NMR and *in vitro* aggregation assays. Preliminary evidence suggests that sHsps can delay aggregation of disease relevant tau mutants and future work will determine if BAG3 can promote aggregation suppression. Furthermore, Rebecca has focused on developing classical chaperone substrate assays, like malate dehydrogenase (MDH) refolding, to focus on sHsp-Hsp70 hand off and to determine if BAG3 or BAG3 derived peptides can influence sHsp activity.

5.3 Notes

Some figures from this Chapter have appeared in the following manuscripts:
Colvin TA, Gabai VL, Gong J, Calderwood SK, Li H, Gummuluru S, Matchuk OH, Smirnova SG, Orlova NV, Zamulaeva IA, Garcia-Marcos M, Li X, Young ZT, **Rauch JN**, Gestwicki JE, Takayama S, Sherman MY. *Hsp70-Bag3 Interactions Regulate Cancer-Related Signaling Networks*. Cancer Research. 2014; 74(17):1-10.

Li X, Colvin TA, **Rauch JN**, Acosta-Alvear D, Kampmann M, Dunyak B, Hann B, Aftab BT, Murnane MR, Cho M, Walter P, Weissman JS, Sherman MY, Gestwicki JE. *Validation of the Hsp70-Bag3 Protein-Protein Interaction as a Potential Therapeutic Target in Cancer*. Molecular Cancer Therapeutics. 2015. [epub ahead of print]

5.4 References

1. Elliott, E., O. Laufer, and I. Ginzburg, *BAG-1M is up-regulated in hippocampus of Alzheimer's disease patients and associates with tau and APP proteins.* J Neurochem, 2009. **109**(4): p. 1168-78.
2. Souza, A.P., et al., *HspBP1 levels are elevated in breast tumor tissue and inversely related to tumor aggressiveness.* Cell Stress Chaperones, 2009. **14**(3): p. 301-10.
3. Knoll, R., et al., *The cardiac mechanical stretch sensor machinery involves a Z disc complex that is defective in a subset of human dilated cardiomyopathy.* Cell, 2002. **111**(7): p. 943-55.
4. Nakamura, J., et al., *Targeted disruption of Hsp110/105 gene protects against ischemic stress.* Stroke, 2008. **39**(10): p. 2853-9.
5. Kai, M., et al., *Heat shock protein 105 is overexpressed in a variety of human tumors.* Oncol Rep, 2003. **10**(6): p. 1777-82.
6. Oda, T., et al., *Prognostic significance of heat shock protein 105 in lung adenocarcinoma.* Mol Med Rep, 2009. **2**(4): p. 603-7.
7. Festa, M., et al., *BAG3 protein is overexpressed in human glioblastoma and is a potential target for therapy.* Am J Pathol, 2011. **178**(6): p. 2504-12.
8. Zhu, H., P. Liu, and J. Li, *BAG3: a new therapeutic target of human cancers?* Histol Histopathol, 2012. **27**(3): p. 257-61.
9. Carrettiero, D.C., et al., *The cochaperone BAG2 sweeps paired helical filament- insoluble tau from the microtubule.* J Neurosci, 2009. **29**(7): p. 2151-61.
10. Elliott, E., P. Tsvetkov, and I. Ginzburg, *BAG-1 associates with Hsc70.Tau complex and regulates the proteasomal degradation of Tau protein.* J Biol Chem, 2007. **282**(51): p. 37276-84.
11. Homma, S., et al., *BAG3 deficiency results in fulminant myopathy and early lethality.* Am J Pathol, 2006. **169**(3): p. 761-73.
12. Norton, N., et al., *Genome-wide studies of copy number variation and exome sequencing identify rare variants in BAG3 as a cause of dilated cardiomyopathy.* Am J Hum Genet, 2011. **88**(3): p. 273-82.
13. Carra, S., S.J. Seguin, and J. Landry, *HspB8 and Bag3: a new chaperone complex targeting misfolded proteins to macroautophagy.* Autophagy, 2008. **4**(2): p. 237-9.
14. Xu, Z., et al., *14-3-3 protein targets misfolded chaperone-associated proteins to aggresomes.* J Cell Sci, 2013. **126**(Pt 18): p. 4173-86.
15. Rousaki, A., et al., *Allosteric drugs: the interaction of antitumor compound MKT-077 with human Hsp70 chaperones.* J Mol Biol, 2011. **411**(3): p. 614-32.
16. Li, X., et al., *Analogs of the Allosteric Heat Shock Protein 70 (Hsp70) Inhibitor, MKT-077, as Anti-Cancer Agents.* ACS Med Chem Lett, 2013. **4**(11).

17. Li, X., et al., *Validation of the Hsp70-Bag3 Protein-Protein Interaction as a Potential Therapeutic Target in Cancer.* Mol Cancer Ther, 2015.
18. Jinwal, U.K., et al., *Chemical manipulation of hsp70 ATPase activity regulates tau stability.* J Neurosci, 2009. **29**(39): p. 12079-88.
19. Wang, A.M., et al., *Activation of Hsp70 reduces neurotoxicity by promoting polyglutamine protein degradation.* Nat Chem Biol, 2013. **9**(2): p. 112-8.
20. Colvin, T.A., et al., *Hsp70-Bag3 interactions regulate cancer-related signaling networks.* Cancer Res, 2014. **74**(17): p. 4731-40.
21. Connarn, J.N., et al., *The molecular chaperone Hsp70 activates protein phosphatase 5 (PP5) by binding the tetratricopeptide repeat (TPR) domain.* J Biol Chem, 2014. **289**(5): p. 2908-17.
22. Selcen, D., et al., *Mutation in BAG3 causes severe dominant childhood muscular dystrophy.* Ann Neurol, 2009. **65**(1): p. 83-9.
23. Arimura, T., et al., *Dilated cardiomyopathy-associated BAG3 mutations impair Z-disc assembly and enhance sensitivity to apoptosis in cardiomyocytes.* Hum Mutat, 2011. **32**(12): p. 1481-91.
24. Ruparelia, A.A., et al., *Zebrafish models of BAG3 myofibrillar myopathy suggest a toxic gain of function leading to BAG3 insufficiency.* Acta Neuropathol, 2014. **128**(6): p. 821-33.

Appendix A

Cysteine Reactivity Distinguishes Redox Sensing by the Heat Inducible and Constitutive Forms of Heat Shock Protein 70 (Hsp70)

A.1 Abstract

The heat shock protein 70 (Hsp70) family of molecular chaperones has important functions in maintaining proteostasis under stress conditions. Several Hsp70 isoforms, especially Hsp72 (HSPA1A), are dramatically upregulated in response to stress; however, it is unclear whether these family members have biochemical properties that are specifically adapted to these scenarios. The redox-active compound, methylene blue (MB), has been shown to inhibit the ATPase activity of Hsp72 *in vitro* and it promotes degradation of the Hsp72 substrate, tau, in cellular and animal models. Here, we report that MB irreversibly inactivates Hsp72 but not the nearly identical, constitutively expressed isoform, heat shock cognate 70 (Hsc70; HSPA8). Mass spectrometry results show that MB oxidizes Cys306, which is not conserved in Hsc70. Molecular models suggested that oxidation of Cys306 exposes Cys267 to modification and that both events contribute to loss of ATP binding in response to MB. Consistent with this model, mutating Cys267 and Cys306 to serine made Hsp72 largely resistant to MB *in vitro* and over-expression of the C306S mutant blocked MB-mediated loss of tau in a cellular model. Further, mutating Cys267 and Cys306 to the pseudo-

oxidation mimic, aspartic acid, mirrored MB treatment: the C267D and C306D mutants had reduced ATPase activity *in vitro* and over-expression of the C267/306D double mutant significantly reduced tau levels in cells. Together, these results suggest that redox sensing by specific cysteine residues in Hsp72, but not Hsc70, may be an important component of the chaperone response to oxidative stress, protecting unfolded substrates from oxidation.

A.2 Introduction

Reactive oxygen species (ROS), such as free radicals and peroxides, are produced as the result of normal metabolic and signaling processes [1-3]. However, an abundance of ROS is also implicated in oxidative damage to lipids, nucleic acids and proteins, contributing to pathology in a number of diseases [4-6]. Thus, to control the accumulation of ROS, organisms are equipped with several scavengers, such as glutathione and ascorbate [7], and redox-sensitive transcription factors, including HIF1α [8], NF-κB [9] and HSF1 [10], that coordinate cellular adaptation to ROS. Another important cellular response is to protect the proteome from acute denaturation and aggregation, which could cause proteotoxicity. This type of ROS protection is often provided by a molecular chaperone that contains a reactive redox sensor (*e.g.* cysteine residue) linked to a system for protecting other proteins from oxidative unfolding. For example, the prokaryotic heat shock protein 33 (Hsp33) contains cysteine residues that are selectively oxidized in response to redox stress, which induces a conformation with high chaperone activity [11].

The heat shock protein 70 (Hsp70) family is a series of highly conserved molecular chaperones that are well known for their activity in maintaining global proteostasis. Hsp70s are involved in most steps in the life of a protein, including the folding of nascent polypeptides, protein trafficking and degradation [12]. Members of the Hsp70 family specifically interact with unfolded substrates through a C-terminal, substrate-binding domain (SBD). In addition, Hsp70s also have a conserved N-terminal nucleotide-binding domain (NBD), which binds and hydrolyzes ATP. These two domains are allosterically coupled, such that ATP hydrolysis within the NBD causes conformational changes in the SBD that enhance affinity for unfolded substrates [13]. In turn, binding of Hsp70s to unfolded proteins protects them against aggregation and assists with their refolding. However, if this process fails, Hsp70s are also involved in triage, shuttling misfolded proteins to the proteasome for turnover [14]. Through these activities, Hsp70s have been linked to diseases associated with aberrant protein quality control, such as cancer and neurodegenerative disease [15, 16].

In humans, the cytosol contains at least six Hsp70 isoforms, including the constitutively expressed Hsc70 (HSPA8) and the major stress inducible isoform, Hsp72 (HSPA1A) [17]. Hsp72 and Hsc70 have very high sequence similarity (85% identical and 94% similar). However, the levels of Hsp72 are typically low under normal conditions and they are only highly induced in response to stress, including redox imbalance [18]. Thus, Hsp72 belongs to a subfamily of Hsp70s, including HSPA6, HSPA7 and HSPA4, which is characterized by elevated

expression in response to stress. One important question is whether the different family members, such as the stress-inducible forms, have any specialized biochemical functions that might distinguish them from the constitutive ones.

Previously, we identified methylene blue (MB) as an inhibitor of the ATPase activity of Hsp72 in a high throughput chemical screen [19]. This compound has been shown to reduce the levels of some Hsp72 substrates, such as tau, polyglutamine fragments and Akt, in cells [19-22]. MB also improves cognitive functions in mouse models of Alzheimer's disease (AD) [20, 23] and it has been explored in Phase IIb clinical trials in AD patients [24]. Although MB is a highly promiscuous compound, it has an enviable safety record and is used clinically for multiple indications [25]. For these reasons, we decided to further explore the mechanism by which it might inactivate Hsp70s. Specifically, we hypothesized that MB might prevent ATP turnover in Hsp72 by oxidizing cysteine residues [26, 27], because MB has been shown to oxidize sulfhydryls in other targets [28]. Here, we report that Hsp72 is indeed oxidized by MB and that treatment with either MB or hydrogen peroxide irreversibly inactivates ATP turnover *in vitro.* Based on modeling studies and mutagenesis, this inhibition appears to be caused by oxidation-induced conformation changes in the NBD that block ATP binding. However, during the course of these studies we also made the unexpected observation that the constitutive Hsp70 family member, Hsc70, is entirely resistant to irreversible inhibition by MB. Mass spectrometry and point mutants revealed that two reactive cysteines, C267S and C306S, are sufficient to

distinguish the special sensitivity of Hsp72 to MB *in vitro* and in cells. Interestingly, Cys306 is also highly conserved in the other stress-inducible Hsp70 isoforms, but it is absent from constitutive forms, supporting the idea that this residue is important in stress-related redox signaling. Thus, these finding suggest a major difference between closely related Hsp70 isoforms, which may be important in redox signaling and protecting cells from oxidative stress. Moreover, this work may provide insight into one mechanism by which MB reduces tau accumulation in cells, animals and AD patients.

A.3 Results

A.3.1 MB and H_2O_2 irreversibly inhibits Hsp72 but not Hsc70

Because MB has been known to directly oxidize sulfhydryls [28], we hypothesized that the inhibition of Hsp70's ATPase activity by MB [19, 29]. may involve oxidation of cysteines. To test this idea, Hsp72 was treated with MB (200 μM) at 37 ^{o}C for 1 hour and then dialyzed to remove any remaining compound. The remaining ATPase activity in the MB-treated Hsp72 sample was then measured using a malachite green assay [30]. Because Hsp72 is a weak ATPase, the stimulatory co-chaperone, DnaJ, was added to enhance nucleotide turnover in these experiments. Using this approach, we found that MB-treated Hsp72 had dramatically reduced ATPase activity (Figure A.1a). Hsp72 was also inhibited by treatment with hydrogen peroxide (100 μM) under similar conditions, suggesting that the loss of activity was due to oxidation (Figure A.1A). Cysteine residues in proteins can be progressively oxidized to sulfenic, sulfinic and then sulfonic acids [31], but only sulfenic acids are readily reversible by glutathione or

DTT [32]. The ATPase activity of MB-treated Hsp72 was only partially recovered after exposure to DTT (1 mM), suggesting that MB irreversibly oxidizes most of the protein.

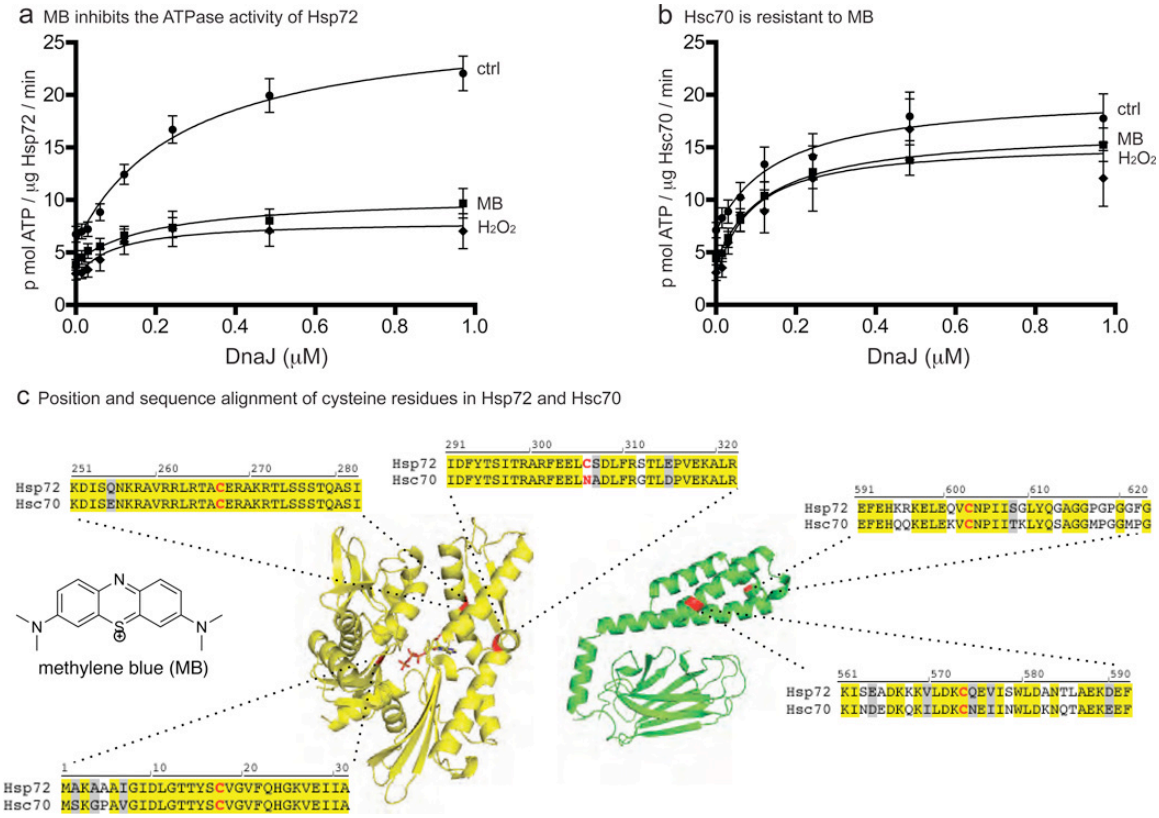

Figure A.1 The ATPase activity of Hsp72, but not Hsc70, is sensitive to oxidation. (A) Purified Hsp72 (0.6 µM) was incubated with either MB, peroxide (H2O2) or a mock control and the remaining compound removed by extensive dialysis. The stimulation of ATPase activity by the model J co-chaperone, DnaJ, was then measured. Results are the average of three experiments performed in triplicate. Error bars are standard error of the mean (SEM). (B) Human Hsc70 is resistant to oxidation. Experiments were performed as described for panel A. (C) The locations of cysteine residues (red) in Hsp72 are shown using the crystal structures of the NBD (pdb # 3JXU) and the SBD (pdb # 1DKX). In the insets, identical residues are shown in yellow, conserved residues in gray and the positions of cysteines are red. Alignments were prepared in Vector NTI (Invitrogen).

Initially as a control, the effects of MB on the ATPase activity of Hsc70 were evaluated. Unexpectedly, we found that MB had no effect on Hsc70 (Figure A.1B). The chemical differences between these two well-conserved (85% identical and 94% similar) Hsp70 isoforms were then more closely examined.

Sequence alignments of the human proteins showed that Hsp72 has five cysteine residues (three in the NBD and two in the SBD) whereas Hsc70 has only four (two each in the NBD and SBD). Thus, one difference between these isoforms is that Hsp72 has a unique Cys306, which is an asparagine in Hsc70 (Figure A.1C). The sequences of a number of inducible or constitutive human Hsp70 family members were then examined, revealing that Cys306 is exclusively found in stress inducible Hsp70s but not in any of the constitutively expressed family members (Figure A.2). Moreover, C267 is conserved in 4 of 5 inducible family members and only 2 of 5 constitutive forms (Figure A.2), suggesting that

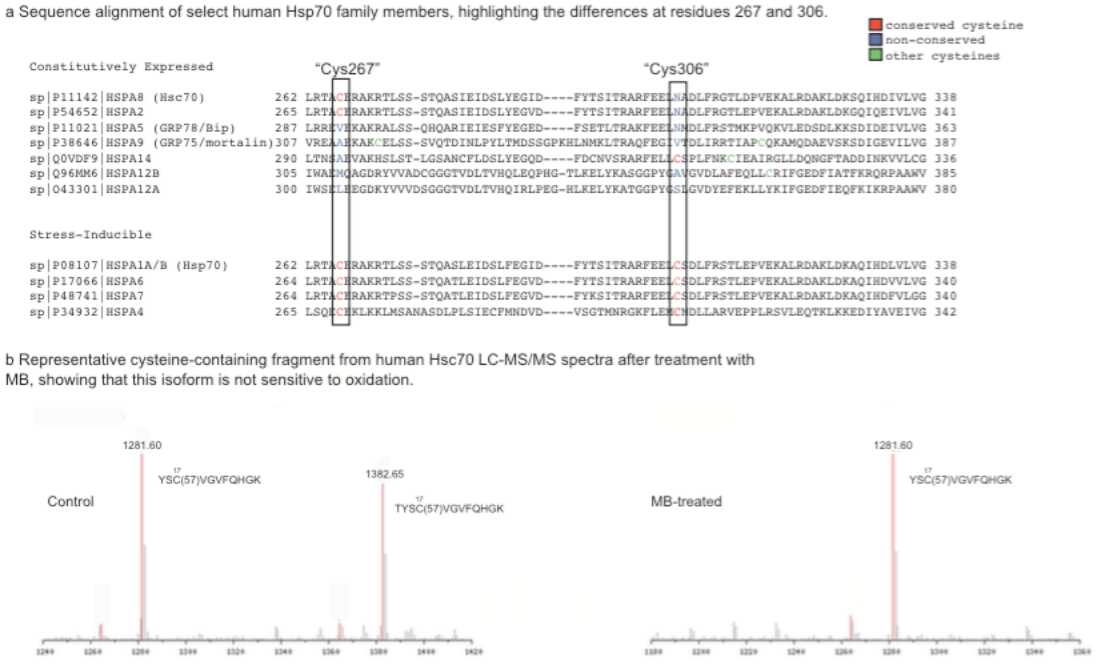

Figure A.2 Stress inducible, but not constitutive forms of the Hsp70 family contain a unique, reactive cysteine at position 306. (a) Sequence alignment of select human Hsp70 family members, showing conservation of cysteine 306 in stress inducible, but not constitutive forms. The 267 and 306 numbers are derived from human Hsp72 (HSP1A1). For more information see Fujikawa et al. (2010) Cell Stress Chaperones 15:193-204. (b) Representative trypsin fragment of human Hsc70 treated with MB (200 μM), as in Fig. 2, showing that Cys17 is not oxidized. In addition, no other fragments in the Hsc70 sequence were oxidized. As discussed in the text, the fragment containing 267 was not observed in the spectra.

both of these residues may be important. Together, these results suggest that MB might selectively compromise ATPase by oxidizing at least one cysteine in Hsp72, but not Hsc70.

A.3.2 MB oxidizes Cys306 of Hsp72

To map which cysteines in Hsp72 were oxidized by MB, a well-established mass spectrometry (MS) method using dimedone (5,5-dimethyl-1,3-cyclohexanedione) was employed. Briefly, dimedone is known to react with oxidized cysteines to form stable thioethers that are readily observed in the MS spectra as a +138 Da shift in molecular mass (Figure A.3A). Accordingly, MB-treated Hsp72 was treated with dimedone and unreacted thiols were capped with carbamidomethyl groups. Subsequent trypsin digestions and analysis by LC-tandem MS/MS

a Reactions of free thiol with iodoacetamide and oxidized cysteine with dimedone

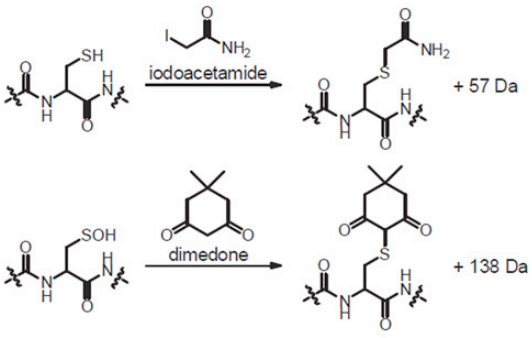

b Mass spectrometry results indicate oxidation of Hsp72 Cys306

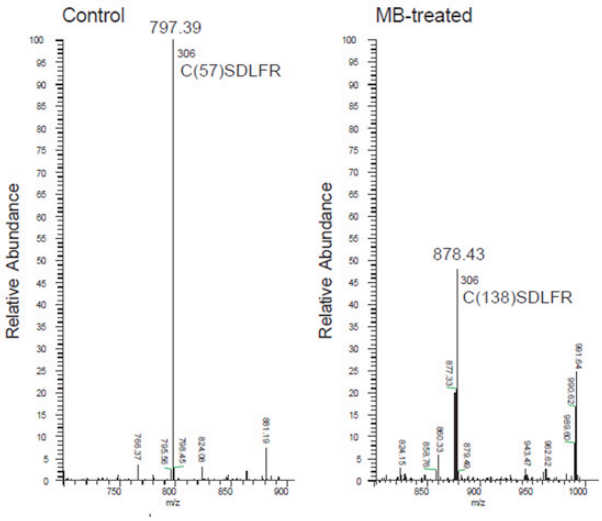

c. Reactivity of cysteines in Hsp72 and Hsc70 to MB

residue	Hsp72		Hsc70		MB (200 µM)
	-	+	-	+	
C17	+57	+57	+57	+57	
C267	n.d.	n.d.	n.d .	n.d.	
C306	+57	+138	n.a.	n.a.	
C574	+57	+57	+57	+57	
C603	+57	+57	+57	+57	

Figure A.3 Hsp72 is oxidized by MB at specific cysteine residues. (A) Schematic of the specific reactions of iodoacetimide with free thiol and dimedone with sulfenic acid, producing a mass shift of +57 or +138 Da, respectively. (B) Select region of the MS/MS spectra focused on the region including the C306 fragment (CSDLFR 306-311). This fragment is 797.39 Da in the mock treated control (indicating iodoacetamide capping) and 878.43 Da in the MB treated (indicating dimedone conjugation). (C) Summary of the mass spectrometry findings, showing that MB only oxidized C306 in Hsp72. n.d. = not detected. n.a = residue not conserved.

revealed that the mass of the fragment containing Cys306 in Hsp72 was oxidized (Figure A.3B). No other residues were modified, although it is important to note that the fragment containing Cys267 was not detected (likely because the nearby region is highly charged) (Figure A.3C). As expected from the ATPase experiments, Hsc70 treated with MB was resistant to modification by dimedone (Figure A.3C and Figure A.2B). Thus, Hsp72 differs from Hsc70 in reactivity of its cysteines at positions 306 and perhaps 267.

A.3.3 Hsp72 Cys to Ser mutations confer resistance to MB

The mass spectrometry studies suggested that MB-based oxidation of specific cysteines might be responsible for the compound's effects on Hsp72's ATPase activity. To test this idea, Cys306, Cys267 or both residues were mutated to serine by site-directed mutagenesis and the resulting mutant proteins were purified. These substitutions did not change the global structure (Figure A.4) or ATPase activity of the mutant chaperones (Figure A.5A-C). However, the ATPase activities of C267S (Figure A.5A) and C306S (Figure A.5B) were

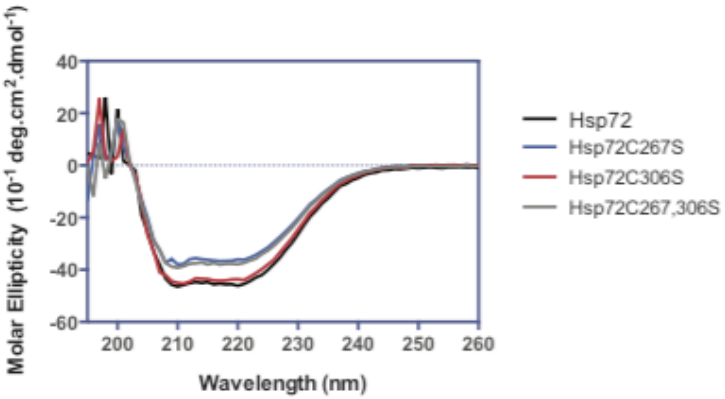

Figure A.4 Serine point mutants Hsp72 C267S and C306S and the double mutant C267/306S) are properly folded, as measured by circular dichroism.

partially resistant to MB (50 μM) and the double mutant (C267/306S) was completely resistant (Figure A.5C). Thus, MB appeared to exert its inhibitory effect on Hsp72 ATPase activity via oxidation of these cysteines and both residues appeared to be involved.

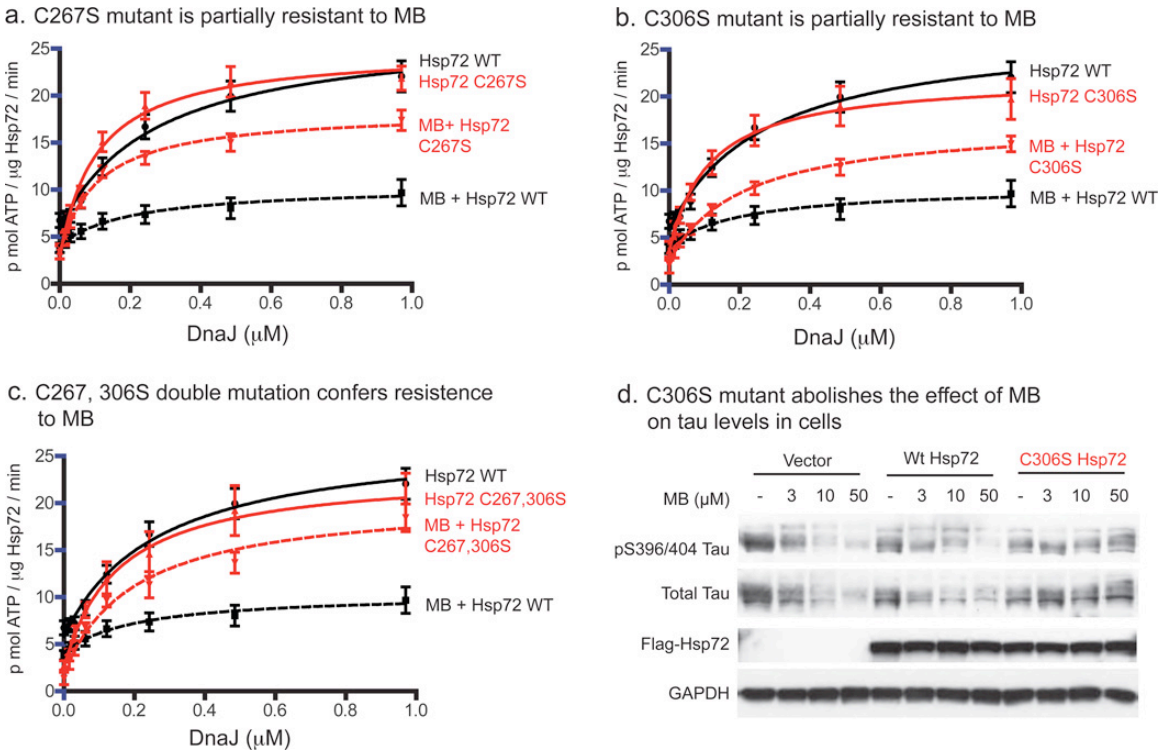

Figure A.5 Serine mutants of Hsp72 are resistant to MB treatment in ATPase and cell-based assays. (A) C267S mutation confers partial resistance to MB (50 μM). (B) C306S confers partial resistance to MB (50 μM). (C) C267, 306S double mutation confers resistance to MB (50 μM). All of the ATPase experiments were performed at least twice in triplicate and error bars are SEM. (D) Over-expression of the C306S mutation blocks MB-mediated clearance of tau. HeLaC3 cells were transfected with vector, Flag-tagged WT Hsp72 or C306S Hsp72 mutant for 48 hours and then treated with MB for 10 minutes. Samples were analyzed by western blot and the results are representative of experiments performed in duplicate.

MB is known to reduce tau levels in cells through a mechanism dependent on Hsp72 [19]. Thus, the over-expression of the C306S, C267S and C267/306S mutants may de-sensitize cells to MB. In fact, when HeLaC3 cells were stably transfected with Hsp72 C306S, MB no longer reduced the levels of

phosphorylated (pS396/404) or total tau (Figure A.5D). Together, these results strongly suggest that MB acts on Hsp72 by oxidizing Cys267 and Cys306, and that this activity is important in regulating the levels of tau.

A.3.4 C267D mutation causes a conformational change and disrupts nucleotide binding

To gain some insight into the structural basis of these observation, the NBD of Hsp72 containing a C267D mutation was modeled using Robetta [33], using the structure of human Hsp72 NBD in the ADP form (3JXU) as a starting point [34]. An aspartic acid substitution was used because it sterically and electronically mimics oxidized cysteine [35]. A comparison of the structures of the wild type Hsp72 NBD and the C267D Hsp72 NBD showed that they were globally very similar, with an RMSD of 1.55Å and a TM-score of 0.94 (Figure A.6A). However, several residues that are specifically involved in nucleotide binding were predicted to be significantly shifted. For example, Gly339, which makes a hydrogen bond interaction with the alpha phosphate group of ADP, was shifted away from the nucleotide by 1.0 Å, likely preventing the formation of this important bond (Figure A.6B). Further, Arg272, which interacts with the adenine ring by pi-stacking, is significantly pulled away by regional rotations in the backbone (Figure A.6C). Collectively, these changes and others resulted in side chain displacements totaling more than 25Å in the nucleotide binding cleft. Very similar results were seen with the C306D mutant, suggesting that these residues might both contribute to conformational rearrangements (Figure A.7A). Interestingly, oxidation of C306 is predicted to swivel residue C267 into the solvent-exposed cleft above nucleotide in the NBD (Figure A.7B), perhaps

making it more accessible to oxidation by MB. Together, these *in silico* observations suggest that oxidation of Cys267 and Cys306 in Hsp72 might damage nucleotide binding and inactivate ATP turnover. Further, these results

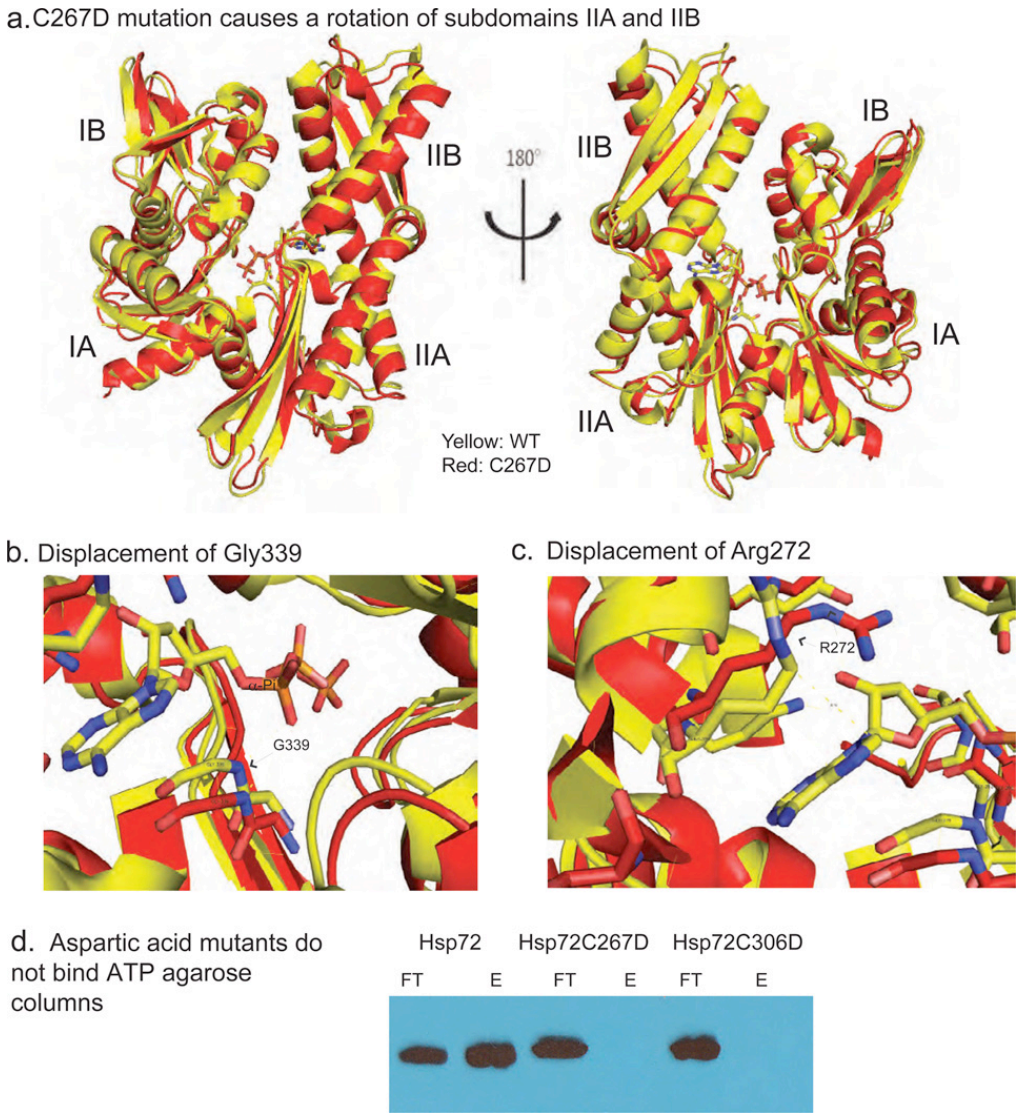

Figure A.6 Modeling of Hsp72 C267D reveals structural changes in residues that contact nucleotide. (A) Overall alignment of the NBDs of Hsp72 (yellow: pdb entry 3JXU) and Hsp72 C267D Model (red: modeled from template 3JXU using Robetta Server). In the C267D model, (B) Gly339 is shifted away from the a-phosphate of nucleotide and (C) Arg272 is shifted away from the adenine ring. In total, C267D caused structural changes totaling 25Å. Similar results were seen in the C306D mutant. (D) Purified C267D and C306D mutants do not bind nucleotide. Purified mutants and wild type Hsp72 (5 μM) were treated with 1 mL of ATP-agarose, washed with 3 mL of Buffer A (25 mM HEPES, 10 mM KCl, 5 mM MgCl2, pH 7.5) and flowthrough (FT) collected. Following three additional washes, the remaining protein was collected in the eluant (E) by washing with 3 mL of Buffer A containing 3 mM ATP. Fractions were analyzed on 1-20% Tris-Tricine gels using a polyclonal anti-Hsp72 antibody (Enzo).

suggest that sequential oxidation of C306 and then C267 may reinforce and promote these conformational changes (Figure A.7C).

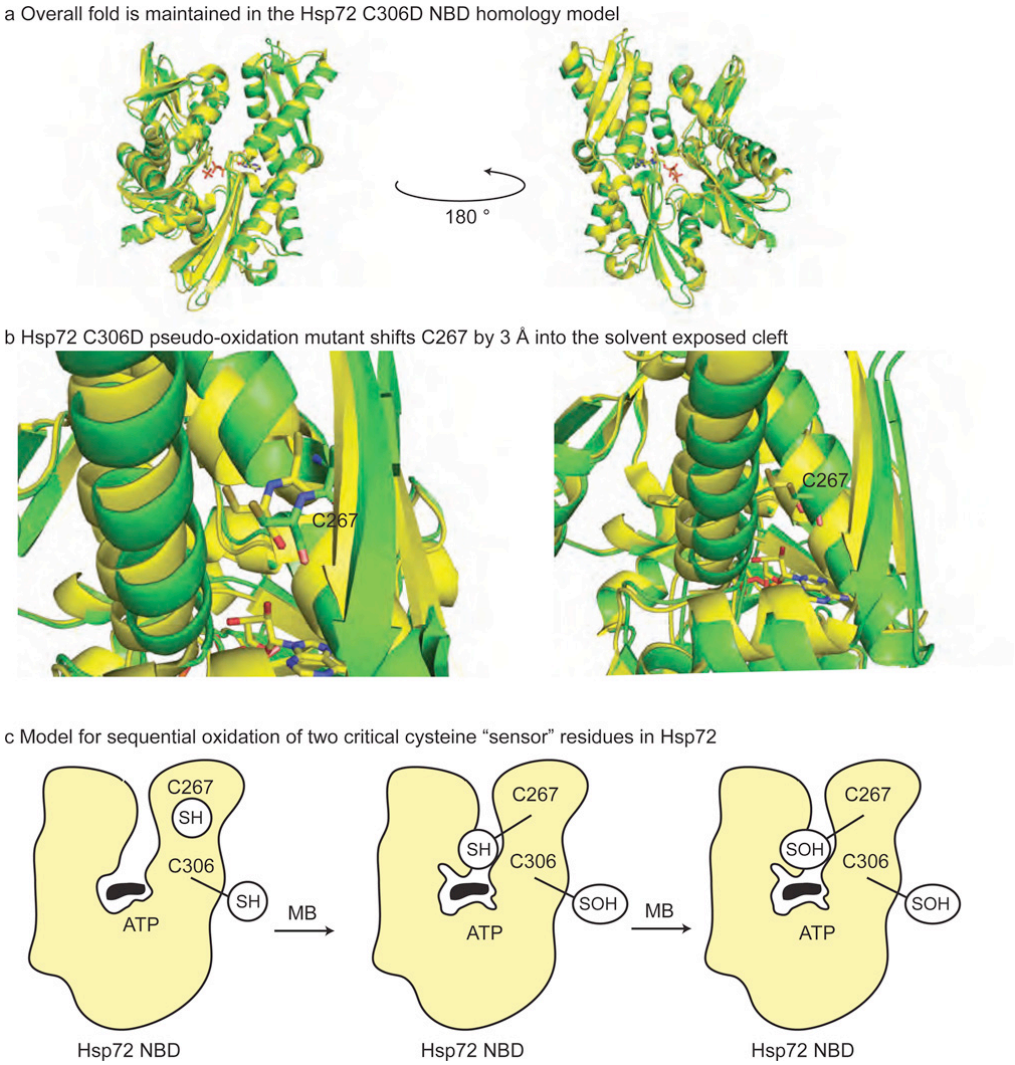

Figure A.7 Homology model of Hsp72 C306D NBD. (A) Pseudo-oxidation of residue 306 does not produce global changes in the NBD fold, similar to what was seen with the C267D mutant. Green is C306D. Yellow is wild type (PDB 3JXU). The C306D and C267D models are nearly identical, with C306D also causing an ~25 Å total displacement of residues associated with nucleotide binding. (B) Close up that illustrates how C306D increases the solvent exposure of Cys267, potentially enhancing its oxidation. C267 moves by ~3 Å in the C306D model. (C) Model for initial oxidation at Cys306, leading to synergistic oxidation of C267 and reduced ATP binding.

A.3.5 Cys to Asp mutations "phenocopies" MB treatment *in vitro* and in cells

To test this model, Cys267 and Cys306 of Hsp72 were mutated to the pseudo-oxidation residue, Asp, and the resulting mutant proteins were purified. Initial attempts to purify the mutants on ATP agarose immediately revealed that they had significantly reduced affinity for nucleotide (Figure A.6D), consistent with the models. Switching to size exclusion, the mutants were purified and found to have normal circular dichroism (CD) spectra (Figure A.8A), suggesting that the global

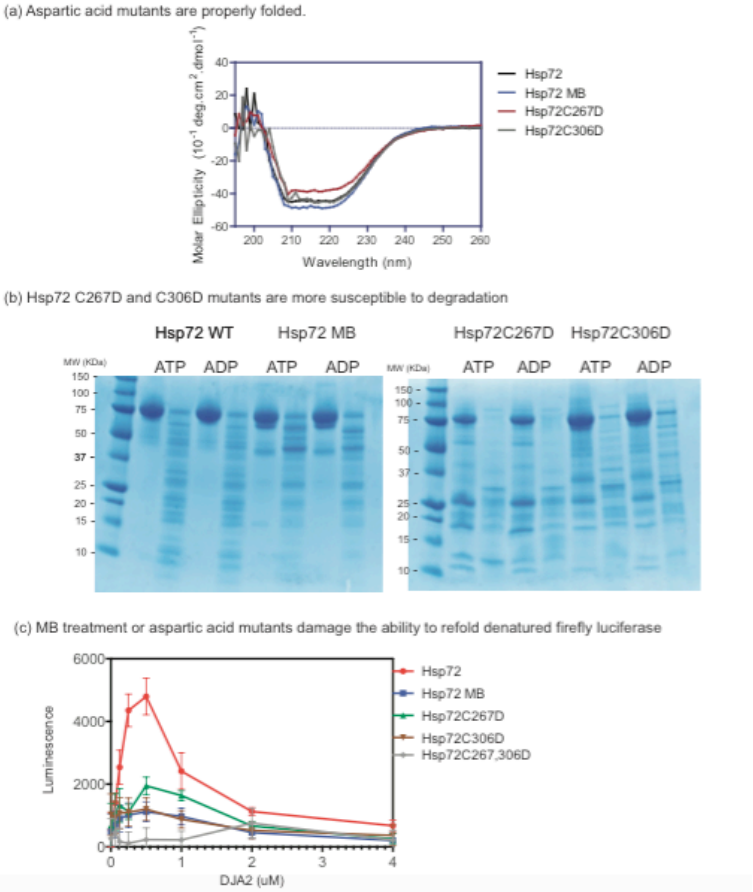

Figure A.8 C267D and C306D mutants have impaired ATP binding and are more flexible. (A) Circular dichroism results indicate that the mutants have similar global structure to the wildtype. Likewise, MB treatment does not cause major changes in structure, as determined by this method. All proteins were used at 2 μM in 50 mM NaF buffer. (B) Hsp70 variants (6 μM) were treated with nucleotide (5 mM) for 30 minutes and then digested with trypsin for 30 min at rt. Reactions were quenched with loading dye, bands separated on 10-20% Tris-Tricine gels and imaged by Coomasie stain. Results are representative of experiments performed in duplicate. (C) Hsp72 and DJA2 could robustly refold denatured luciferase, but Hsp72 treated with MB (50 μM) or Hsp72 with Asp mutants had greatly reduced activity. Results are the average of at least three independent experiments performed in triplicate. Error is SEM.

structure was not significantly disrupted by the Asp mutations. However, partial proteolysis showed that the mutants were more prone to digestion (Figure A.8B), suggesting that they may be more flexible. Interestingly, MB-treated wild type Hsp72 is also prone to proteolysis (Figure A.8B), further enforcing the similarities between the Asp point mutants and the oxidized wild type.

To further explore this possibility, enzymatic activities of the Hsp72 pseudo-oxidation mutants were examined using ATPase assays, showing that the C267D and C306D mutants had dramatically decreased enzymatic activity (Figure A.9A). These mutants essentially behaved like Hsp72 that had been treated with MB. We next tested the ability of Hsp72 and the mutants to refold denatured firefly luciferase. These experiments showed that Hsp72 treated with MB and the C267D, C306D and C267/306D double mutants all had reduced refolding activity (Figure A.8C). Taken together, these studies suggest that the Asp mutants phenocopy some aspects of MB-treated Hsp72.

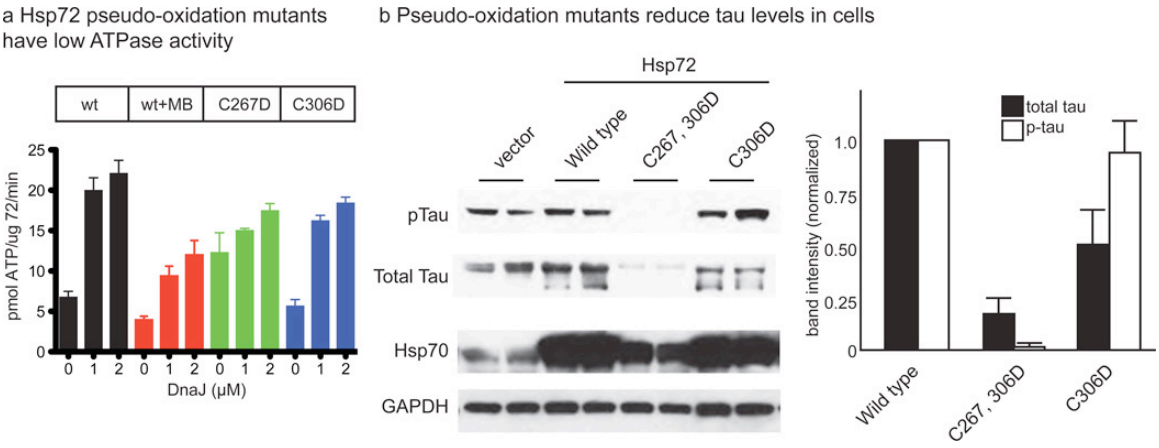

Figure A.9 Pseudo-oxidation mutants phenocopy MB treatment. (A) The DnaJ-stimulated ATPase activities of purified Hsp72 mutants were reduced, resembling MB-treated wild type. These experiments were performed at least three times using two independently prepared samples. Error bars represent the standard error of the mean (SEM). (B) Over-expression of wild type Hsp72 had little effect on tau levels, but the C306D and C267/306D mutants reduced tau. The gels show two independent replicates and the quantification of band intensities includes SEM.

In HeLaC3 cells, over-expression of the C306D mutant produced modest (~40%) reductions in total tau levels and no significant effect on phosphorylated tau (Figure A.9B). Over-expression of the double mutant (C267/306D) substantially (>70%) reduced both tau and phosphorylated tau levels (Figure A.9B). Together, these findings provide strong support for MB acting through oxidation of specific cysteine residues in Hsp72 to reduce tau levels.

A.4 Discussion

One “arm” of the cellular response to redox stress likely involves the acute protection of proteins from oxidation-induced unfolding and aggregation. Here, we were specifically interested in understanding how the Hsp70 family of chaperones, especially the stress inducible forms, might be linked to these types of redox responses. We found that Hsp72, but not Hsc70, was sensitive to oxidation by either MB or peroxide. A recent large-scale proteomic study positively identified Hsp72 as sensitive to oxidation by peroxide in HeLa cells [36], consistent with this finding. Our mass spectrometry, modeling and point mutagenesis results suggest that oxidation of Hsp72 occurs selectively at two cysteine residues, Cys267 and Cys306. Importantly, Cys306 is uniquely conserved in the stress-inducible Hsp70 family members and is absent from the constitutive ones. Although it might be initially surprising for such highly homologous proteins to have different biochemical properties, Goldfarb, *et al.* recently demonstrated that Hsp72 and Hsc70 have opposing effects on the surface expression of murine epithelial sodium channel [37], further suggesting

that even highly conserved Hsp70 isoforms can sometimes have distinct functions. Together, our findings suggest that Hsp72, and possibly other stress-inducible Hsp70 family members, are specially adapted for sensing and responding to redox stress. Based on the observed effects on tau stability, this redox response may involve switching the triage decision to favor degradation of misfolded Hsp72 substrates, perhaps clearing the cytosol of folding intermediates that are particularly prone to oxidative damage.

What is the molecular mechanism linking oxidation of Hsp72 to a loss of ATPase activity? We propose a model in which oxidation of the unique and solvent exposed Cys306 leads to re-arrangement of Cys267, such that this residue is now also sensitive to oxidation. Thus, although Hsc70 has Cys267, it lacks the critical initiator (*i.e*. residue Cys306) and, therefore, treatment with either MB or peroxide does not inactivate it. This model further suggests that oxidation of both Cys267 and Cys306 causes numerous, subtle re-arrangements in residues that normally contact nucleotide. These changes destabilize a number of key contacts, including hydrogen bonds with ATP, hydrogen binds with the phosphate, and a number of hydrophobic interactions. Consistent with this idea, the purified mutants, C267D and C306D, lacked the ability to bind ATP *in vitro*. Thus, we propose a model in which a cascade of oxidations severely damages the binding of Hsp72 to nucleotide. How this re-arrangement favors degradation of bound substrates, such as tau, is not yet clear.

Another goal of this work was to better understand the mechanism by which MB reduces tau levels in cellular and mouse models of AD [19, 23]. Although MB is clearly a promiscuous compound that lacks a classic “drug-like” profile, it is remarkably non-toxic and, thus, it is used in humans for the treatment of a variety of indications, including inherited and acute methemoglobinemia, prevention of urinary tract infections, ifosfamid-induced neurotoxicity, vasoplegic adrenaline resistant shock and pediatric malaria [25]. Because of MB’s particular promise as an AD therapeutic, we were interested in understanding whether any of its effects on tau accumulation may be mediated by oxidation of Hsp72. In this work, we found that mutating Hsp72 Cys267 and/or Cys306 to serine blocked the ability of MB to reduce tau levels in cells. This is an important finding because it strongly links Hsp72 oxidation to effects on tau accumulation. To further enforce this idea, over-expression of the corresponding C267/306D pseudo-oxidation mutant was a strong “dominant negative” and it dramatically reduced tau levels. Together, these results suggest that Hsp72 oxidation is one important way by which MB reduces tau accumulation in AD models. These findings may aid in the discovery of additional AD therapeutics that take advantage of this under-explored mechanism.

Treatments with high levels of MB are tolerated in cells [38] and, moreover, it is relatively non-toxic in humans [25]. On first glance, the global inactivation of Hsp70s might be hypothesized to be acutely and dramatically toxic, given the proposed roles of this chaperone family in “housekeeping” activities. However,

another point of view is that the stress-inducible Hsp72 isoform is specifically concerned with degrading only the substrates that have been damaged or misfolded in response to stress [39], protecting the cytosol from the accumulation of proteotoxic intermediates. In normal cells, the levels of Hsp72 and such misfolded substrates may be low due to the action of other components of the protein quality controls system. Thus, MB may have low toxicity because of its unusual selectivity for the stress-inducible Hsp70 family members. This is an important finding in the continued search for Hsp70-modifying compounds with low toxicity and favorable therapeutic benefits.

A.5 Methods

A.5.1 Proteins and reagents.

Unless otherwise specified, reagents were purchased from Sigma (St. Louis, MO) or Fisher Scientific (Pittsburgh, PA). Human Hsp72, Hsc70 and *E. coli* DnaJ were purified according to published schemes [40]. Site directed mutagenesis primers were designed based on previous reports [41] and mutagenesis of Hsp72 was carried out following the user manual for the QuickChange site-directed mutagenesis kit (Stratagene, La Jolla, CA). The Hsp72 C267S, C306S and C267/306S mutants were expressed and purified using the same protocol as Hsp72 (42). The Hsp72 C267D and C306D mutants were expressed as previously described (42) and purified using nickel-nitrilotriacetic acid His·Bind® resin (Novagen, Darmstadt, Germany), then buffer exchanged into a 25mM HEPES buffer (10mM KCl, 5mM $MgCl_2$ pH 7.5).

A.5.2 Oxidation of Hsp72/Hsc70.

Protein (10 μM) and MB (5 mM) were incubated at 37 °C for 1 hour. For H_2O_2 oxidation, protein sample (10 μM) was incubated with 1 mM H_2O_2 at 37 °C for 1 hour. Treated protein samples were subsequently dialyzed against buffer A (100 mM Tris-HCl, pH 7.4, 20 mM KCl, 6 mM $MgCl_2$) at 4 ^oC.

A.5.3 ATPase activity.

ATPase activity was measured according to the previously published method [30]. Briefly, malachite green-based assays were used to measure phosphate release from purified Hsp72, Hsc70 or mutants (1 μM). Reactions were initiated with 1 mM ATP, performed for 60 minutes and quenched before measuring absorbance. Absorbance readings were converted to pmol of ATP using a phosphate standard curve.

A.5.4 Preparation of dimedone-modified Hsp70s.

MB-treated or untreated Hsp70s (10 μM) were incubated with 5 mM dimedone (5,5-dimethyl-1,3-cyclohexanedione) in buffer A (100 mM Tris-HCl, pH 7.4, 20 mM KCl, 6 mM $MgCl_2$) at room temperature for 1 hour. The samples were analyzed by SDS-PAGE and stained with colloidal Coomassie blue (Invitrogen, Carlsbad, CA). Bands corresponding to Hsp72 were excised and stored at -20 °C until use.

A.5.5 Mass spectrometry.

In-gel digestion was performed as previously described [42]. After reduction (10 mM DTT) and alklylation (65 mM iodoacetamide) of the free cysteines at room temperature for 30 minutes, proteins were digested overnight with trypsin

(Promega). Resulting peptides were resolved on a nano-capillary reverse phase column (Picofritcolumn, New Objective) using a 1% acetic acid/acetonitrile gradient at 300 nL/min and subjected to LC-tandem MS using LTQ Orbitrap XL mass spectrometer. MS/MS spectra were searched against the database considering either carbamidomethyl- or dimedone-modified cysteine.

A.6 Notes

A portion of this work was published as Miyata Y*, **Rauch JN***, Jinwal UK, Thompson AD, Srinivasan S, Dickey CA, Gestwicki JE. *Cysteine reactivity distinguishes redox sensing by the heat-inducible and constitutive forms of heat shock protein 70***.** Chemistry & Biology. 2012; 19:1391-9. (*co-first author)

A.7. References

1. Forman, H.J., M. Maiorino, and F. Ursini, *Signaling functions of reactive oxygen species.* Biochemistry, 2010. **49**(5): p. 835-42.
2. Giles, N.M., et al., *Metal and redox modulation of cysteine protein function.* Chem Biol, 2003. **10**(8): p. 677-93.
3. Paulsen, C.E. and K.S. Carroll, *Orchestrating redox signaling networks through regulatory cysteine switches.* ACS Chem Biol, 2010. **5**(1): p. 47-62.
4. Waris, G. and H. Ahsan, *Reactive oxygen species: role in the development of cancer and various chronic conditions.* J Carcinog, 2006. **5**: p. 14.
5. Lin, M.T. and M.F. Beal, *Mitochondrial dysfunction and oxidative stress in neurodegenerative diseases.* Nature, 2006. **443**(7113): p. 787-95.
6. Patten, D.A., et al., *Reactive oxygen species: stuck in the middle of neurodegeneration.* J Alzheimers Dis, 2010. **20 Suppl 2**: p. S357-67.
7. Apel, K. and H. Hirt, *Reactive oxygen species: metabolism, oxidative stress, and signal transduction.* Annu Rev Plant Biol, 2004. **55**: p. 373-99.
8. Majmundar, A.J., W.J. Wong, and M.C. Simon, *Hypoxia-inducible factors and the response to hypoxic stress.* Mol Cell, 2010. **40**(2): p. 294-309.
9. Morgan, M.J. and Z.G. Liu, *Crosstalk of reactive oxygen species and NF-κB signaling.* Cell Res, 2011. **21**(1): p. 103-15.
10. Zhang, Y., et al., *HSF1-Dependent Upregulation of Hsp70 by Sulfhydryl-Reactive Inducers of the KEAP1/NRF2/ARE Pathway.* Chem Biol, 2011. **18**(11): p. 1355-61.

11. Kumsta, C. and U. Jakob, *Redox-regulated chaperones.* Biochemistry, 2009. **48**(22): p. 4666-76.
12. Hartl, F.U., A. Bracher, and M. Hayer-Hartl, *Molecular chaperones in protein folding and proteostasis.* Nature, 2011. **475**(7356): p. 324-32.
13. Mayer, M.P., et al., *Multistep mechanism of substrate binding determines chaperone activity of Hsp70.* Nat Struct Biol, 2000. **7**(7): p. 586-93.
14. Mayer, M.P. and B. Bukau, *Hsp70 chaperones: cellular functions and molecular mechanism.* Cell Mol Life Sci, 2005. **62**(6): p. 670-84.
15. Patury, S., Y. Miyata, and J.E. Gestwicki, *Pharmacological targeting of the Hsp70 chaperone.* Curr Top Med Chem, 2009. **9**(15): p. 1337-51.
16. Evans, C.G., L. Chang, and J.E. Gestwicki, *Heat shock protein 70 (hsp70) as an emerging drug target.* J Med Chem, 2010. **53**(12): p. 4585-602.
17. Hageman, J., et al., *The diverse members of the mammalian HSP70 machine show distinct chaperone-like activities.* Biochem J, 2011. **435**(1): p. 127-42.
18. Lindquist, S., *The heat-shock response.* Annu Rev Biochem, 1986. **55**: p. 1151-91.
19. Jinwal, U.K., et al., *Chemical manipulation of hsp70 ATPase activity regulates tau stability.* J Neurosci, 2009. **29**(39): p. 12079-88.
20. Congdon, E., et al., *Phenothiazine induces autophagy and attenuates tauopathy in vitro and in vivo.* Autophagy, 2012. **8**(4).
21. Koren, J., 3rd, et al., *Facilitating Akt clearance via manipulation of Hsp70 activity and levels.* J Biol Chem, 2010. **285**(4): p. 2498-505.
22. Wang, A.M., et al., *Inhibition of hsp70 by methylene blue affects signaling protein function and ubiquitination and modulates polyglutamine protein degradation.* J Biol Chem, 2010. **285**(21): p. 15714-23.
23. O'Leary, J.C., 3rd, et al., *Phenothiazine-mediated rescue of cognition in tau transgenic mice requires neuroprotection and reduced soluble tau burden.* Mol Neurodegener, 2010. **5**: p. 45.
24. Wischik, C., et al., *Tau aggregation inhibitor (TAI) therapy with Rember^{TM} arrests disease progression in mild and moderate Alzheimer's disease over 50 weeks*, in *Alzhimer's and Dementia*. 2008. p. T167.
25. Schirmer, R.H., et al., *"Lest we forget you--methylene blue...".* Neurobiol Aging, 2011. **32**(12): p. 2325.e7-16.
26. Oz, M., D.E. Lorke, and G.A. Petroianu, *Methylene blue and Alzheimer's disease.* Biochem Pharmacol, 2009. **78**(8): p. 927-32.
27. Liu, Q., E.J. Levy, and W.J. Chirico, *N-Ethylmaleimide inactivates a nucleotide-free Hsp70 molecular chaperone.* J Biol Chem, 1996. **271**(47): p. 29937-44.
28. Kelner, M.J. and N.M. Alexander, *Methylene blue directly oxidizes glutathione without the intermediate formation of hydrogen peroxide.* J Biol Chem, 1985. **260**(28): p. 15168-71.
29. Miyata, Y., et al., *Molecular chaperones and regulation of tau quality control: strategies for drug discovery in tauopathies.* Future Med Chem, 2011. **3**(12): p. 1523-37.

30. Chang, L., et al., *High-throughput screen for small molecules that modulate the ATPase activity of the molecular chaperone DnaK.* Anal Biochem, 2008. **372**(2): p. 167-76.
31. Reddie, K.G. and K.S. Carroll, *Expanding the functional diversity of proteins through cysteine oxidation.* Curr Opin Chem Biol, 2008. **12**(6): p. 746-54.
32. Poole, L.B., P.A. Karplus, and A. Claiborne, *Protein sulfenic acids in redox signaling.* Annu Rev Pharmacol Toxicol, 2004. **44**: p. 325-47.
33. Kim, D.E., D. Chivian, and D. Baker, *Protein structure prediction and analysis using the Robetta server.* Nucleic Acids Res, 2004. **32**(Web Server issue): p. W526-31.
34. Wisniewska, M., et al., *Crystal structures of the ATPase domains of four human Hsp70 isoforms: HSPA1L/Hsp70-hom, HSPA2/Hsp70-2, HSPA6/Hsp70B', and HSPA5/BiP/GRP78.* PLoS One, 2010. **5**(1): p. e8625.
35. Permyakov, S.E., et al., *Oxidation mimicking substitution of conservative cysteine in recoverin suppresses its membrane association.* Amino Acids, 2011.
36. Leonard, S.E., K.G. Reddie, and K.S. Carroll, *Mining the thiol proteome for sulfenic acid modifications reveals new targets for oxidation in cells.* ACS Chem Biol, 2009. **4**(9): p. 783-99.
37. Goldfarb, S.B., et al., *Differential effects of Hsc70 and Hsp70 on the intracellular trafficking and functional expression of epithelial sodium channels.* Proc Natl Acad Sci U S A, 2006. **103**(15): p. 5817-22.
38. Yaglom, J.A., V.L. Gabai, and M.Y. Sherman, *High levels of heat shock protein Hsp72 in cancer cells suppress default senescence pathways.* Cancer Res, 2007. **67**(5): p. 2373-81.
39. Pratt, W.B. and D.O. Toft, *Regulation of signaling protein function and trafficking by the hsp90/hsp70-based chaperone machinery.* Exp Biol Med (Maywood), 2003. **228**(2): p. 111-33.
40. Chang, L., et al., *Mutagenesis reveals the complex relationships between ATPase rate and the chaperone activities of Escherichia coli heat shock protein 70 (Hsp70/DnaK).* J Biol Chem, 2010. **285**(28): p. 21282-91.
41. Zheng, L., U. Baumann, and J.L. Reymond, *An efficient one-step site-directed and site-saturation mutagenesis protocol.* Nucleic Acids Res, 2004. **32**(14): p. e115.
42. Brady, G.F., et al., *Regulation of the copper chaperone CCS by XIAP-mediated ubiquitination.* Mol Cell Biol, 2010. **30**(8): p. 1923-36.